CHEMOENZYMATIC PREPARATION OF PROBES FOR IN VITRO AND CELLULAR ELUCIDATION OF COMPLEX BACTERIAL POLYSACCHARIDES

by

Amanda Joy Reid

A dissertation submitted to the faculty of
The University of North Carolina at Charlotte
in partial fulfillment of the requirements
for the degree of Doctor of Philosophy in
Nanoscale Science

Charlotte

2021

Approved by:

_____
Dr. Jerry Troutman

_____
Dr. Craig Ogle

_____
Dr. Yuri Nesmelov

_____
Dr. Swarnapali De Silva Indrasakara

_____
Dr. Mark Clemens

ABSTRACT

AMANDA JOY REID. Chemoenzymatic Preparation of Probes for *in vitro* and Cellular Elucidation of Complex Bacterial Polysaccharides. (Under the direction of DR. JERRY TROUTMAN)

Bacteria play a major role in our health and wellbeing. The microbe-host interaction is often mediated by sugar polymers at the cell surface. An incredibly diverse amount of glycan variation exists throughout these structures, which makes identification of surface components difficult. The composition of the surface is unique to bacteria and acts as molecular fingerprint which can distinguish even subspecies apart. Better methods to decipher what those glycan identities are or how to reproduce them may help develop future advancements towards exploiting them as therapeutic targets. The major challenge addressed herein is to simplify the tools used to track the formation of these natural materials. To do this, we expand on the chemoenzymatic preparation of a tagged lipid substrate central to early stages of biosynthesis for many surface polysaccharides. Further, we identify conditions in which these unnatural substrates can be used *in vitro*. Lastly, we develop methodologies to detect BP and polysaccharide intermediates in live cells. These tools have facilitated robust detection and reconstruction of glycan assembly building blocks. This research may lay the ground work for future applications technologies towards novel therapeutics, such as glycoconjugates vaccines.

DEDICATION

In the memory of a faithful furry friend, Ebony.
Your unconditional companionship helped me through a great number of challenges from elementary to my second year of graduate school.

ACKNOWLEDGEMENTS

This project would not have been possible without the support and encouragement of a great deal of people.

First, I would like to thank my advisor Dr. Jerry Troutman whose expertise and inspiration was essential for the success of this project. I am extremely grateful for his open-door policy (which I didn't hesitate to take advantage of) and enthusiasm for this project.

I would also like to thank all current and past members of the Troutman lab that I've had the pleasure to work alongside with. I owe a great deal of gratitude in particular to Kate Erickson and Beth Scarbrough for encouraging my development as a confident researcher and who were always willing to provide advice in any number of personal or professional challenges I faced during my time here.

The support from my friends and family has been invaluable. Thank you for always listening to me talk (for far too long) about my research endeavors and never failing to ask for updates.

I would also like to thank the NIH for awarding me with the F31 which funded my graduate studies. This includes help from Dr. Mark Clemens, who provided a great deal of insight for preparing the proposal, as well as Ida and Peter, who were integral for managing the behind-the-scenes aspects of dispersing the award when there was no

established system for doing so.

I gratefully acknowledge the support of my committee members for their commitment to excellence and my growth as a researcher. The support of the departmental faculty, including Dr. Cliff Carlin and Jon Merkert, were invaluable for maintaining instruments and supplies essential for this research.

Lastly, I would like to thank my furry children, Ebony and Ivory, whose emotional support is unmatched.

TABLE OF CONTENTS

LIST OF TABLES

LIST OF FIGURES

LIST OF ABBREVIATIONS

AP	Acid phosphatase
Az	3- Azidoanilino- (clickable moiety)
BP	Bactoprenyl phosphate
BPP	Bactoprenyl diphosphate
cef	cell envelope fraction
2CN	2-cyanoanalino- (fluorescent moiety)
DBCO	Dibenzocyclooctyne
DiNAcBac	N,N-diacetylbacillosamine
DMSO	Dimethylsulfoxide
Fl-BP	Fluorescently tagged BP
FPP	Farnesyl diphosphate
Gal	Galactose
GalNAc	N-Acetylgalacoseamine
Glc	Glucose
GlcNAc	N-Acetylglucoseamine
GPP	Geranyl diphosphate
HexNAc	N-Acetyl-Hexosamine
HPLC	High performance liquid chromatography
IPP	Isopentenyl diphosphate
LCMS	Liquid chromatography mass spectroscopy
LPS	Lipopolysaccharide
NBD	Nitro-benzoxadiazoylamino- (fluorescent moiety)

NMR	Nuclear magnetic resonance spectroscopy
PCR	Polymerase chain reaction
Pgl	Protein glycosylation
PGT	Phosphoglycosyltransferases
RCF	Relative Centrifugal Force
Rcs	Regulation of capsule synthesis
SBA	Soybean Agglutinin
SDS-PAGE	Sodium dodecyl sulfate Polyacrylamide Gel Electrophoresis
SIM	Scanning ion mode
TB	Terrific Broth
UDP	Uridine diphosphate
UppP	Undecaprenyl diphosphate phosphatase
UppS	Undecaprenyl diphosphate synthase
Und-P	Undecaprenyl phosphate

CHAPTER 1: INTRODUCTION

Overview

Our bodies host a complex population of microbes that have a profound influence on our overall health. Their important role is often unrecognized until we fall ill, either as a result of absent symbiotic bacteria or the presence of infectious pathogens. This seemingly ambivalent relationship can be better understood by considering the different species and sub-species of bacteria we encounter. *Escherichia coli*, for example, has over 100 different serotypes that differentiate symbionts from pathogens. These serotypes are categorized based on differences in their surface composition which are predominantly comprised of polysaccharides. Further, various protective glycans on the bacterial cell surface can also be responsible for virulence or can be a response leading to antibiotic resistance. Therefore, characterizing the composition of surface polysaccharides and how they are assembled is essential to understanding their influence over our health. The biggest challenge in the field of bacterial glycobiology is the immense hyper-diversity present in bacterial glycan composition. This chapter will review historically important and current methods for elucidating bacterial glycan bioassembly, as well as identify gaps in the field that are addressed in the research presented herein.

Bacteria and Their Influence on Our Health

Trillions of microscopic organisms reside in and on the human body.[1] These complex bacterial communities comprise the human microbiome and they play a direct role in maintaining our health. They act as a barrier to prevent pathogens from invading, and they even digest foods or produce vitamins that we otherwise are incapable of.[2] Some major diseases, such as obesity or type II diabetes, have also been linked to our gut microflora.[3] Additionally, beneficial bacteria may also contribute to the early development of our immune system, and may result in autoimmune disorders later in life if not present.[4, 5] Conversely, pathogens also

undermine our health by causing diseases which can be spread between people or ingested in the food we eat. Discerning precisely how pathogens and commensals differ may help better our understanding of the interactions which are critical for our health. One major difference lies in the composition of the bacterial cell wall.

Many structural motifs of the bacterial cell wall are shared among commensal and pathogenic good and bad bacteria alike. Broad-spectrum antibiotics like penicillin target these common features, and inadvertently increases our susceptibility to opportunistic pathogens or even contributes to antimicrobial resistance.[6-8] Even though there are many similarities in the cell wall landscape, a great deal of variation exists in the precise chemical identity. Yet, probing their composition has been difficult due to the intrinsically rare and unusual chemical composition of those structures. Better methodologies to investigate their step-wise assembly are needed in order to facilitate advances towards mitigating their negative influence on our health.[9]

Cell Surface Chemistry

Anatomy of the Cell Surface

Most bacteria belong in one of two broad categories based on general patterns of cell wall organization. For purposes herein, we included discussion on only gram positive and gram-negative bacteria and have omitted a smaller 'gram-variable' category. Both classes of bacteria possess a formidable barrier at their cell envelope (**Figure 1.1**). One common feature between gram negatives and positives is the presence of a phospholipid bilayer, which largely protects the cell against passive diffusion of hydrophilic molecules such as water. Pores and efflux pumps on the cell surface aid in nutrient acquisition of relatively small, hydrophilic analytes on the order of ~600 Da.[10-12] The presence of a double lipid bilayer in gram negative species, such as *E. coli,* largely contributes to the difficulty of gaining access to the cytosol in gram negative species. The additional lipid barrier poses a challenge for some hydrophilic antibiotics.[13]

Gram negative species possess two lipid bilayers, a symmetrical inner phospholipid membrane as well as an asymmetrical outer lipid membrane. The outer membrane is a distinguished feature of gram-negative species, where the outer leaflet is thought to be primarily comprised of lipopolysaccharide (LPS), while the inner leaflet is comprised of only phospholipids. LPS (also called endotoxin) consists of three major components: first, a glycolipid moiety with acyl tails which anchor into the membrane; next a conserved core region of phosphorylated glycans; and last, a variable length glycan polymer known as O-antigen.[14, 15] Divalent cations help stabilize the highly anionic environment in the core region of LPS which is thought to be a result of charge shielding. Likewise, this region is believed to be crucial to maintain the cell wall barrier function.[13] Unlike the core region, the O-antigen demonstrates tremendous diversity with ~180 variants in *E. coli*.[16] The precise length and composition of the O-antigen accounts for the high degree of natural variation and can fundamentally differentiate between virulent and avirulent subspecies.[17]

Peptidoglycan is another important glycopolymer of the cell wall. The monomeric unit is comprised of a NAG/NAM repeating disaccharide (N-actylglucosamine and N-acetylmuramic acid) and a polypeptide of four to five amino acids. Crosslinking of the polypeptide contributes to cell shape, rigidity, and prevents lysis in environments with low osmolarity.[18] In gram positive species, the peptidoglycan may extend tens of nanometers from the cell surface and is anionically charged due to the presence of teichoic acids, polymers of alternating glycans, and glycerophosphate. In gram negative species the peptidoglycan is sandwiched between the two membrane bilayers, in a space called the periplasm, and is notably much thinner than in gram positive species (~10 nm).

Gram positive bacteria are distinct in that, unlike gram negatives, they lack LPS altogether. Instead, gram positive bacterial species possess a thick peptidoglycan layer which can extend upwards of 100 nm from the cell surface. Modifications of the peptidoglycan are an important mechanism to combat natural defenses against infection. For example lysozymes, such as those produced in tears, are commonly produced as a host defense by catalyzing the hydrolysis of the NAG/NAM disaccharide.[19] O-acylation of NAM in pathogenic *S. aureus*, however, inhibits lysozyme leading to opportunistic colonization such as those found in conjunctivitis, better known as pink eye.[20, 21]

Several accessory surface glycans may also be present which can aid in virulence, surface adhesion, or preventing desiccation. Broadly, these materials are referred to as exopolysaccharides and can include covalently linked capsules or glycan polymers that are excreted into the immediate environment. Colanic acid is an example of an exopolysaccharide which is common to virulent members of the *Enterobacteriaceae* family, which includes *E. coli* and *Salmonella*, and may act as a scaffold for biofilm formation.[22] Bacterial biofilms form as the result of the accumulation of glycopolymers and other biological material in complex bacterial communities. Biofilm formation can make it harder for therapeutics to access the bacterial cell wall and can lead to persistent infections.[23] Other types of non-essential cell wall modifications can be important for virulence such as an important oligosaccharide which modifies surface proteins of the common food pathogen *Campylobacter jejuni*. Attenuation of *C. jejuni* can be achieved by blocking the formation of this oligosaccharide, although the precise mechanism for how is not known.[24]

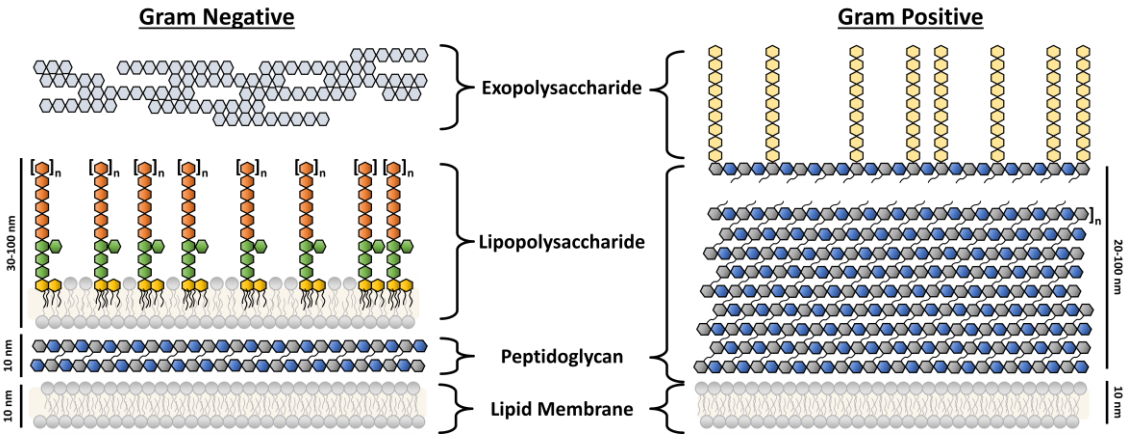

Figure 1.1 Anatomy of the gram positive and negative bacterial cell walls
Gram positive bacteria contain an outer membrane and a thick peptidoglycan layer which can extend tens of nanometers from the cell surface. Gram negative bacteria in contrast have both and inner and outer phospholipid bilayer. The outer leaflet is made from LPS which is comprised of a glycolipid, core, and variable O-antigen region. The peptidoglycan in gram negative species is sandwiched in between the outer and inner membranes. Both types of bacteria can have exopolysaccharides that may be covalently attached to the cell wall or excreted into the environment around the cell.

Unique Glycan Fingerprints

The specific combination of LPS, O-antigen, exopolysaccharides, and some surface proteins present in the cell wall creates a bacterial 'fingerprint' which give rise to subspecies variants. For instance, there are over 2,500 subspecies, or serotypes, of *Salmonella* and less than 100 of those are human pathogens. Identifying the specific chemical composition in each and every microbe becomes a monumental task. This challenge is exacerbated by the fact that bacteria utilize on the order of 500 common glycans. In comparison, mammalian cells utilize just 30.[25] The natural glycan hyper-diversity is an attractive target for novel therapeutic or diagnostic development as there is a smaller chance for cross-reactivity with us or with our microflora. The dilemma therein lies in the fact that these glycans are rare and therefore have low natural abundance. There is a dearth of cheap commercial sources and they often require custom synthesis, which often start at ~$10,000 for milligram quantities. Thus, a fundamental and field-wide challenge lies in producing these rare glycans in the lab. This can be done through chemical or sometimes chemoenzymatic synthesis if the glycan identity is known ahead of time.[26, 27] For pathways with unknown glycan composition, finding alternative methods that do not rely on

glycan availability are needed to expedite glycopolymer discovery and subsequent therapeutic development.

A Common Lipid Anchor for Surface Polysaccharide Bioassembly

Virtually all surface glycans are synthesized on the cytosolic face of the phospholipid membrane. A lipid carrier, bactoprenyl phosphate (BP), acts as a scaffold for oligosaccharide assembly at the membrane. BP is thought to be a universal lipid carrier for many bacterial surface glycans including LPS, peptidoglycan, and capsule assembly. Oligosaccharide synthesis occurs most commonly by the addition of a glycan via a phosphoanhydride linkage to the phosphoryl group of BP, or less often by phosphoryl- esters. Nucleotide-linked sugar donors provide the necessary substrate for either initiating phosphoglysocyl- or glycosyl- transferase enzymes, respectively, to catalyze these linkages. The oligosaccharide is then stepwise synthesized by either transferase or glycan modifying enzymes for a particular pathway. Polysaccharides, such as capsules, are exported and the oligosaccharide repeating unit is polymerized prior to cell surface presentation. Alternatively, glycans may instead be transferred onto surface presenting features rather than polymerized. Importantly, BP is regenerated as a result of either processes and subsequently reused for glycan assembly.

De novo BP is synthesized by the enzymes undecaprenyl diphosphate synthase (UppS) and undecaprenyl diphosphate phosphatase (UppP) (**Figure 1.2**). First, eight successive condensation additions of isopentenyl diphosphate onto a farnesyl diphosphate are catalyzed by UppS to produce bactoprenyl diphosphate (BPP). This process is thought to be carried out in the cytosol, as UppS is a soluble protein, and the lipid carrier is inserted into the inner membrane bilayer by an unknown mechanism. Then, cleavage of the terminal phosphoanhydride is then carried out by the membrane protein UppP to produce bactoprenyl phosphate. Then, the first phospho-glycan is added by a phosphoglycosyltransferase (PGT) marking the first committed

step for pathway divergence. The oligosaccharide is then built over the course of subsequent glycan additions or modifications, and the substrate is flipped to the periplasmic side of the cell. The oligosaccharide may then be covalently attached to the cell wall or polymerized and exported to the cell surface. Importantly, BP is regenerated at the end of either process and recycled for subsequent glycosylation.

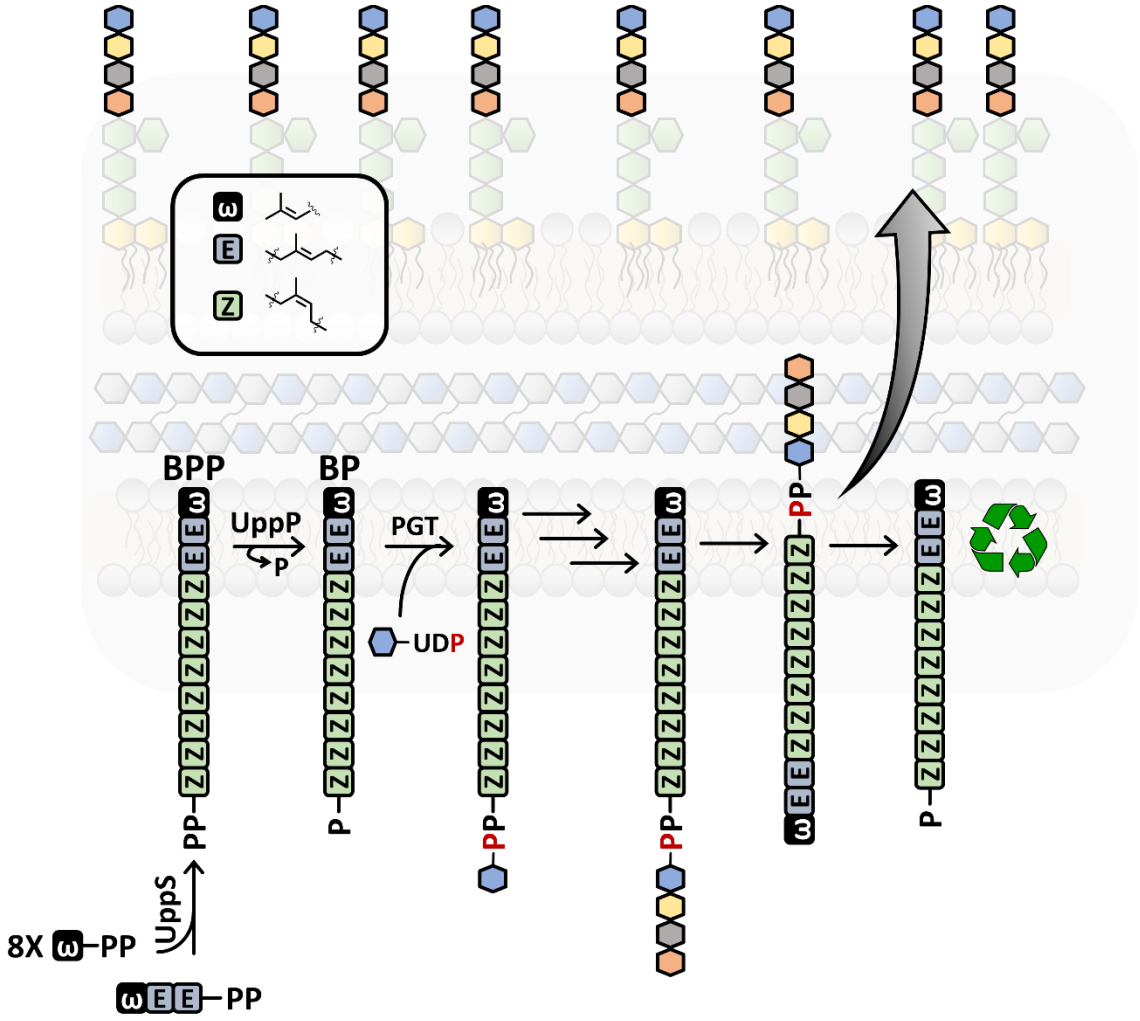

Figure 1.2 General biosynthesis of early polysaccharide bioassembly.
First the common lipid carrier BPP is synthesized from early isoprenoid building blocks by UppS. The lipid scaffold is then embedded in the membrane and dephosporylated by UppP. A PGT then adds the first phospho-glycan, followed by subsequent glycan addition or modification. The repeating unit is then flipped toward the periplasmic face and then is polymerized and exported or exported to build the cell wall.

Methods for Elucidating Glycan Bioassembly *in vitro*

Glycan Probes

Glycan based molecular probes are among the most widely used tools throughout glycobiology. Of historical importance are radiolabeled glycans, which has helped identify the lipid scaffold and sugars responsible for cell wall components such as colanic acid.[28, 29] These types of probes have detection limits as low as attomoles, and are most similar to their native structures but come with additional considerations such as the cost and challenges of resource sharing.[30] For most other biomolecules such as proteins or nucleic acids, fluorescent modifications have largely replaced radiolabeling techniques. Unlike these other biomolecules, bacterial glycans have the possibility of forming non-linear linkages. Therefore, the design of fluorescent modifications of monosaccharides needs to take this into consideration.

Within the last 20 years, advancements in bioconjugate chemistry has allowed for diversification of fluorophore choices.[9] In particular, "Click" chemistry has been popularized in glycobiology as it provides modular reactions between a pair of small molecules that readily react in biological environments. Huisgen cycloaddition had been widely adapted to install relatively small "click-handles" in the form of an azide or alkyne groups on a biomolecule and molecular probe. Significant progress was made when Bertozzi and coworkers developed a strained octyne click-companion to drive the reaction, rather than a copper catalyst which is known to be cytotoxic.[31] This has enabled *in vivo* tracking of peptidoglycan bioassembly which revealed insights on cell wall synthesis in exquisite detail and was not previously possible. While commercially available, this approach is largely exclusive to peptidoglycan because the amino acid, and not the glycan, contain the click-handle (**Figure 1.3**).[32]

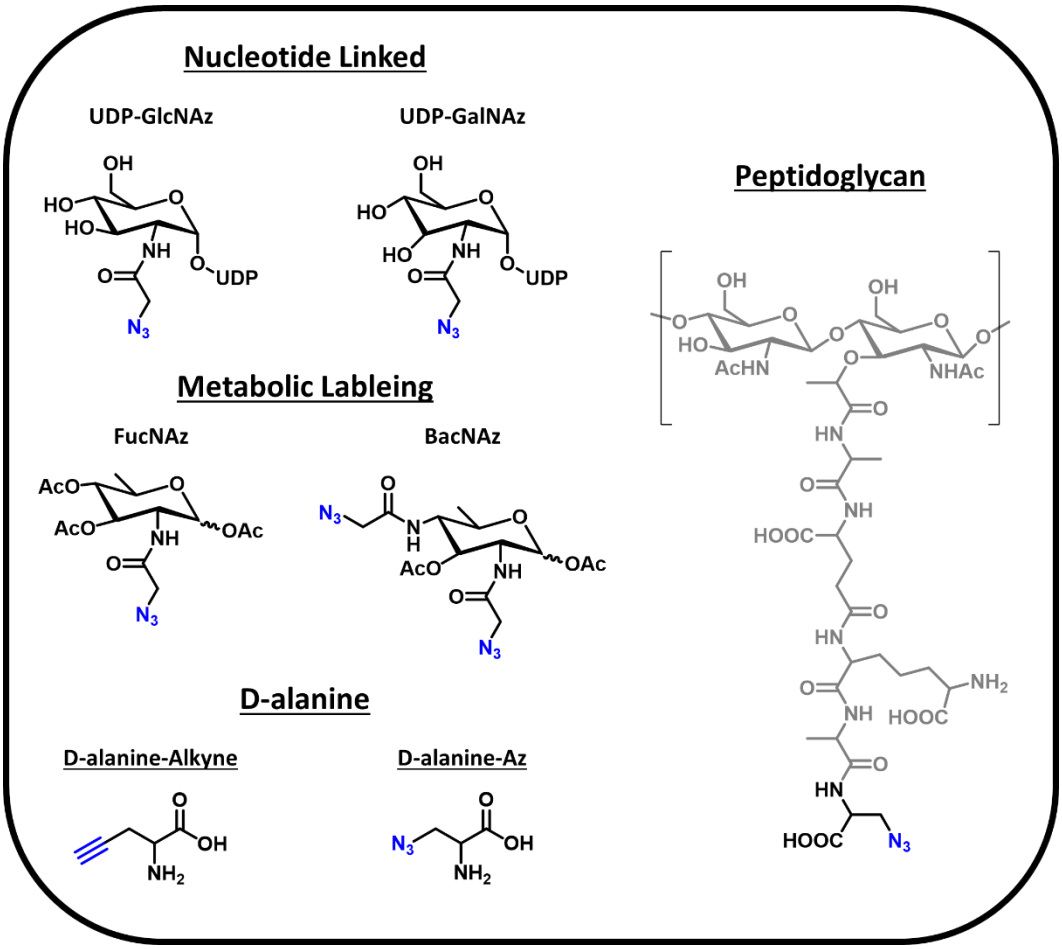

Figure 1.3 Click-tools used for glycan labeling.
Metabolic labeling of peptidoglycan was made possible through the incorporation of click-able amino acids such as azido and alkyne labled D-alanine. Alternatively, glycans with direct chemical modifications can be synthesized for metabolic labeling such as fucose (Fuc) or bacillosamine (Bac). The more naturally abundant glycans UDP - glucosamine (UDP-Glc) or –galactosamine (UDP-Gal) are commercially available with nucleotide linkages.

There is a critical lack of commercial sources of bacteria specific glycan libraries. More often, dedicated efforts are undertaken to generate each individual glycan, such as an azide labeled fucose or bacillosamine found in *E. coli* and *C. jejuni*, respectively (Figure 1.3). The synthesis of labeled glycans, such as those used for metabolic incorporation, are produced in well over 10 synthetic steps.[9, 33] Yet these efforts have been extremely fruitful in discovering several unique glycans in key infectious species.[34] Lesser found are nucleotide-linked glycans, such as a glucosamine or galactosamine, needed for *in vitro* recapitulation (**Figure 1.3**). Only three years ago was the first report utilizing two enzymes to append UDP-linkages to label bacterial specific

glycans.[35] It remains to be determined if the substrate specificity of these enzymes could permit broader use to other rare glycans.

Alternative Lipid Substrates

Modifications of the common lipid scaffold have also been investigated to solve persistent problems throughout *in vitro* recapitulation of glycan assembly such as cost and solubility. Commercial sources of BP are both rare and expensive totaling up to $2,000 for 50 milligrams. Alternatively, these can be synthesized from isoprenoid building blocks over iterative isoprenoid additions, which can total in excess of 25 steps if building the full-length BP.[36] Some reports even obtained crude BP from the bacterial membrane, but there are not established methods to quantify the amount of BP present in them.[29, 37-39] Often BP is solubilized with co-solvents since enzymatic reactions require aqueous conditions. Recently a semi synthetic approach was undertaken to extract plant undecaprenol from Bay leaves and append click-handles or photoaffinity tags to the end of the isoprenoid scaffold.[40] However, the C_{55} isoprenoid undecaprenol, which differs by one *E*-configuration double bond in the place of a *Z*-configuration, is equally hydrophobic as BP and may therefore share many of those challenges (**Figure 1.4**).

Isoprenoids, other than undecaprenol and bactoprenol, are readily obtained from plant sources including prenol, geraniol, and citronellol. These naturally abundant fragrance and food additives are very cheap, unlike BP. Because of some of the challenges associated with obtaining or solubilizing BP, shorter isoprenoids have been used as substrate replacements for glycan bioassembly (**Figure 1.4**). When these "short" monophosporylated substrates consist of three 5-carbon isoprenoid monomer units or fewer (e.g. neryl-, geranyl-, and farnesyl-) glycosyltransferase activity is generally absent.[41, 42 43, 44] Isoprenoids over four units become

increasingly less abundant in nature, however enzyme activity is markedly enhanced within the "medium" regime of 4-6 isoprene units in many accounts.[41-43, 45-48] Enzyme activity for "long" substrates (≥7 isoprene units) has the most discrepancy in the literature, varying from least to most preferred when compared to other isoprenoid sizes.[42, 44, 45, 48-50] This disparity is proposed to be the result of differing *in vitro* components (e.g. surfactants, DMSO, organic alcohols).[45] Often each enzyme has unique preferences or tolerances to those various additives which must be determined empirically.

Interestingly, isoprenoid geometry pays a role in substrate recognition as well (**Figure 1.4**). Native BP is comprised of a terminal farnesyl- group (ω, 2*E*) followed by eight cis prenyl-additions (8*Z*) closest the phosphate where transferase activity occurs. Thus, it is no surprise that isoprenoids containing only *E* configurations of any length are poor substrates for glycosyltransferases.[50] At least one α-*Z* unit is needed for activity, and two or more enhance transferase activity.[41, 42, 45, 47, 50] Lesser understood are the effects of saturation on activity. For example, citronellyl monophosphate, with an alpha *Z* isoprenoid and unsaturated ω isoprenoid, permitted assembly of the first lipid-linked glycan product of peptidoglycan but not the second.[42, 45] When lipid-linked oligosaccharides are synthetically pre-formed with a saturated undecyl- acyl tail, two enzymes involved in later stages of peptidoglycan and LPS synthesis was observed.[51, 52] It remains unclear if initiating phosphoglycosyltransferases could also use such substrates. Partially α-saturated lipid containing isoprenoids, such as dolichol phosphates found in mammalian cells, have variable activity with initiating phosphoglycosyltransferases.[44, 49, 50] This may be due to the fact that they are found as varying n-lengths and share similar challenges associated with lipid solubilization and enzyme optimization.

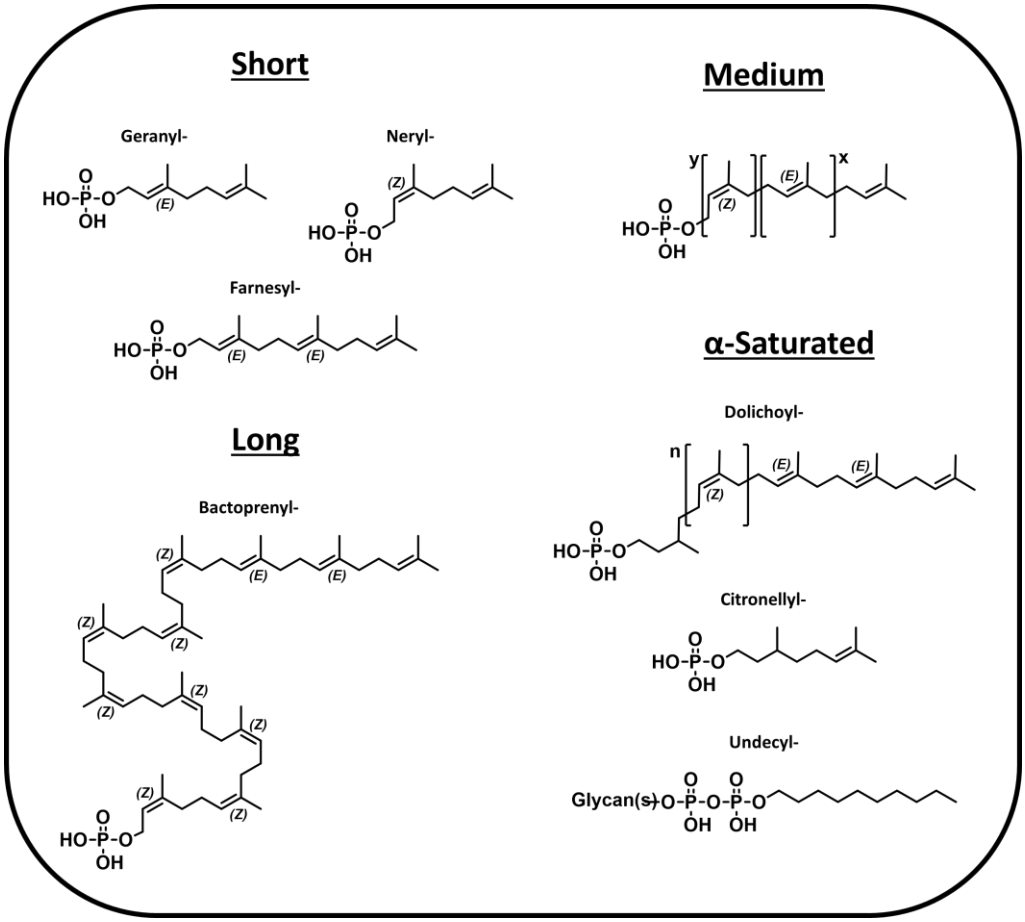

Figure 1.4 Alternative lipid substrates used for in vitro glycan assembly
Medium length isoprenoids, where x and y equal 4-6, tent to be preferred substrate replacements. Short, 3 units or shorter, and long isoprenoids, over 7 units, are generally poor substrate replacements in comparison. Lipids containing saturated α-isoprenes are also sometimes used.

Isoprenoid Probes

Isoprenoid based probes, although fundamental to nearly all cell wall synthesizing components, are less discussed in the literature. This may be due to the fact that there are far fewer probes to choose from, unlike those reported with glycans, and they have only just recently been applied to bacterial glycan synthesis. Within the last decade, Troutman and coworkers developed methodologies to produce fluorescently modified BP.[53-55] These substrates were then subsequently used to identify the enzyme roles associated with the oligosaccharide repeating units of a capsular polysaccharide from *Bacteroides fragilis* and colanic acid from *E. coli*.[26, 27] Both reports use a chemoenzymatically synthesized BP with a 2-cyano anilino fluorophore. This was achieved by incorporating the 2CN tag onto GPP (2CN-GPP), an analogous structure of FPP

(**Figure 1.5A**). Then, 2CN-GPP was supplied to UppS from *B. fragilis* ($UppS_{Bf}$) to generate fluorescently modified BPP followed by subsequent dephosphorylation by a general phosphatase (**Figure 1.5B**).

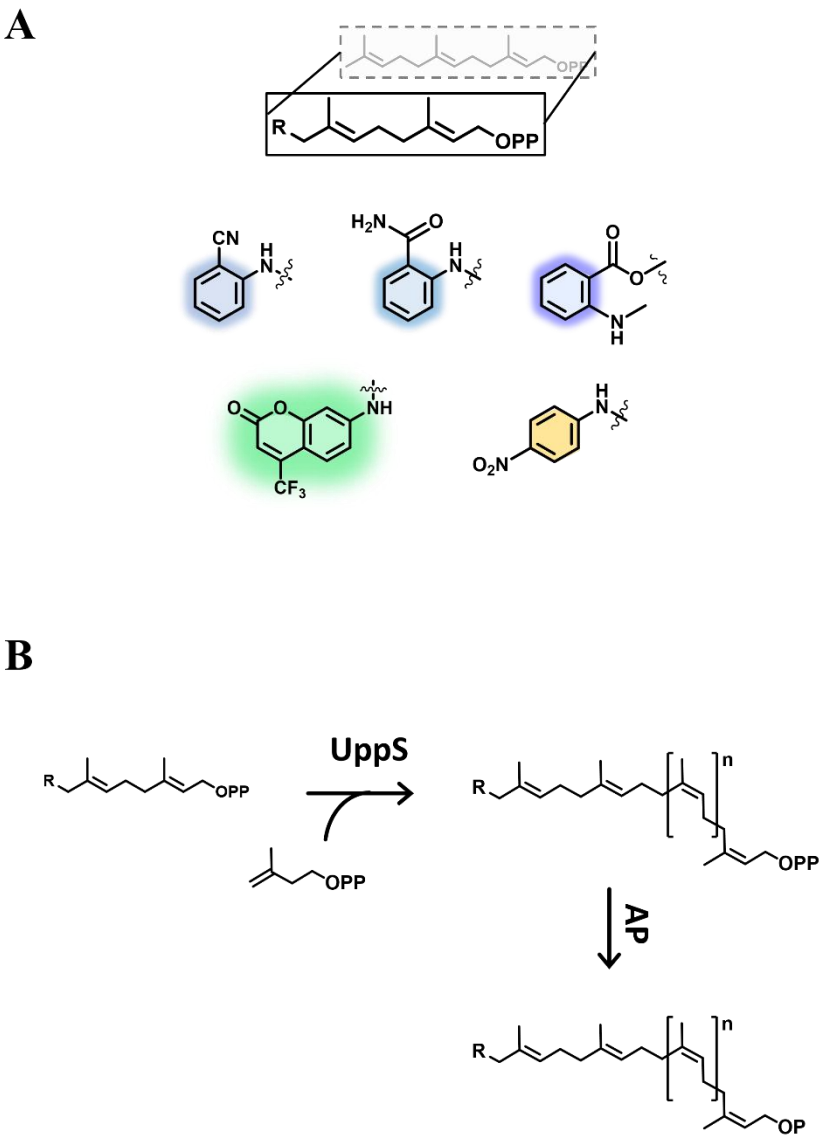

Figure 1.5 Analogues Farnesyl Diphosphate Substrates for UppS
(A) Reported substrates that act as FPP replacements for BPP synthesis. (B) Chemoenzymatic synthesis scheme for the production of tagged BP substrates for polysaccharide bioassembly.

Fluorescently modified isoprenoids were used to probe UppS polymerization nearly 10 years before applications in glycan bioassembly. In fact, kinetic analysis was enabled through the

use of a trifluoromethyl-coumarin (TFMC) analogue, for which $UppS_{Ec}$ could only catalyze the first IPP addition.[56] This was believed to be the result of steric hindrance between the fluorophore and a hydrophobic tunnel in UppS associated with lipid elongation. The length of this tunnel is thought to act as a molecular ruler for BP length determination, and it was hypothesized to exclude entry of TFMC. Since then, a handful of smaller chromophores including 2CN-, nitroaniline-, anthranilamide-, and a N-methyl-aminobenzoyl- (MANT) probe were sufficiently small to permit elongation of isoprenoid probes (**Figure 1.5A**).[57] Interestingly, UppS from either *E. coli*, *B. fragilis,* or *Vibrio vulnificus* were demonstrated to have different preferences for 2CN- tagged lipid substrates.[54] This suggests that differences in the amino acid sequence between these species yield differences in the hydrophobic tunnel size or demonstrate relaxed substrate specificity. Later, it was also determined that the size of the isoprenoid could be tuned by supplying specific surfactants, an artifact of *in vitro* UppS reaction conditions exploited to control isoprenoid length.[55]

The Current Gaps and Research Goals Presented

Several gaps in the field need to be addressed before rapid progress can be made towards future prospects of glycan use in therapeutics or diagnostics. Appending probes to isoprenoids, rather than glycans, can do this by broadening the range of cell wall components that can be synthesized *in vitro*. To do this we first sought to diversify the types of tags available to isoprenoid-based probes, such as those that already applied to click glycans. Moreover, the strategic placement of the tag on the isoprenoid, as opposed to the glycan, allows for applications where preserving the native glycan identify might be important. Lastly, we demonstrate that oligosaccharides can be detected from cell extracts. Addressing these challenges increases the

accessibility of tools that can be used through virtually all isoprenoid-based cell wall synthesizing components.

Currently, the isoprenoid probes used for characterizing glycan assembly lie in the UV region. Not only does that contribute to higher background noise, but techniques throughout cell imaging are primarily amenable to excitations in the visible spectrum. Extended use of UV-light for live cells, such as those needed for *in vivo* analysis, may damage cells. Therefore, we first developed and optimized the production of a fluorophore that emits in the visible spectrum. To ensure that this new probe would be a substrate for glycosylation, we validated it with a number of PGTs important for either O-antigen or capsule synthesis from four different organisms. We also scaled up the chemoenzymatic synthesis and optimization of parameters important for narrow size product distributions. We incidentally identified unique solubility requirements resulting from the addition of hydrophilic fluorophores.

Our second goal was to employ isoprenoid probes for applications other than for tracking glycan bioassembly. Detecting surface glycans in point of care diagnostics is not widely used. Developing such assays depend on reproducing biological targets and immobilizing them, or conjugating them to other biomolecules. To close this gap, we reproduced an important oligosaccharide from the food pathogen *C. jejuni* with a click-ready azido moiety installed on the isoprenoid. With cost considerations in mind, we identified an alternative method to produce an expensive sugar used to make this oligosaccharide. Most excitingly, we found that installing an azido tag permitted us to use the short and naturally abundant isoprenoid neryl- to build the oligosaccharide. The azido tag indeed allowed us to immobilize the oligosaccharide while maintaining the native structure of the glycan which we were able to detect with a fluorescently conjugated lectin. This is especially advantageous for

future sensing applications of the glycan and represents an early developmental tool for novel glycan sensing diagnostics.

Lastly, we tackled the challenge of using a cell to produce sugars for us in place of purchasing them or making them in the lab. To do this we developed an LC-MS method that could detect native untagged BP and BPP-linked glycans extracted from cells. We then use *E. coli* strains bearing single enzyme mutants to accumulate intermediates of colanic acid. This allowed us to visualize each step of colanic acid bioassembly by using sugars and enzymes present in the cell. This method is an exciting step towards reducing the burden of producing or buying rare glycans. Extending this protocol to uncharacterized pathways could help narrow the glycan identities associated with unknown oligosaccharides. Altogether this illustrates a powerful technique to identify and recapitulate glycans inside of live cells as they occur in nature. These findings will ultimately further our understanding on the stepwise construction of species-specific glycan ‘fingerprints’ and inspire novel methods for them to positively influence our health and wellbeing.

CHAPTER 2: GENERAL UTILIZATION OF FLUORESCENT POLYISOPRENOIDS WITH SUGAR SELECTIVE PHOSPHOGLYCOSYLTRANSFERASES

Author Contributions: Amanda Reid, Jerry Troutman, and Beth Scarborough acquired all data, performed analysis, and contributed to the final project design and methodology. Early conceptualization of the project design, including original mutant work, were carried out by Tiffany Williams and Claire Gates. Colleen Eade were responsible for preparing the final C43 ΔwecA mutant. Preliminary analysis essential for this project was carried out by Tiffany Williams and Claire Gates. This manuscript was written and prepared by Amanda Reid and Jerry Troutman, and the final version edited by all authors.

Overview

The protective surfaces of bacteria are comprised of polysaccharides and are involved in host invasion and colonization, host immune system evasion, as well as antibacterial resistance. A major barrier to our fundamental understanding of these complex surface polysaccharides lies in the tremendous diversity in glycan composition among bacterial species. The polyisoprenoid bactoprenyl phosphate (or undecaprenyl phosphate) is an essential lipid carrier necessary for early stages of glycopolymer assembly. Because of the ubiquity of bactoprenyl phosphate in these critical processes, molecular probes appended to this lipid carrier simplify identification of enzymatic roles during polysaccharide bioassembly. A limited number of these probes exist in the literature or have been assessed with such pathways, and the limits of their use are not currently known. Herein, we devise an efficient method for producing fluorescently modified bactoprenyl probes. We further expand our previous efforts utilizing 2-nitrileaniline, and additionally prepare nitrobenzoxadizol tagged bactoprenyl phosphate for the first time. We then assess enzyme promiscuity of these two probes utilizing four well characterized initiating phosphoglycosyltransferases: CPS2E (*Streptococcus pneumoniae*), WbaP (*Salmonella enterica*), WecA (*Escherichia coli*) and WecP (*Aeromonas hydrophilia*). Both probes serve as substrates for these enzymes and could be readily used to investigate a wide range of bacterial glycol assembly pathways. Interestingly, we have also identified unique solubility requirements for the

nitrobenzoxadizol moiety for efficient enzymatic utilization that was not observed for the 2-nitrileaniline.

Introduction

The unique composition of the bacterial cell surface accounts for a large degree of diversity observed among microbial communities. One species of bacteria, such as *Escherichia coli*, may have numerous sub-types that possess a unique composition in O-antigen, lipopolysaccharide, or capsule.[58] A common lipid carrier, bactoprenyl phosphate (BP) (also referred to as undecaprenyl phosphate), is utilized for the bioassembly of cell wall glycans, or modifications of these materials. The addition of the first sugar residue to BP marks a critical step in establishing the ultimate glycan end product. Thus, BP expenditure is considered to sequester this common anchor from a finite pool, and ultimately influences cell physiology, cell shape, as well as adaptations for antibiotic resistance.[59-61] Because of its ubiquity among surface polysaccharide bioassembly, BP is essential to recapitulate surface glycan synthesis *in vitro* but is difficult to detect.

Our group has previously demonstrated that fluorescently tagged BP (fl-BP) can be utilized *in vitro* for two polysaccharide assembly pathways: *E. coli* colanic acid, and *Bacteroides fragilis* capsular polysaccharide A.[26, 27] Tagged glycans, including fluorescent and radiolabeled moieties, have been extensively employed in the literature to serve a similar purpose.[33, 62] Bacteria utilize a plethora of glycans, generating the considerable diversity among bacterial serotypes. Commercial sources of all known glycans are limited, and a smaller fraction are available labeled. Efforts to prepare these synthetically have been successfully reported, and require a different synthetic strategy for each individual glycan. The primary advantage of fl-BP is that this anchor is ubiquitous throughout bacterial surface glycan assembly, and preserves the native glycan structure. However, the consequences associated with the isoprenoid tag structure and their influence on enzymatic

activity have yet to be broadly assessed.

As the glycan oligomer is built on fl-BP, the terminal tag is increasingly distanced from the catalytic site. Therefore, we reason that the initial glycosylation step to fl-BP could be a limiting factor for broader use of these probes. Initiating phosphoglycosyltransferases (PGTs) are integral membrane proteins that catalyze the transfer of hexose-1-phosphates or N-acetylhexosamine-1-phosphates to BP. This first step is then followed by subsequent glycosylation by highly specific pathway-dependent enzymes. A few well studied examples of initiating PGTs include: CPS2E from *Streptococcus pneumoniae,* which aids in capsule formation; WbaP from *Salmonella enterica,* WecA from *Escherichia coli,* and WecP from *Aeromonas hydrophilia,* the latter of which aids in formation of O-antigen.[37, 39, 63, 64]

The above well characterized PGTs are herein used to assess fl-BP tag influence on enzymatic activity (**Figure 2.1**). Broadly, the fl-BPs are promising tools to probe PGT activity and glycan specificity with their native, unlabeled nucleotide-linked sugar substrates. The fluorescent moiety used in previous works, 2-nitrileaniline (2CN), is prepared by chemical and enzymatic synthesis to produce variable-length isoprenoids, which are length tunable by surfactant choice.[55] While the 2CN analogue has been very useful in these applications, the primary shortcomings of this probe include poor detection limit (relative to larger fluorophores or radiolabels) and high UV-background noise. We sought to address these issues by selecting to install a nitrobenzoxadizol (NBD) fluorophore to both increase the detection limit and reduce background noise since the excitation and emission lie in the visible range. Farnesyl labeled NBD probes have been developed for mammalian protein prenylation, but this moiety has not been applied to elongated isoprenoids necessary for bacterial glycobiology.[65] Since BP is common to many surface polysaccharide assembly systems, highly fluorescent BP poses an attractive method for following these

fundamental processes that is comparable with current methods in glycan labeling.[33, 66]

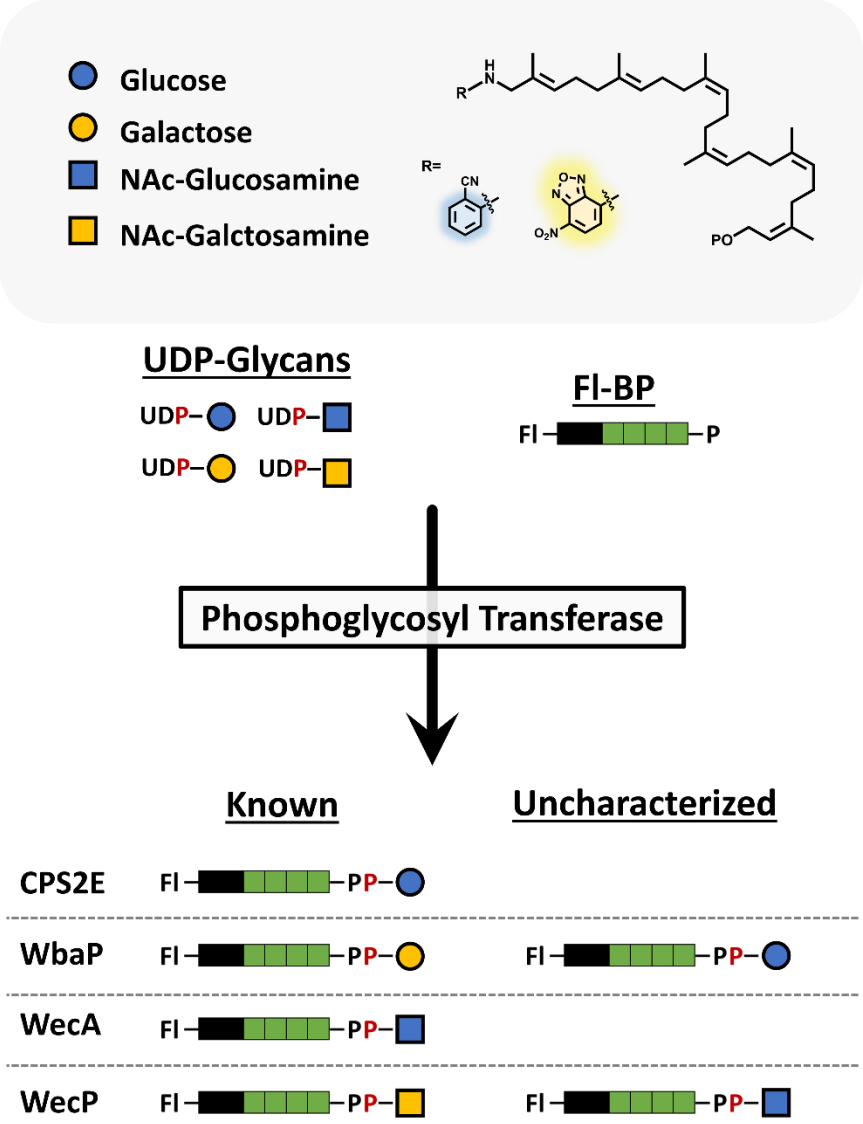

Figure 2.1 Model PGTs and their transferase activity towards two fluorescently modified substrates
Shortened polyisoprenoids have been chemoenzymatically prepared with one of two fluorescent tags (fl-BP). These alternative substrates were then assessed for transferase activity among four model PGTs with known functions. Both fl-BPs were suitable substrates for all PGT's in the presence of their preferred UDP-linked glycan substrates. Additional specificity analysis revealed previously uncharacterized transferase activity in two of the model PGTs.

We report herein the development of a new fl-BP that is based on the well characterized NBD fluorophore. Moreover, we have scaled fl-BP production 100 fold relative to our previous efforts by exploiting a highly efficient chemoenzymatic procedure to afford 10 µmol of fl-BPP. We have found that 2CN and NBD are near equivalent substrates for the model PGT enzymes used

here. We have also identified previously uncharacterized alternative glycan substrate specificities for two of these PGTs, WbaP and WecP (**Figure 2.1**). This work also highlights the conditional dependence of fl-BP enzymatic substrate utilization in the presence of *n*-propanol, suggesting new insights into the molecular arrangements of these polyisoprenoids in substrate utilization by PGTs. The use of fl-BPs is promising for future applications as effective probes for solubilized enzyme kinetics, background cell envelope fraction activity, and specificity of common bacterial PGTs. The use of bactoprenyl probes has been successful for the identification of enzymatic roles involved in several polysaccharide bioassembly pathways, requiring only nanomolar concentrations for detection. These materials have potential to help with not just fundamental characterization, but also metabolic labeling of live cells which greatly aid our understanding of how these materials behave *in situ*. An efficient and robust method for producing bactoprenyl probes is therefore required to obtain sufficient material downstream applications. Several variables are optimized herein to scale up 100-fold production of tagged BP from previous efforts. This includes: the selection of isoprenoid tags which will be later applied *in vitro* and *in vivo*; UppS activity which differs among various bacterial amino acid sequences; phosphatase activity; and also methodology for efficient semi-preparatory purification.

Results and Discussion

Preparation of Highly Fluorescent Bactoprenyl Diphosphate

Chemical preparation of farnesyl diphosphate analogues of 2CN and NBD have been previously reported in the literature.[54, 65] Efficient enzymatic preparation of fluorescently modified 2CN bactoprenyl diphosphate (fl-BPP) has been achieved with recombinant undecaprenyl diphosphate synthase (UppS) from *Bacteroides fragilis* ($UppS_{Bf}$).[54] The 2CN analogue was shown to be effective for monitoring enzyme activity with an increase in fluorescence intensity observed upon isoprenoid chain elongation, which was attributed to an increasingly hydrophobic

environment around the fluorophore. Similar to 2CN, the NBD fluorophore is known to be highly sensitive to its molecular environment. To rapidly assess if the NBD-GPP compound was a substrate for $UppS_{Bf}$ and to determine if a similar increase in fluorescence could be observed with the NBD analogue upon elongation, $UppS_{Bf}$ reactions were prepared in 96-well plate format and chain elongation of 5 μM 2CN-GPP or NBD-GPP was monitored by fluorescence increase (**Figure 2.2**). We observed a minimum increase in fluorescence in the NBD-GPP reactions over 50 min (1.1 fold), while 2CN-GPP fluorescence increased 2.5 fold. HPLC analysis of products demonstrated that very little substrate had been consumed with the NBD-GPP analogue, while nearly all of the 2CN-GPP had been consumed under identical conditions (data not shown). We were then curious to examine if UppS from different bacterial species would be more effective at utilizing tagged substrates. We found that the enzyme encoded by *Staphylococcus aureus* ($UppS_{Sa}$) was highly effective for the elongation of both 2CN- and NBD-GPP. A 4.8 fold increase in fluorescence with NBD-GPP was observed relative to a 3.5 fold increase with 2CN-GPP under identical conditions (**Figure 2.2**) with the *S. aureus* protein.

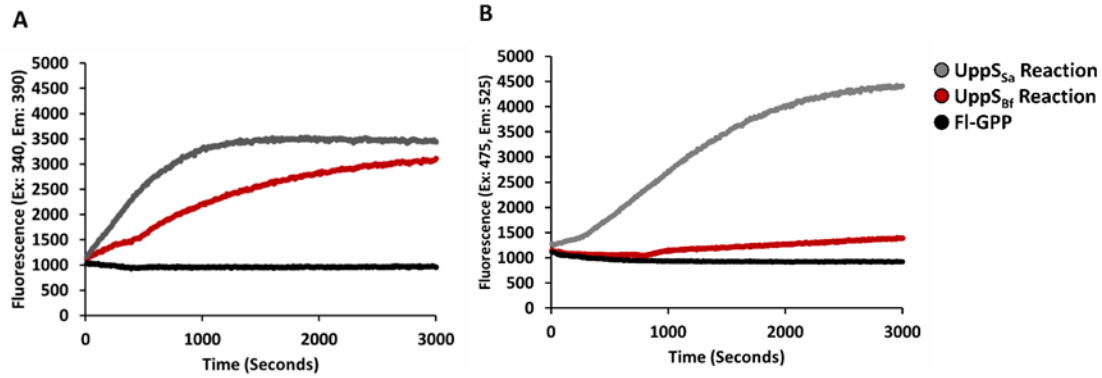

Figure 2.2 UppS reactions with 2CN- or NBD-GPP.
(A) or NBD-GPP (B) monitored. Black lines show the GPP control, in the absence of IPP or UppS. Red lines show reaction using UppS from *B. fragilis*, while gray lines show reactions using UppS from *S. aureus*.

From these data it was clear that $UppS_{Sa}$ was able to accept the NBD-labeled analogue more readily than the $UppS_{Bf}$, suggesting that subtle differences in the structures of these proteins

could lead to more promiscuous activity with alternative substrate structures. A trifluoromethyl (TFM) coumarin based fluorescent analogue was previously shown to be an ineffective substrate with UppS from *E. coli* ($UPPS_{Ec}$), where the analogue was capable of only accepting a single isoprene unit before being released from the enzyme.[56] Analysis of the X-ray crystal structure of $UppS_{Ec}$ suggested that the terminal isoprene of FPP moves through a narrow hydrophobic tunnel beneath the active site of the enzyme as isoprene units are added.[67] It was proposed that this analogue was a poor substrate for $UppS_{Ec}$ because the bulky TFM-coumarin-fluorophore could not fit through this hydrophobic tunnel and was therefore released after just a single isoprene unit addition. The NBD and TFM-coumarin moieties have a similar estimated size relative to an isoprene unit or the smaller 2-nitrileaniline. NBD-GPP was also found to be a poor substrate for $UppS_{Ec}$ (data not shown). The ineffectiveness of NBD-GPP with *B. fragilis* and *E. coli* UppS may have been similarly related to factors that made the TFM-coumarin analogue an ineffective substrate for $UppS_{Ec}$. It is interesting to consider if the more promiscuous *S. aureus* protein would utilize the TFM-coumarin analogue more readily, and if this protein could be generally used to prepare BPP analogues with bulkier fluorophores.

Two step formation of fl-BP

In previous work our focus has been on relatively small (100 nmol) preparations of fl-BPP.[54] We sought to exploit the robust nature of $UppS_{Sa}$ by scaling up BPP production to 10 µmols in the same 1 mL volume used previously, or 100 µmols by scaling the volume ten-fold. Typical soluble protein expression yields from a 1 L culture of $UppS_{Sa}$ were around 30-40 mg of purified protein, which could be stored at -80 °C for several weeks. Variable length isoprenoid production was expected, and is tunable based on surfactant choice – herein designated *nZ* where n is the number of isoprene additions in *Z* configuration.[55] Additionally, we found that a narrow distribution of isoprenoid additions could be modulated by sequential addition of isopentenyl

diphosphate, in the presence of relatively high concentrations of $UppS_{Sa}$ (Figure A1**)**. This approach enabled us to achieve a range of fl-BPPs of 2CN and NBD with 4-6*Z* additions (Error! Reference source not found.). Generally, for practical purposes, shorter isoprenoids (4-6*Z*) were preferred for their solubility and ease of handling.

An essential step for BP production is phosphoanhydride hydrolysis, which provides a polyisoprenyl monophosphate substrate for bacterial PGTs. Previous work from our group utilized an alkaline phosphatase to convert the diphosphate to monophosphate after separation and purification of UppS products. However, we found that there is considerable batch-to-batch variation with alkaline phosphatase activity prompting us to look for an alternative method. Additionally, separation of BPP prior to dephosphorylation was time consuming and decreased overall yield for this process. To address this problem, we chose instead to use commercially available potato acid phosphatase.[56, 68] Since acidic conditions were required for the acid phosphatase, a two-step sequential reaction was employed. To do this, we first chose to extract $UppS_{Sa}$ reaction products with *n*-butanol, and then treat the dried extract with acid phosphatase in an acidic buffer. Reactions containing 5 mM of each fl-BPP were readily converted to monophosphate with 20 μg/mL acid phosphatase (Sigma 0.5-3 units/mg) in the presence of 20% *n*-propanol (Error! Reference source not found.). Alternatively, acid phosphatase reactions could be carried out directly from *n*-butanol extracts (with up to 5% *n*-butanol carryover) in addition to all other reaction components. Monophosphate product formation was confirmed by LCMS (Figure A2**)**, and these were isolated by semi-preparatory HPLC according to isoprenoid size. Dried fractions were optimally resuspended in a single phase mixture of Acetone:Hexanes:DMSO (6:5:0.5 v/v/v) and concentrated as described in methods and materials. Purity and identity of the isolated fl-BP products were confirmed by LCMS and then quantitated by the extinction

coefficients associated with the fluorophores. We also tested whether the acid phosphatase reaction could be monitored in a plate reader format, but detected no significant change in fluorescence upon diphosphate hydrolysis (data not shown). Fl-BP with four *Z*-isoprene additions were further utilized to test the HPLC limit of detection for the isoprenoids. Using three standard deviations of peak-to-peak chromatogram noise, the approximate limit of detection was found to be 5 and 1 pmol for 2CN and NBD, respectively, demonstrating that we had indeed increased the limit of detection for labeled bactoprenyl from our previous attempts by five-fold (Figure A3**)**.

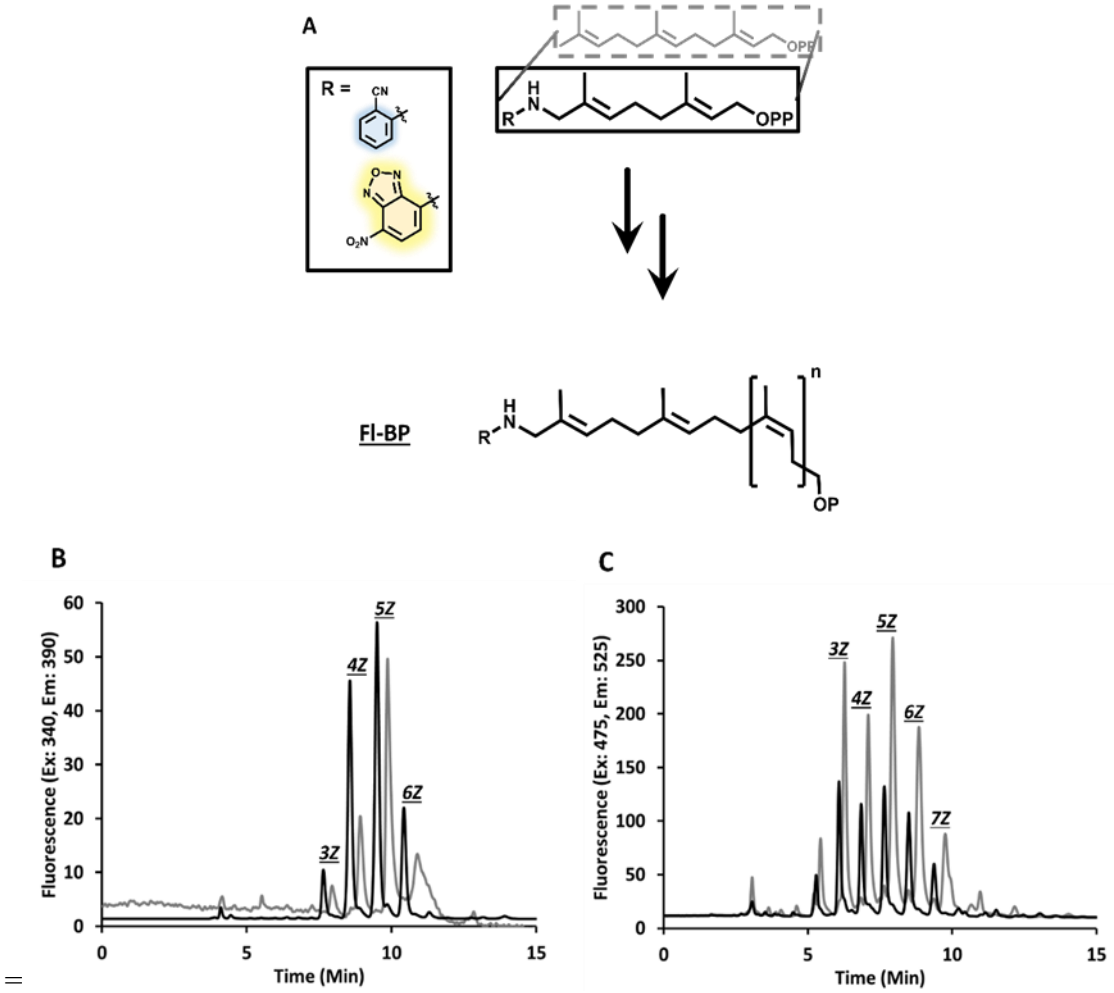

Figure 2.3 Two-step formation of multi-milligram scale fl-BP.
A general scheme for two-step fl-BP formation (A) with representative HPLC of 2CN (B) and NBD (C). The black line shows fl-BPP formation from $UppS_{Sa}$ reaction, while the gray line shows fl-BP formation upon potato acid phosphatase treatment in the presence of 20% *n*-propanol.

The hydrophobic nature of phospho-polyisoprenoids has led to a number of challenges associated with their limited solubility at high concentrations. Fluorescently tagged materials have somewhat increased solubility, albeit still relatively difficult to solubilize in aqueous amenable solvents alone. We employed a number of solutions to ensure efficient recovery of fl-BPs. Dried fl-BP elutions were resuspended in a single phase solution of Acetone:Hexanes:DMSO, which could then be readily transferred to microcentrifuge tubes. The volatiles were then removed under a ReactiVap thus reducing the total number of transfer steps and ultimately yielding DMSO solubilized fl-BPs. Given the scalability of the chemoenzymatic preparation and robustness of $UppS_{Sa}$, the fundamental bottleneck for purification is column loading capacity during HPLC purification.

NBD-BP and 2CN-BP are nearly equivalent substrates for the PGT WecP

We were next interested in whether these fluorescent moieties altered the substrate effectiveness for isoprenoid utilizing enzymes. The PGT WecP, which transfers N-acetyl-galactosamine phosphate (GalNAc-P) to BP, is a transmembrane protein; however, previous work has demonstrated that the functional form of the full length protein can be solubilized away from membranes and purified.[64] We chose to use this protein as a representative because, unlike many other PGTs, it was easily purified away from cell envelope fraction (cef) and therefore would not have complicating factors in its analysis. The *wecP* gene was commercially synthesized then incorporated into a pET-24a vector for overexpression and subsequent purification. As expected the protein initially fractionated with the cef, and we were able to extract and purify it to homogeneity (Figure A4**)**. We tested WecP activity with UDP-GlcNAc and -GalNAc, with the expectation that it would only be capable of transferring GalNAc-P to our fl-BP. GalNAc-P was transferred by the protein to both NBD-B(*4Z*)P and 2CN-B(*4Z*)P analogues. Interestingly, while GalNAc-P was clearly a better substrate for the enzyme, the protein was also able to catalyze the

transfer of GlcNAc-P to a limited extent (**Figure 2.4**). Neither UDP-glucose (Glc) nor UDP-galactose (Gal) was a substrate for the enzyme under these conditions. LCMS analysis confirmed that the new fluorescent peaks in these reactions were indeed NBD- and 2CN- B(*4Z*)PP-linked GlcNAc and GalNAc (Figure A5 and Figure A6).

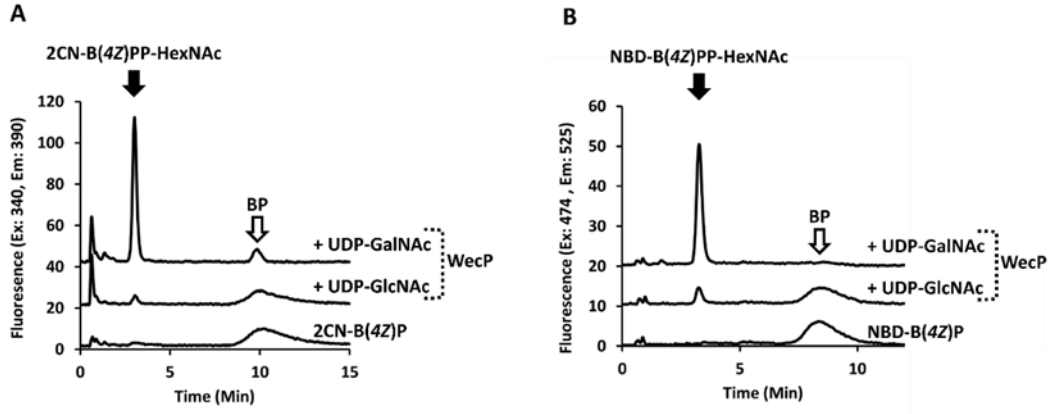

Figure 2.4 WecP activity with 2CN and NBD-B(4Z)P.
Transferase activity is observed with UDP-GalNAc and UDP-GlcNAc with 2CN- and NBD-B(*Z*4)P's, A and B respectively. A co-eluting contaminate is present in the 2CN-4Z-BP standard, which appears at 10 min only after 2CN-BP consumption.

Chain length and tag identity have little influence on isoprenoid utilization by WecP

To determine how well fl-BPs serve as substrates, we chose to perform kinetic analysis on WecP with analogues of varying chain length and tags. Our fl-BP provides a unique opportunity to readily measure kinetics, and are considerably more facile to detect than unlabeled isoprenoids. Optimization of WecP activity was first carried out to identify an optimal concentration of divalent cations and surfactant (Figure A7 and Figure A8). Reactions were next prepared with 2CN-B(*4Z*)P and 2CN-B(*7Z*)P at variable concentration with 225 μM UDP-GalNAc (**Table 2.1**). Under these conditions the apparent k_{cat}, $K_m^{isoprenoid}$, and $k_{cat}/K_m^{isoprenoid}$ were nearly identical suggesting that the length of the isoprenoid within this range had no influence on enzyme recognition with the 2CN analogue. When the isoprenoid was changed to the NBD-B(*7Z*)P the analogue was utilized slightly less efficiently (1.5 fold) than the 2CN-B(*7Z*)P ($^{app}k_{cat}/K_m^{isoprenoid}$) due to a slightly lower $^{app}k_{cat}$. When the smaller NBD-B(*5Z*)P was utilized, the efficiency ($^{app}k_{cat}/K_m^{isoprenoid}$) was

indistinguishable from the other compounds, although the turnover rate ($^{app}k_{cat}$) was 2.7 fold lower, as the $^{app}K_m^{isoprenoid}$ proportionally decreased relative to $^{app}k_{cat}$. Overall, there was little influence on the WecP isoprenoid utilization by altering the tag or changing the length of the isoprenoid substrate.

Table 2.1 WecP Kinetics with UDP-GalNAc

	fl-BP			UDP-GalNAc		
Isoprenoid	k_{cat} ($s^{-1}\cdot10^{-2}$)	K_m (μM)	k_{cat}/K_m ($M^{-1}\cdot s^{-1}\cdot10^{3}$)	k_{cat} ($s^{-1}\cdot10^{-2}$)	K_m (μM)	k_{cat}/K_m ($M^{-1}\cdot s^{-1}$)
2CN-B(*4Z*)P	1.49 ± 0.23	3.0 ± 1.2	4.9 ± 2.0	1.13 ± 0.05	520 ± 89	21.7 ± 3.8
2CN-B(*7Z*)P	1.77 ± 0.24	3.5 ± 1.3	5.1 ± 2.1	1.00 ± 0.09	166 ± 54	60.4 ± 20.4
NBD-B(*5Z*)P	0.55 ± 0.08	1.3 ± 0.5	4.2 ± 1.7	1.03 ± 0.07	293 ± 60	35.2 ± 7.6
NBD-B(*7Z*)P	1.00 ± 0.18	2.9 ± 1.1	3.5 ± 1.5	0.97 ± 0.05	152 ± 31	63.7 ± 13.5

Reaction mixtures were prepared with 200 mM Bicine pH = 8.5, 20 mM $MgCl_2$, 4 mM KCl, 0.019% *n*-dodecyl-β-D-maltoside (DDM 2.4 x CMC) and 10-30 nM WecP. When held constant BP concentration was 2.5 μM and UDP-GalNAc was 225 μM. All parameters are apparent steady-state kinetic values from a non-linear fit to the Michaelis-Menten equation with a minimum of three repeats of six concentrations.

Chain length, but not tag identity influences UDP-GalNAc utilization by WecP

Since there was little change in the utilization of isoprenoids by WecP, we next tested whether UDP-GalNAc activity was altered by changing the acceptor isoprenoid substrate. To do this, the isoprenoid concentration was held at 2.5 μM and UDP-GalNAc concentration was varied. The $^{app}k_{cat}$ of these reactions was unaffected by the isoprenoid chain length or fluorophore. However, the isoprenoid structure did have a major impact on the UDP-GalNAc $^{app}K_m^{GalNAc}$. With both the 2CN-B(*7Z*)P and NBD-B(*7Z*)P, the $^{app}K_m^{GalNAc}$ was similar at 166 and 152 μM, respectively. However, when the 2CN-BP was changed to the four *Z*-configuration isoprene the $^{app}K_m^{GalNAc}$ increased over three-fold. When the NBD-BP isoprenoid was changed to the five *Z*-configuration isoprene analogue the $^{app}K_m^{GalNAc}$ increased nearly two-fold. This data suggests that the length of the isoprene has an important influence on the interaction of the UDP-GalNAc with the enzyme.

UDP-GlcNAc is nearly 50-fold less effective as a substrate with WecP

Our data suggested that UDP-GlcNAc could also be a substrate for WecP although the product formed in our assay was considerably lower than with UDP-GalNAc. We next quantified the effectiveness of UDP-GlcNAc as a substrate by testing 2.5 µM 2CN-B(*7Z*)P with varying concentrations of the sugar donor (**Table 2.2**). Surprisingly, the $^{app}K_m^{GlcNAc}$ was only two-fold higher than that of UDP-GalNAc. However, the $^{app}k_{cat}$ was 24-fold lower with UDP-GlcNAc as the donor substrate. These data suggested that the lack of activity with UDP-GlcNAc was more influenced by defective catalysis rather than simply a decrease in the ability of the nucleotide-linked sugar to interact with the protein.

Table 2.2 WecP Kinetics with UDP-GlcNAc

k_{cat} ($s^{-1}\cdot10^{-2}$)	K_m (µM)	k_{cat}/K_m ($M^{-1}\cdot s^{-1}$)
0.041 ± 0.004	330 ± 140	1.25 ± 0.54

Reaction mixtures were prepared and kinetics analyzed as in Table 1 with 30-90 nM WecP, and 2.5 µM 2CN-B(*7Z*)P with varying UDP-GlcNAc.

Endogenous E. coli transferases are active with fl-BPs

Because both the NBD and 2CN BP analogues were accepted as substrates by WecP, we next chose to test whether or not these analogues could serve as substrates for other important model PGTs. WecA is a well-established membrane localized protein known to transfer GlcNAc-P to BP. This protein originating from *E. coli* has not previously been purified to homogeneity, and all attempts herein did not yield purified protein.[44, 69] Because WecA is native to *E. coli*, we first tested whether native cef from C43 *E. coli* strains, commonly used for protein overexpression, could serve as a functional source of the protein. When cef was incubated with 1 mM UDP-GlcNAc and either 2CN- or NBD-B(*4Z*)P, partial consumption of the fl-BPs was observed at a retention time and mass consistent with fl-BPP-GlcNAc formation (Figure A10**)**. Alternatively, a pET-24a

construct with the *wecA* gene inserted (p*wecA*) was commercially prepared and transformed into C43 protein expression cells. The cef of these cells containing overexpressed recombinant WecA protein (Figure A4**)** was also able to convert fl-BPs with far lower concentrations of UDP-GlcNAc (**Figure 2.5**).

We next wanted to ensure that endogenous WecA was indeed responsible for the transfer of GlcNAc-P to the fl-BPs and also avoid this background activity in subsequent cef preparations. We attempted two routes to inhibit endogenous WecA transferase activity and to identify it as the protein responsible for fl-BPP-GlcNAc formation. First, we prepared a Δ*wecA* mutant in the C43 background strain. Neither the 2CN nor NBD BP analogues led to the formation of the presumed fl-BPP-GlcNAc when the *wecA* gene was removed. However, transferase activity was restored through complementation with p*wecA* overexpressing the *wecA* gene (**Figure 2.5**). The second route we chose to verify endogenous WecA transferase activity was to supplement reactions with an inhibitory concentration of tunicamycin, the well-known inhibitor of WecA.[70] Background WecA activity was abolished under these conditions. Reactions containing cef led to the formation of a new, unanticipated fluorescent material (•) at a retention time of 6.2 and 6.4 min for 2CN and NBD BP, respectively, and the peaks were most prominent when WecA activity was ablated. This unidentified product formed with cef controls, and would form even when sugar was not added to the reaction mixture.

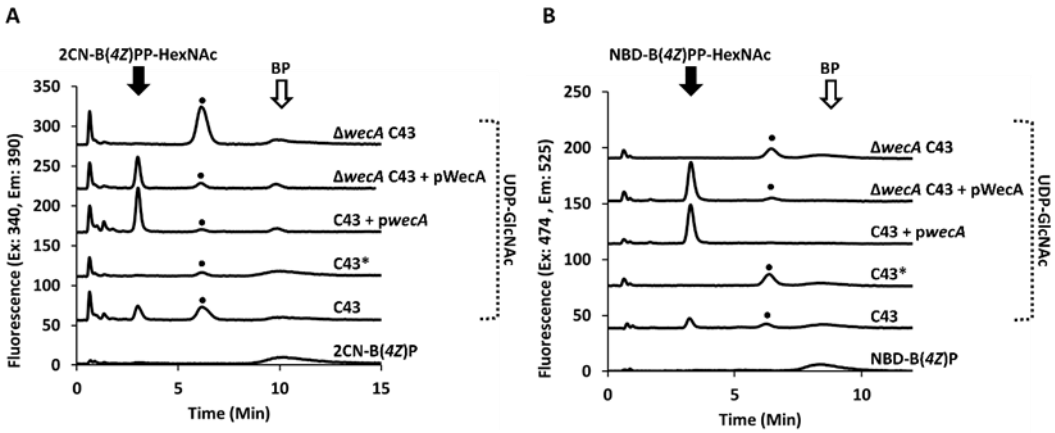

Figure 2.5 WecA UDP-GlcNAc transferase activity with fl-BPs.
Cef from indicated strains was incubated with either 2CN (A) or NBD-B(*4Z*)P (B) and UDP-GlcNAc as the donor sugar. The cef C43 forms fl-BPP-HexNAc at a retention time of 3.0 and 3.4 for 2CN and NBD, respectively, when co-incubated with UDP-GlcNAc. Adding 1 µg/mL of tunicamycin, designated by (*), eliminates transferase activity. An additional fluorescence peak (•) is observed at 6.2 and 6.4 min for 2CN and NBD respectively. A co-eluting contaminate is present in the 2CN-B(*4Z*)P standard, which appears at 10 min only after BP consumption.

Phosphohexosetransferases utilize fl-BP substrates

The above data clearly demonstrated that the phospho-HexNAc transferases WecA and WecP could utilize both the 2CN and NBD fl-BP analogues as substrates. We were next interested in testing whether or not two model phosphohexosetransferases could also utilize fluorescently tagged BP probes. Previous work from our group has shown that the *S. pneumoniae* protein CPS2E will catalyze the transfer of a Glc-P from UDP-Glc to a 2CN fl-BP analogue.[26] WbaP from *S. enterica* is known to transfer Gal-P to BP, but has not yet been assessed with a fl-BP.[37] Both phosphohexosetransferases were prepared as cefs from plasmid constructs similar to those for WecP and WecA, and their presence was verified by SDS-PAGE and western blot (Figure A4**)**. We next tested these cef preparations with the two fl-BP probes. The fl-BPP-Hexoses eluted at a similar retention time as fl-BPP-HexNAc under our HPLC conditions. 2CN-B(*4Z*)P was an effective substrate for both phosphohexosetransferases and their respective glycan donors **(Figure 2.6**). Surprisingly, NBD was only an effective substrate for CPS2E, and not WbaP. Previous work with WbaP suggested that isoprenoid chain length may influence the ability of the protein to utilize shorter substrates.[49] However, utilizing a longer NBD-B(*7Z*)P also did not produce a

corresponding product (Figure A11**)**. This data suggests that the NBD fluorophore itself, and not chain length, influences catalytic activity for WbaP. The fact that NBD-BPs were ineffective substrates for WbaP was unexpected considering their effectiveness with all other PGTs tested in this work.

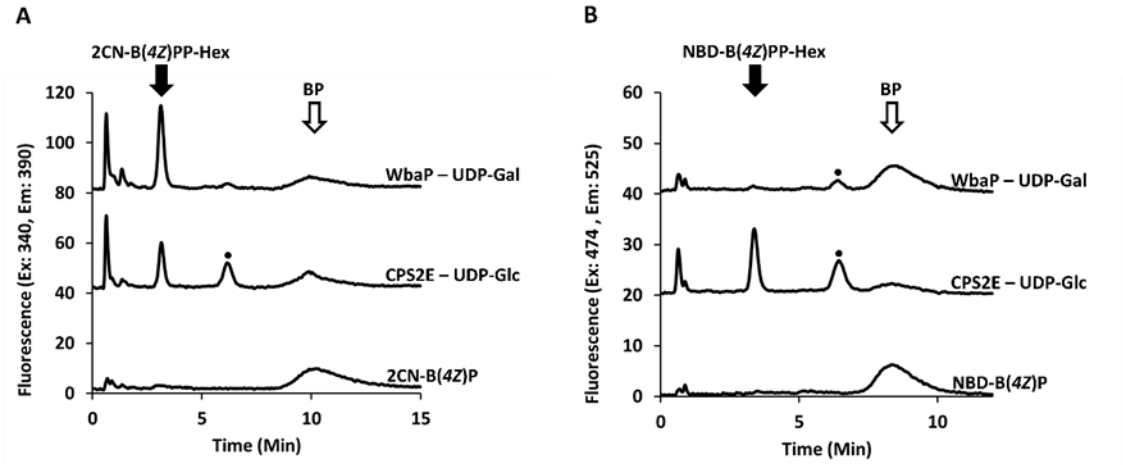

Figure 2.6 Phosphohexosetransferase activity with fl-BPs.
Formation of fl-BPP-Hexose appears at a retention time of 3.0 and 3.4 for 2CN (A) and NBD (B), respectively, when co-incubated with their respective UPD-linked sugar donor. NBD-B(*4Z*)P does not appear to be a substrate for WbaP. An additional fluorescence peak (•) is observed at 6.2 and 6.4 min for 2CN and NBD respectively.

WbaP activity with NBD-BP is recovered when surfactant is replaced with n-propanol

While surfactants are commonly employed in PGT reactions, previous work has shown that organic alcohols are needed in addition to prevent aggregation of isoprenoids.[71] We found that the surfactant could be replaced entirely with the addition of fl-BPs solubilized in *n*-propanol, amounting to 5% *n*-propanol in the total final reaction volume (**Figure 2.7**). Notably, WbaP activity was recovered with NBD-B(*4Z*)P under these conditions, demonstrating that all model PGTs were in fact functionally compatible with both fl-BPs. In the presence of *n*-propanol WecA activity was completely suppressed, as was the formation of the unidentified material. For all PGTs , there was a limit to how much *n*-propanol could be added (≥15%) before enzymatic activity was quenched, presumably due to protein denaturation. When reactions were supplemented with 5% *n*-propanol after the fl-BP had already been added in DMSO, the turnover was markedly decreased

(Figure A12**)**. This suggests that the effect organic alcohol has is limited to the initial solution of BP. Perhaps, the way BPs are introduced to solvent conditions changes their availability to enzymes in reaction conditions.

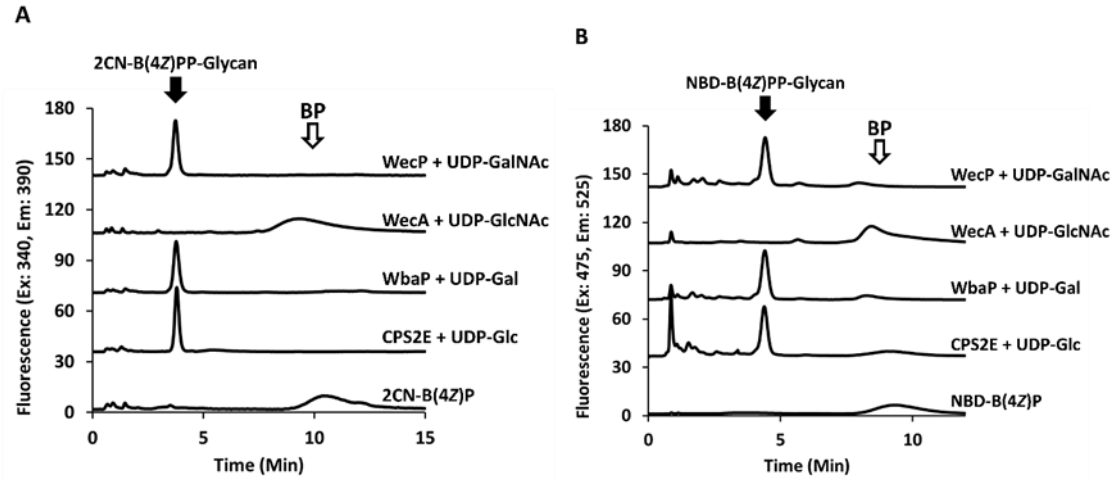

Figure 2.7 PGT activity with fl-BPs in the presence of 5% n-propanol.
Formation of fl-BPP-glycans appears at a retention time of 3.8 and 4.7 for 2CN (A) and NBD (B), respectively, when co-incubated with their respective UDP-linked sugar donor. WecA transferase activity is, however, not observed under these conditions. NBD-B(*4Z*)P is a substrate for WbaP only when cholate is replaced with 5% *n*-propanol.

Polyisoprenoids have also been proposed to take on organized micellar structures *in vitro*.[68] The role of organic alcohol addition to the isoprenoid reactions to prevent aggregation is corroborated by previous work describing acid phosphatase activity on polyisoprenoids.[68] Likewise, the supplementation of either 15% methanol and/or surfactants have been essential for enzymatic turnover for full length BP.[48, 49, 70, 71] Notably, when crude endogenous BP is used instead, *in vitro* reactions do not necessitate the use of surfactants or organic alcohols.[37, 38, 64, 69] It has also been recently suggested that the unique geometry of BP may aid in binding to PGTs and may also facilitate interactions at the membrane interface.[72] It is possible that lipophilic polyisoprenoids, when added with surfactants or organic alcohols, do not necessarily share these same properties as an artifact of exogenous supplementation.

An interesting consideration arises in the fact that the NBD fluorophore is more

hydrophilic, and presumably more amenable to aqueous conditions, than the 2CN tag or the native isoprene. Thus solubility alone cannot explain WbaP inactivity with surfactants. Phospholipids bearing an NBD tag on the acyl chain are thought to "loop-back" to the polar headgroup.[73, 74] The unique hydrophilicity of NBD could lead to changes in the ability of the PGT enzymes to interact with the isoprenoid, particularly if a severe alteration in the micelle structure is induced by the potentially bolaamphiphilic isoprenoid. Perhaps it is the addition of *n*-propanol that changes the orientation of NBD-B(*4Z*)P in solution, which then makes the phosphate more available for catalysis. This is supported by the fact that co-solubilization of the fl-BP and *n*-propanol simultaneously is required for efficient catalysis.

WecA fails to exhibit activity with any quantity of organic alcohol (**Figure 2.7**). One trivial explanation for this difference is that WecA may exhibit poor tolerance of organic solvents, likely due to protein denaturation. In addition, all other PGTs used here exhibit distinctly similar topology whether predicted or experimentally determined, except for WecA which is predicted to have 11 transmembrane domains. It is not yet clear based on these results if a change in BP orientation or WecA conformation has a larger influence on the lack of activity. These findings highlight the trade-off between the positive influence of solubilizing fl-BP and the protein denaturation effect of *n*-propanol. Likewise, we naturally questioned whether these alcohols could replace the need for a surfactant in UppS reactions, but no observable activity was detected at any concentration in these organic alcohols (data not shown).

Alternative glycan donor specificity with phosphoglycosyltransferases

Because our fluorescent probes provide a unique opportunity to assess transferase promiscuity, we next performed glycan specificity analysis with the three PGTs (CPS2E, WbaP, WecA) with all four donor substrates (UDP-Glc, -Gal, -GalNAc, or -GlcNAc) in the presence of

surfactant (Figure A13 and Figure A 14). Additional transferase promiscuity was observed only for WbaP with UDP-Glc as the donor sugar (**Figure 2.8**). Similarly, when cholate was replaced with *n*-propanol, WbaP NBD-B(*4Z*)P was also active with UDP-Glc (**Figure 2.8**). Predictive topology suggests a similar structure of WbaP to WcaJ, a Glc-P transferase.[75] However, complementation with *wbaP* in a Δ*wcaJ* mutant was unable to restore the mucoid phenotype expected to result from production of the exopolysaccharide colanic acid. This may be indicative of poor substrate utilization of UDP-Glc by WbaP *in vivo*.

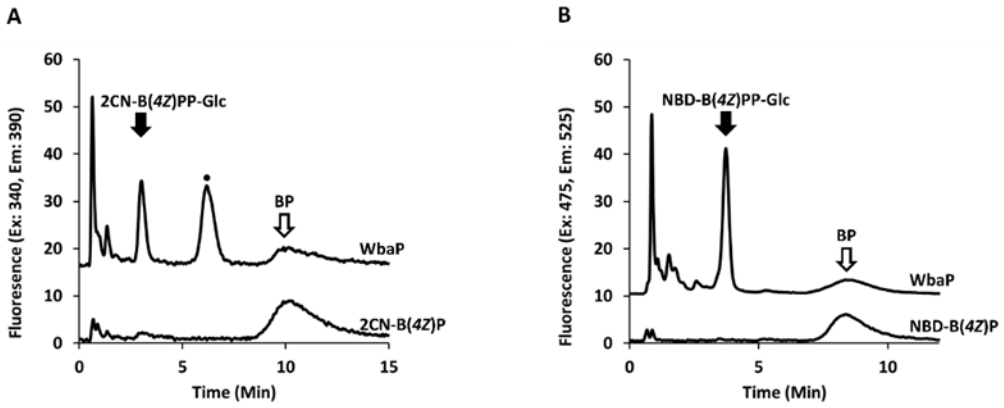

Figure 2.8 WbaP catalyzes the transfer of UDP-Glc to fl-BPs.
Promiscuous transferase activity is demonstrated with cholate and 2CN (A) or 5% *n*-propanol supplementation and NBD (B). Fl-BPP-Glc is observed at 3.0 and 3.7 min for 2CN and NBD, respectively. A prominent unanticipated fluorescence peak (•) is observed at 6.3 min for 2CN only.

All cef displayed UDP-GlcNAc transferase activity was inhibited by tunicamycin suggesting that this activity was due to native WecA. To ensure that background WecA activity (and not enzymatic promiscuity for UDP-GlcNAc) was responsible for this, PGTs were incubated in the same concentration of tunicamycin with their respective sugar. Expectedly, enzyme function was still observed for all PGTs, except for WecA (**Figure 2.9**). Despite also demonstrating additional activity towards UDP-GlcNAc, WecP was not inhibited by tunicamycin. The topology of WecP is reported to be more similar to WbaP than with the HexNAc transferase WecA. In fact, WecA topology is strikingly different from CPS2E, WbaP, or WecP. Members of the HexNAc-

phosphate transferase family that utilize UDP-GlcNAc as a donor sugar are expected to demonstrate potent inhibition by tunicamycin, a transition state analogue containing GlcNAc and isoprenoid character. Under reaction conditions used here, WecP was still able to catalyze fl-BPP-GlcNAc transfer, suggesting that efficient inhibition is affected by the stereochemistry of the inhibitor sugar moiety.

Figure 2.9 PGT transferase activity in the presence of tunicamycin
2CN-B(4Z)P is used here in the presence of cholate only, as WecA activity is not observed with *n*-propanol. Fl-BPP-glycan products are seen at a retention time of 3.0.

Conclusion

In vitro characterization of bacterial glycopolymers depends on the presence of an isoprenoid carrier. The full length, $C_{55,}$ lipid carrier with correct stereochemistry is sparse on the

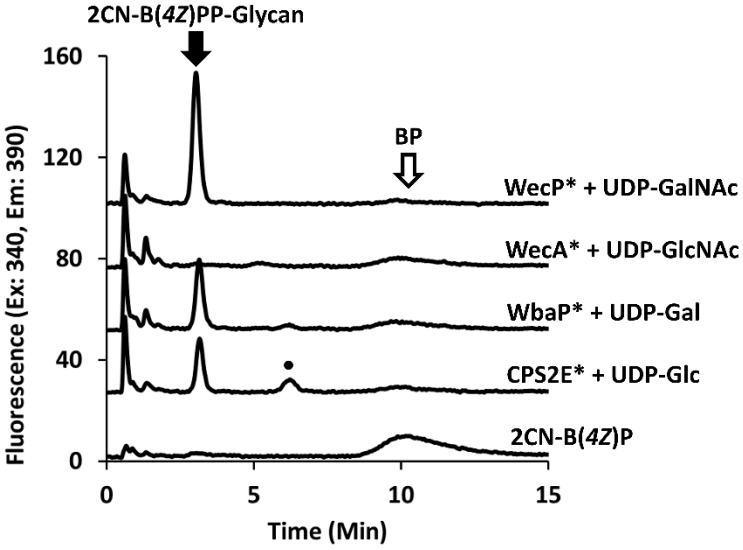

commercial market. Other polyisoprenoids that are more accessible are often derived from plant sources, and may not represent the isomer configuration most tolerable to individual bacterial enzymes.[71] Recently it was demonstrated that isoprenoid geometry was critical for binding of PglC, a PGT from *Campylobacter jejuni*, to BP. [72] Alternative to commercial sources, BP has been obtained either through crude isolation from bacterial cell membranes, by chemical synthesis of full or partial length polyisoprenoids, or through shortened isoprenoids which are commercially

available but are not necessarily the preferred double bond configuration.[36-38, 76, 77] Owing to the importance of BP as a carrier lipid, and the biological importance of glycosyltransferases, it is reasonable for native transferases to be present in the cef background of protein expression cell lines. Endogenous WecA activity appears to be one such transferase exerting activity in the background of our specificity analysis. Therefore, it is reasonable to hypothesize that other such endogenous transferases native to *E. coli* could explain the unanticipated peak present in our cef reactions. Further, this peak is completely absent in the case of our standards and solubilized WecP reactions. This unanticipated material formed with a great deal of variability only when cef was added to the reaction, and was most prominent in the absence of fl-BPP-GlcNAc formation by WecA. The new peak was not dependent on exogenous UDP-Glc, -Gal, -GalNAc, or -GlcNAc suggesting that none of these sugar donors were substrates for proteins co-isolated in the cef (Figure A13 and Figure A 14). This suggests that the transferase substrate (possibly a sugar) is also native to the membrane. We are curious to explore such types of proteins, and where they might obtain their sugar source in the absence of exogenous substrate. The identity of this new product is the subject of upcoming work from our laboratory.

Experimental Procedures

General.

All reagents were ACS grade or higher and purchased from Sigma-Aldrich, VWR, or Fisher Scientific unless otherwise stated. TLC was performed on fluorescent plates and *p*-anisaldehyde stain was used for detection. Preparation of NBD-GPP has been adapted from the literature with some modifications.[65, 78, 79] Preparation of IPP and tris(tetra n-butyl ammonium) diphosphate (TTNBA-PP) have been previously reported.[80] Characterization of all compounds were carried out on 500 MHz Jeol for ^{1}H and ^{13}C NMR for intermediates, and ^{1}H and ^{31}P for final products (NBD-

GPP, IPP, and TTNBA-PP) in Figure A 15. Sequences in the Appendix A were used to generate recombinant proteins in the vector backbone of pET24a (Genscript). Overexpression of proteins was conducted in *E. coli* strains C41 (UppS) or C43 (WbaP, WecA, and WecP). UppS and WecP were used as soluble proteins, where as WecA and WecP were used as cef. CPS2E, also prepared as cef from BL21-AI, was provided by the Yother lab and has been previously reported in the literature.[63] Induction times and temperatures, as well as detailed purification conditions can be found in the SI. All HPLC analysis was performed using a reverse phase Agilent Eclipse XDB-C18, 3.5 µM 4.6 x 50 mm column on an Agilent 1100 HPLC system, unless noted otherwise. All LCMS analysis was performed using a Waters Xbridge Peptide BEH C18 3.5 uM, 4.6 x 50 mm column on an Agilent 1260 Single Quadrupole with a TEE connector splitting the column eluant between the MSD and FLD. All LC solvent conditions are as specified below.

Two-step fl-BP Preparation with Potato Acid Phosphatase

Preparation of fl-BPP was carried out in a total volume of 10 mL in a conical tube. Reaction mixtures contained: 10 mM fl-GPP (2CN or NBD), 60 mM IPP, 50 mM bicine (pH 8.5), 5 mM KCl, 0.5 mM $MgCl_2$, 2.4% octyl thioglucoside (OTG), and 100 µM UppS. Using this quantity of enzyme was critical to the success of this preparatory scale reaction. After incubating at 37 °C for 1 h, the reactions were evaluated by HPLC. More IPP was added to encourage a desired product length (4-6 *Z* additions), such that an additional 10 and 40 mM of IPP was added to the 2CN and NBD reactions, respectively. Reactions were quenched with the addition of 1 mL *n*-butanol with vortexing, followed by a brief centrifugation at 2,500 relative centrifugal force (RCF) for 2 min. The upper layer containing *n*-butanol and fl-BPP (approx. 100 mM) was then separated and either stored at -20 °C for several weeks, used immediately, or lyophilized. To prepare large scale fl-BPs, mixed fl-BPPs in *n*-butanol (5% n-butanol carry over) were added to 20% of *n*-propanol, 0.1% Triton-X100, and 50 mM sodium acetate buffer (pH 4.5) and then were generously vortexed

and sonicated to promote complete solubilization. Finally, 20 μg/mL of potato acid phosphatase was added and the reaction was allowed to incubate at 37 °C overnight. Suspensions of 2 mg/mL potato acid phosphatase (3.2 M ammonium sulfate pH 5.0 in 20% glycerol) were used here and could be stored at -80 °C for several weeks. HPLC analysis was used to ensure complete hydrolysis, since downstream purification would result in fl-BP/BPP mixtures.

Purification of fl-BP was performed on an Eclipse XDB-C18 (9.4 x 250 mm, 5 μm) column with a stepping gradient. For 2CN (4-7 *Z*) the column was first equilibrated to 55:45 *n*-propanol:100 mM ammonium bicarbonate, and then *n*-propanol was incrementally stepped up after the elution of each size fl-BP (55% 0-15 min, 60% 15-25 min, 75% 25-35 min). For NBD (3-7 *Z*) the column was first equilibrated to 40:60 *n*-propanol:100 mM ammonium bicarbonate and then *n*-propanol was incrementally stepped up after the elution of each size fl-BP (40% 0-20 min, 45% 20-30 min, 50% 30-40 min, 65% 40-50 min). A 10 min rinse at 95% *n*-propanol was used in both methods to elute any remaining fl-bactoprenol formed using acid phosphatase (typically <5% of the product). Fractions were lyophilized, and the purified fl-BP's were then resuspended in a single phase mixture of Hexanes:Acetone:DMSO (10:10:0.5) which permitted rapid and efficient solubilization of fl-BPs from glass tubes. This solution of fl-BPs was transferred to a clear non-binding tube (2CN) or amber tubes (NBD) and the volatile solvents were removed under a gentle stream of air resulting in DMSO solubilized fl-BP. The concentrations were determined spectrophotometrically (2CN ε_{DMSO} = 2,400 $M^{-1}cm^{-1}$ and NBD ε_{DMSO} = 20,885 $M^{-1}cm^{-1}$) and could be stored at -20 °C for several months. Both HPLC and LCMS were used to characterize the length of purified fl-BP material.

Plate Reader Assay

Kinetic reads were performed on a Molecular Devices M5 plate reader with SoftMaxPro software. Representative enzyme reactions occurred in 96-well opaque plate, with two fluorescent reads (excitation/emission 340/390 and 475/525) occurring simultaneously. Fluorescence was taken in 30 s intervals over 60 min. Pre-mixed reactions contained 25 mM bicine (pH 8.5), 0.1% DDM, 5 mM KCl, 0.5 mM MgCl, 10 μM fl-FPP, and 100 nM UppS from either *S. aureus* or *B. fragilis*. This reaction premix was allowed to incubate at 37 °C for 5 min to equilibrate the temperature. In a separate, but adjacent, well IPP was also allowed to prewarm. After the 5 min incubation period, a multichannel pipettor was used to transfer the IPP (or water for the control) to the premixed reactions so that the final concentration of IPP was 1 mM.

WecP Kinetic Assays

WecP reactions mixtures were prepared in 200 mM Bicine pH = 8.5, 20 mM $MgCl_2$, 4 mM KCl, 0.019% *n*-dodecyl-β-D-maltoside and 10-30 nM WecP. When held constant fl-BP concentration was 2.5 μM and UDP-GalNAc was 225 μM. When UDP-GlcNAc was used as the sugar donor 30-90 nM WecP was used. Each reaction was sampled by HPLC through multiple injections over a period of two hours, where product was still being produced linearly with respect to time. Reaction yield at each time point was determined by peak integrals of product and substrate. The fluorescence integral of the substrate and product did account for 100% of signal with no appreciable changes after transfer of the phosphor-sugar. Rates were calculated based on the input fl-BP substrate and product formed over time. Rates were fit to the Michaelis-Menten equation $v/Et=k_{cat}^{app}[S]/(K_m^{app}+[S])$ where v/Et was the reaction rate per total enzyme and S was the concentration of the varied substrate.

PGT Glycan Specificity Reactions

Standard reactions were carried out in a total volume of 40 µL in the presence of 1 µM fl-BP, 100 µM UDP-sugar, and 0.10 mg/mL total protein cef. For CPS2E, WbaP, WecA, and WecP reactions buffers consisted of 200 mM bicine pH 8.5, 5 mM $MgCl_2$, 100 mM KCl, and 15 mM cholate. Alternatively, 5% *n*-propanol was used in place of cholate as a component of the fl-BP solvent. All reactions were allowed to sit at 37 °C for 2 h and then were quenched with an equal volume of *n*-propanol.

Expression and Purification of UppS

A 5 ml starter culture was prepared overnight. Terrific broth, 1 L, (yeast extract 24 g/L, tryptone 20 g/L, glycerol 4 mL/L, and 90 mM phosphate buffer pH 7.4) supplemented with 1% glucose was inoculated with 1 mL of the overnight culture with 50 µg/mL kanamycin. The culture was then incubated at 37 °C with shaking until an OD_{600} of 0.6 was reached. Overexpression was induced with the addition of 1 mM of IPTG to each culture for 4-6 hours at 30 °C. Cultures were then centrifuged at 10,000 g for 5 min, and cell pellets were suspended in 40 mL of lysis buffer containing 50 mM Tris-HCl pH 8.0, 200 mM NaCl, and 20 mM imidazole. Cells were then lysed via sonication at 25% power for 3 min with a pulse of 1 s on and 2 s off. The resulting lysate was centrifuged under vacuum at 91,635 RCF for 60 min at 4 °C. The supernatant was then added to a column containing 2.0 mL of packed nickel-nitrolotriacetic acid resin (Ni-NTA, PerfectoPro, 5 Prime Inc.) and the lysate was passed through twice. The column was then washed with 20 mL of wash buffer (50 mM Tris-HCl pH 8.0, 200 mM NaCl, and 50 mM imidazole). The protein was then eluted in six half-column volume fractions (1 mL) with elution buffer (100 mM Bicine pH 8.0, 200 mM NaCl, 50 mM KCl, 5 mM $MgCl_2$, and 500 mM imidazole). SDS-PAGE analysis was performed on all fractions (lysate, flow through, wash, and elutions) to determine which fractions contained protein. Elutions containing protein were pooled together and dialyzed thrice in 1 L

dialysis buffer (100 mM Bicine pH 8.0, 200 mM NaCl, 50 mM KCl, 5 mM $MgCl_2$) at 4 °C with at least 4 h intervals in between buffer changes. The final concentrations, typically in excess of 500 uM, were calculated spectrophotometrically with an extinction coefficient of ε_{UppSSa} = 36,900 $M^{-1}cm^{-1}$.

Expression, purification, and solubilization of WecP

Bacterial cultures baring p*wecP* were prepared as described above and incubated at 37 °C with shaking until an OD_{600} of 1.0 was reached. Overexpression was induced with the addition of 1 mM of IPTG to each culture for 3 hours, maintaining the temperature at 37 °C. Cultures were then centrifuged at 10,000 g for 5 min, and cell pellets were suspended in 20 mL of buffer containing 50 mM Tris-HCl pH 8.0 and 200 mM NaCl. Cells were then lysed via sonication at 25% power for 3 min with a pulse of 1 s on and 2 s off. The resulting lysate was then briefly centrifuged at 2,500 g for 10 min to remove unlysed cell debris. The supernatant, containing soluble and membrane proteins, was further centrifuged under vacuum at 91,635 RCF for 60 min at 4 °C. The cell envelope fraction was homogenized in 20 mL lysis buffer (50 mM Tris-HCl pH 8.0, 200 mM NaCl, 20 mM imidazole, and 1% Triton-X100) supplemented with 1% Triton-X100. The suspension was then agitated for 4 h at 4 °C. Then, 0.5 mL of nickel-nitrolotriacetic acid resin (Ni-NTA, PerfectoPro, 5 Prime Inc.) was added and the homogenate was agitated 4 h to overnight while at 4 °C. The flow-through was eluted and the column was washed with 12 mL of wash buffer (50 mM Tris-HCl pH 8.0, 200 mM NaCl, 50 mM imidazole, and 1% Triton-X100). Solubilized WecP was eluted from the column in six half-column volume fractions (250 μL) with elution buffer (50 mM Tris-HCl pH 8.0, 200 mM NaCl, 500 mM imidazole, and 1% Triton-X100). SDS-PAGE analysis was performed on all fractions (lysate, flow through, wash, and elution's) to determine which fractions contained protein. Elutions that contained protein were pooled together and dialyzed thrice in dialysis buffer (50 mM Tris-HCl pH 8.0, 300 mM NaCl) at 4 °C with at least

4 h intervals between buffer changes. A Bradford assay was used to determine the final total protein content of solubilized WecP, due to possible absorption from Triton-X100.

Expression and cef preparation of CPS2E, WbaP, and WecA

The overexpression of membrane bound proteins was identical to that of WecP, except 250 mL of TB was used. Induction occurred after an OD of 1.0 was reached by the addition of 1 mM IPTG (or 0.2% Arabinose for CPS2E). Cells were induced for 3 h for WbaP and WecA, or 0.5 h for CPS2E (as previously reported). Following induction and culture centrifugation, the cell pellet was suspended in lysis buffer containing 50 mM Tris-HCl pH 8.0, and 200 mM NaCl. Cells were then lysed and centrifuged as described above. The cell envelope fraction was homogenized in 1 mL of the above buffer and was used directly in activity assays. A Bradford assay was used to determine the final total protein content of cef.

ΔWecA C43 Deletion Mutant

E. coli MG1655 was transformed with pKD46 and plated on LB + 100 µg/mL ampicillin to select for successful transformants. After a 24 h transformation incubation, 6 colonies from the selection plate were inoculated into 5 mL LB, 100 µg/mL ampicillin, and 0.2% glucose (to repress the arabinose-inducible promoter on pKD46). This culture was grown with shaking at 30 °C overnight, then diluted 1:100 into LB with 100 µg/mL ampicillin and grown shaking at 30 °C. After 2.5 h, 10 mM arabinose was added to induce expression of the *γ*, *β*, and *exo* genes on pKD46. This induction proceeded for 1 hr, then the culture was centrifuged, then the pellet was washed twice in 0.3 M sucrose, and finally resuspended in 0.3 M sucrose at 1/50 the original culture volume. These induced, electrocompetent cells were stored at -80 °C until use.

Primers were designed to amplify the FRT-flanked neo^R gene (conferring kanamycin resistance, from the pRED/ET kit, Gene Bridges) and also append 50 base pairs homologous to

the genome sequence flanking the *wecA* gene in *E. coli*. Gel electrophoresis confirmed a PCR amplicon of 1,737 base pairs. Next, 2 µg of this amplicon was combined with 50 µL of the previously prepared electrocompetent MG1655 pKD46 cell preparation and electroporated at 2,500 V. SOC media (1 mL) was added immediately following electroporation and cells were recovered at 37 °C for 2.5 h. This reaction was plated on LB with 50 µg/mL kanamycin, and incubated at 37 °C overnight. The following day, colonies that grew on this selective media were restreaked on LB with 50 µg/mL kanamycin to purify, then PCR was used to confirm the correct insertion using the primers WecA_pRED_Fwd and WecA_ck_Rev (**Table A1**), which produced a 1,858 base pair product by gel electrophoresis, indicating insertion of the amplicon in place of the native *wecA* gene. This mutation was then moved into a C43 background by P1 transduction, and propagated in LB/Kan to select for Δ*wecA*.

Preparation of 2-[[(2E)-3,7-dimethyl-2,6-octadienyl]oxy]tetrahydropyran (HO-G-THP)

To a round bottom flask, 1 equivalent of geraniol, 1.5 equivalents of 3,4-dihydropyrane and 0.1 equivalents of PPTS was added in dichloromethane at room temperature for 12 h. The solvent was then removed and the crude reaction was placed in a separatory funnel and extracted with diethyl ether and brine. The organic layer was collected and dried with sodium sulfate for 1 h resulting in quantitative yield of G-THP. The crude product was analyzed by TLC in hexanes/ethyl acetate (3:1) and visualized with p-anisaldehyde (R_f = 0.78).

Preparation of (2E,6E)-2,6-Dimethyl-8-[(tetrahydro-2H-pyran-2-yl)oxy]-2,6-octadien-1-ol (HO-G-THP)

Into a round bottom was added 4 equivalents of tert-butyl hydroperoxide 70% (v/v), 0.1 equivalent of salicylic acid, and 0.1 equivalent of selenium dioxide at room temperature until homogenous. The solution was cooled to 0 °C, after which 1 equivalent of G-THP was added. The

reaction was allowed to sit for 36 h after which time the solvent was removed. The resulting oil was then placed into a separatory funnel with ethyl ether and washed with 5% (w/v) sodium bicarbonate, saturated copper sulfate, saturated thiosulfate (X2), water, and then brine. The organic layer was then collected and dried with sodium sulfate for 1 h. The crude reaction was analyzed by TLC in hexanes/ethyl acetate (7:3; R_f = 0.24). The crude reaction was purified by flash chromatography over silica gel with from hexanes until remaining G-THP was eluted. Then hexanes/ethyl acetate (4.5:1) was used to elute the aldehyde product. Lastly, the desired alcohol product (HO-G-THP) was eluted with hexanes/ethyl acetate (7:3) with typical yields of 20-30 %.

Preparation of 2-[(2E,6E)-2,6-Dimethyl-8-[(tetrahydro-2H-pyran-2-yl)oxy]-2,6-octadien-1-yl]-1H-isoindole-1,3(2H)-dione (Pt-G-THP)

Into a round bottom flask 1 equivalent of phthalimide, 1 equivalent of triphenylphosphine (recrystallized from hot ethanol) and 1 equivalent of HO-G-THP was added with diethyl ether. The slurry was cooled in a salted ice bath. One equivalent of diethyl azodicarboxylate (DEAD, 40 % in toluene) was added dropwise and the reaction was left to warm to room temperature for 12 h after which time the solvent was removed. The solids were removed by filtration, and the solvent removed. Product formation, Pt-G-THP, was monitored by TLC in hexanes/ethyl acetate (3:1; R_f = 0.46, 60% yield) and purified with hexane/ethyl acetate (6:1).

Preparation of (2E,6E)-2,6-Dimethyl-8-[(tetrahydro-2H-pyran-2-yl)oxy]-2,6-octadien-1-amine (NH_2-G-THP)

Into a round bottom flask, 1 equivalent of Pt-G-THP, 6 equivalents of hydrazine monohydrate and dry ethanol (0.04 mmol mL^{-1}) was added and left at room temperature for 12 h. The solution was filtered and the solvent removed after this time. The reaction was purified and analyzed by TLC with a mixture of chloroform:methanol:ammonium hydroxide (100:10:1, 42%

yield). TLC plates were pre-treated in this mixture by allowing them to saturate in the TLC chamber and then dry completely prior to use.

Preparation of 7-nitrobenzo(1,2,5)oxadiazol-4-yl-1-(2,6-dimethyl-8-(tetrahydro-pyrane-2-yloxy)- 2,6-octadien-1-amine (NBD-G-THP)

To a round bottom flask containing acetonitrile/25 mM sodium bicarbonate buffer (1:1), 1 equivalent of H_2N-G-THP was added. A solution of 1.5 equivalents of NBD-Cl in acetonitrile was added dropwise. The mixture was stirred for 1 h at room temperature and a second solution of 1.5 equivalents of NBD-Cl in acetonitrile was added dropwise for 1 h. The solution was then poured into a separatory funnel and extracted with methylene chloride and washed with brine solution. The organic layer was collected and then dried with sodium sulfate for 1 h and then the solvent was removed. The reaction was monitored and purified with methylene chloride with theoretical yield (R_f = 0.18, 84% yield).

Preparation of 3,7,-dimethyl-8-(7-nitro-benzo[1,2,5]oxadiazo-4-ylamino)-octa-2,6-dien-1-ol (NBD-GOH)

To a round bottom flask, 1 equivalent of NBD-G-THP was dissolved in ethanol. The reaction was heated to 60 °C for 3 h. The reaction was transferred to a separatory funnel and extracted with diethyl ether and washed with brine solution. The organic layer was collected and dried with sodium sulfate and filtered. The solvent was removed and purified with cyclohexane/ethyl acetate (1.5:1) and the reaction was monitored with hexanes/ethyl acetate (1.5:1; R_f = 0.1, 98-100% yield).

Preparation of tris-ammonium(3,7,-dimethyl-8-(7-nitro-benzo[1,2,5]oxadiazo-4-ylamino)-octa-2,6-dien-1) pyrophosphate (NBD-GPP)

To a flame dried flask under argon, 1 equivalent of NBD-G-OH and 0.5 equivalents of 1 M PBr3 in dichloromethane was added. The reaction was immediately checked by TLC in

hexanes/ethyl acetate (7:3) for the formation of the bromide. Three equivalents of tris(tetra-butylammonium) diphosphate in acetonitrile was added upon formation of the bromide. The reaction was allowed to sit for no more than one hour and was monitored by TLC (R_f = 0). The volatiles were then removed without the use of heat. The crude product was then added to an ion exchange column (ammonium form), followed by two 0.5 mL washes of 25 mM ammonium bicarbonate. The column was eluted with ammonium bicarbonate buffer and the flow through was monitored for a drop in pH to pH 4. The elutant was collected until pH 7 and lyophilized overnight. The solid was dissolved in 1 mL of ammonium bicarbonate with acetonitrile (80:20) and purified by reverse phase HPLC as previously reported (15-24 % yield). ^{1}H NMR (300 MHz) in D_20: δ 8.26 (d, 1H), 6.16 (d, 1H), 5.31 (t, 1H), 5.23 (t, 1H), 4.27 (t, 2H), 3.91 (s, 2H), 2.03 (t, 2H), 1.91 (t, 2H), 1.51 (s, 6H). ^{31}P NMR (300 MHz): -7.2 (d, 1P), -9.8 (d, 1P).

Appendix A: Supplemental Information

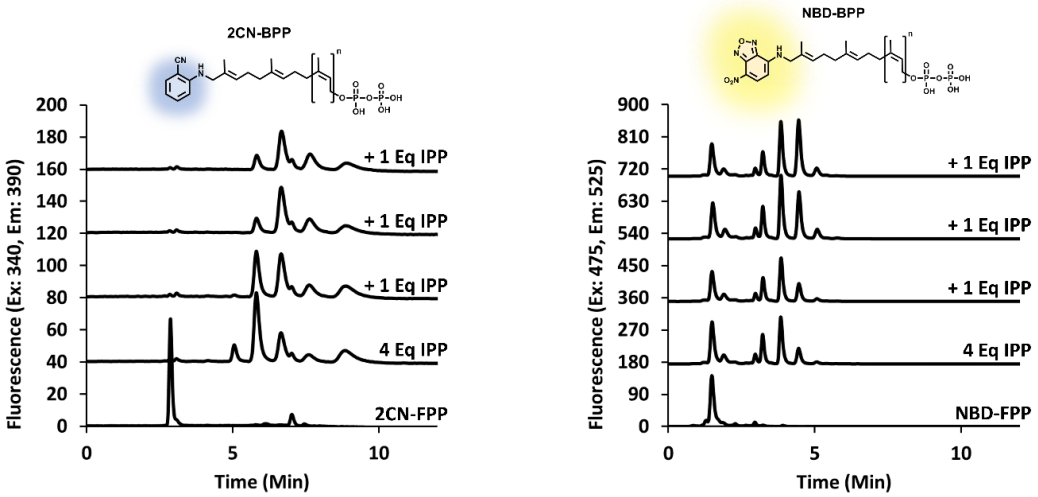

Figure A1. Tunable size of fl-BPPs.
Representative UppS reactions were set up starting with 4 equivalents of IPP. Sequential additions of one equivalent isopentenyl diphosphate increases the size fl-BPP, while maintaining a relatively narrow distribution of BPP sizes.

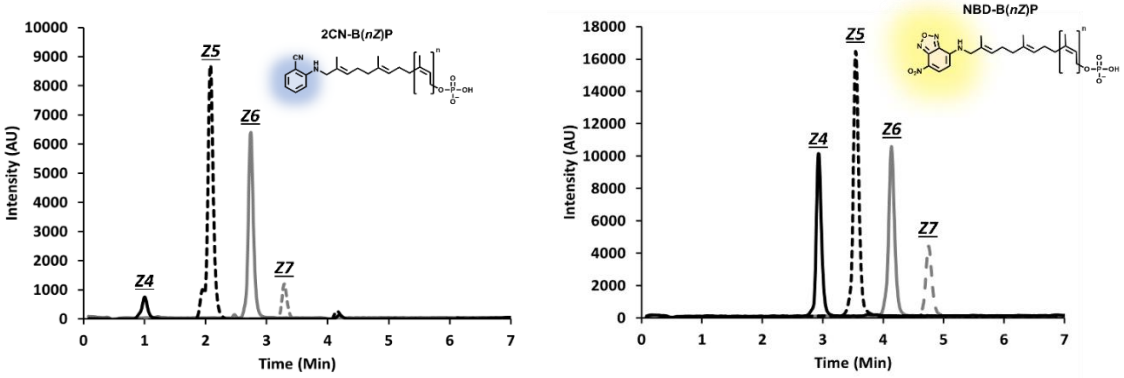

Figure A2. LCMS detection of fl-BPs.
Variable length fl-BP's are observed in SIM mode on LCMS. n-Propanol was increased at a rate of 4% per min, and started at either 40% for 2CN or 20% for NBD with 60% and 80% 100 mM ammonium hydroxide, respectively, as the co-solvent. Mass values for Z3-Z8 fl-BPs that were scanned for are in Table 1. Signals for fl-BP were approximately 10-fold lower than for fl-BPP of the same size. Thus, products were generally analyzed by LCMS after monophosphate following acid phosphatase reactions. Alternatively, fl-BPP products could be detected using the corresponding fl-BP value for *in situ* degradation to the monophosphate during ionization.

Table A1. SIM m/z values for fl-BPs.
All presented values are the $[M-H]^-$ species for each size.

	m/z	
nZ	**2CN**	**NBD**
3	554.4	615.3
4	622.4	683.4
5	690.5	751.4
6	758.5	819.5
7	826.6	887.6
8	894.6	955.6

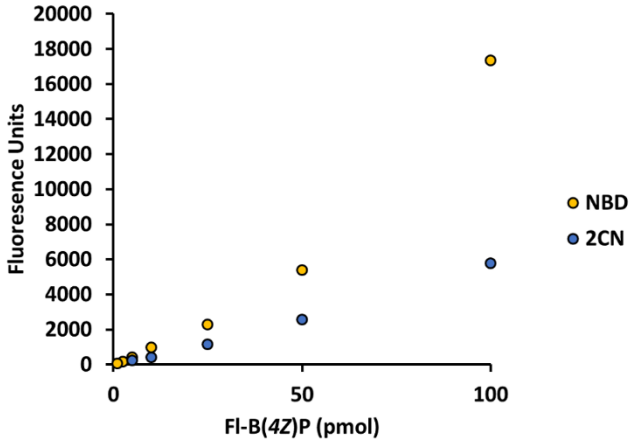

Figure A3. Limit of detection for fluorescent probes.
Fluorescence units include area under the curve of fl-B(*4Z*)P of 2CN and NBD. Limit of detection is defined by the concentration at which the minimum detectable concentration is observed. For 2CN and NBD the limit of detection corresponded to 5 and 1 pmol, respectively.

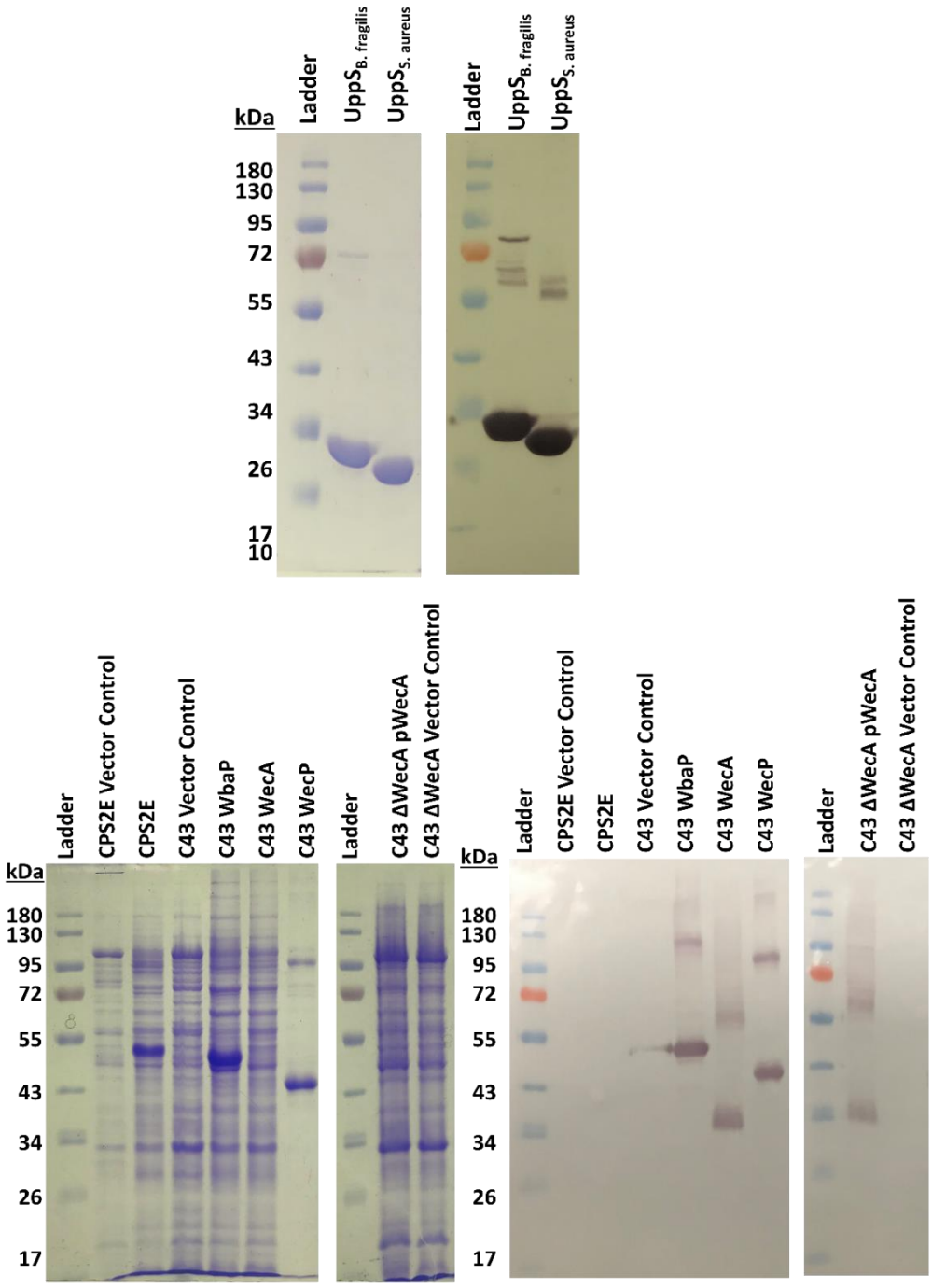

Figure A4. SDS-PAGE and corresponding western blot.
SDS-PAGE stained with coomassie. All western blots were treated first with primary rabbit anti-His antibody (1:5,000 dilution), followed by secondary goat anti-rabbit antibody conjugated to alkaline phosphatasse (1:20,000 dilution). Staining occurred with a 1-Step BCIP/NBT substrate solution for <5 min.

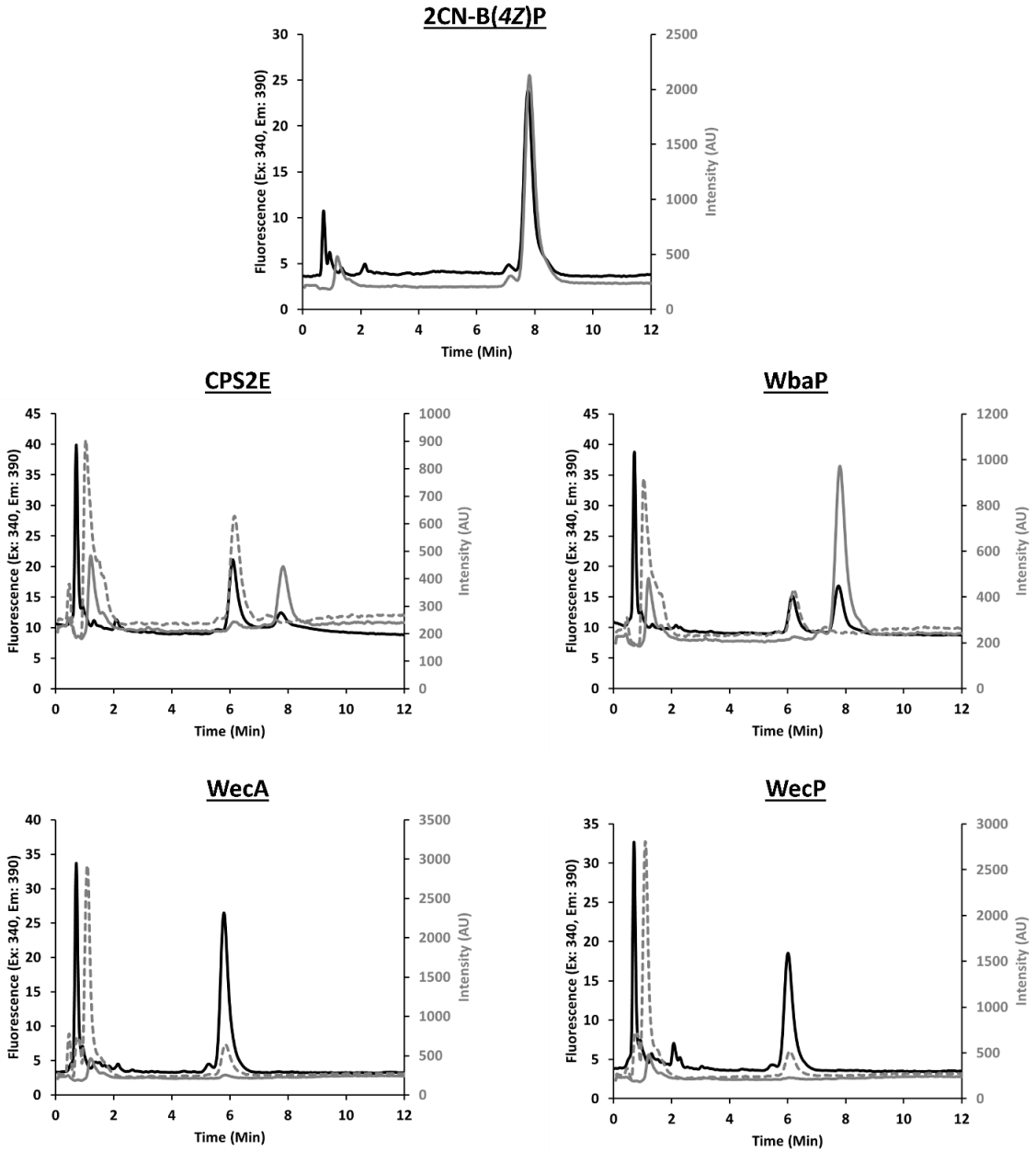

Figure A5. LCMS characterization of PGT activity with 2CN.
LCMS analysis was carried out at 26% propanol isocratic with a TEE connector to the fluorescence detector (left axis) and mass spec of respective masses on SIM mode (right axis). The 2CN-B(*4Z*)P standard appears at a retention time of 7.8 min, with a corresponding $[M-H]^-$ solid gray line (621.4 m/z). 2CN-BPP-Hexose and 2CN-BPP-HexNAc both appear at a retention time of 6.0 min and an overlapping $[M-H]^-$ in dashed gray line (863.4 and 904.4 m/z, respectively).

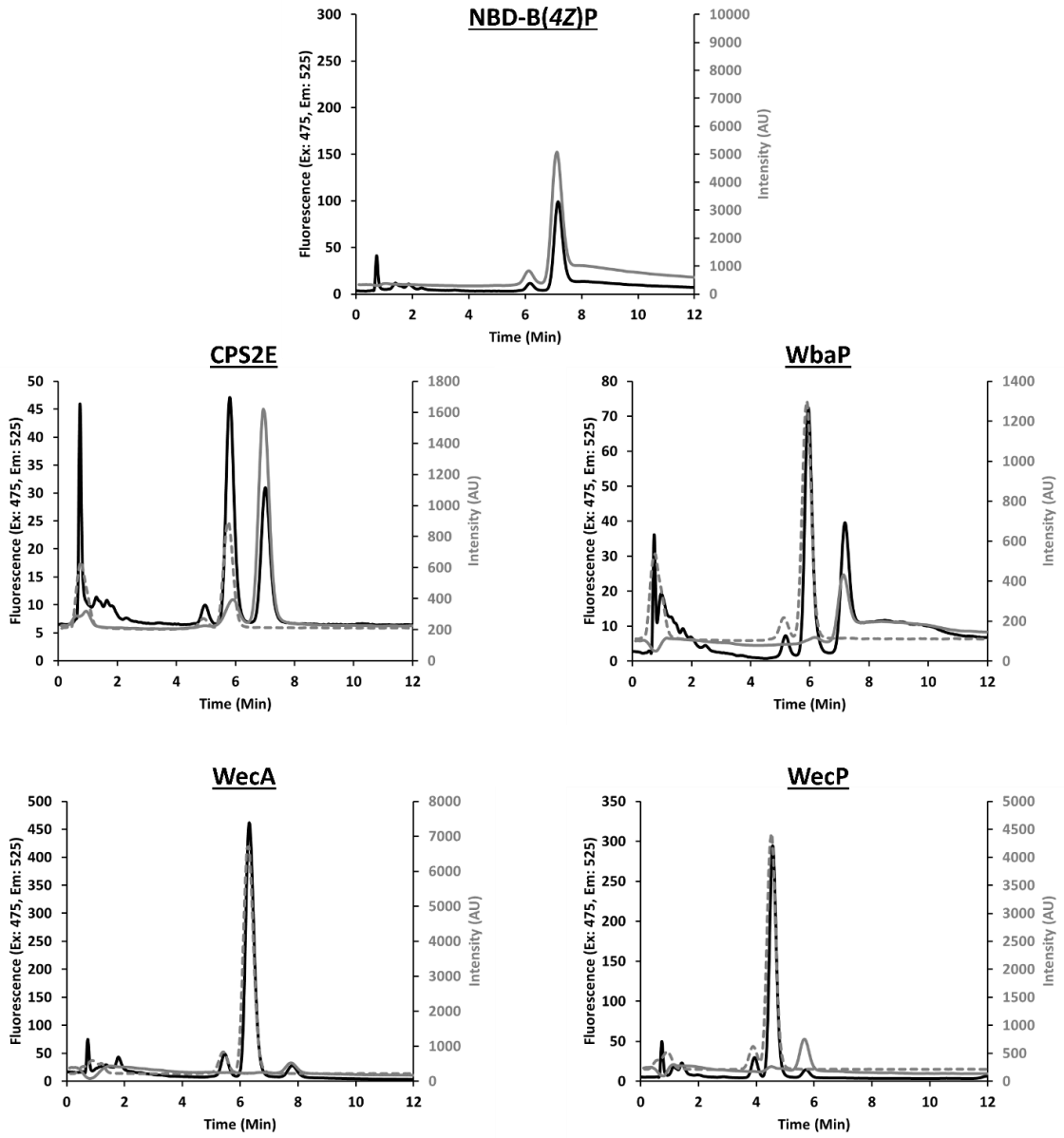

Figure A6. LCMS characterization of PGT activity with NBD.
LCMS analysis was carried out at 24% propanol isocratic as described in Figure S5. The NBD-B(*4Z*)P standard appears at a retention time of 7.1 min, with a corresponding $[M-H]^-$ in solid gray line (683.4 m/z). NBD-BPP-Hexose and NDB-BPP-HexNAc both appear at a retention time of 5.8 min and an overlapping $[M-H]^-$ in dashed gray line (925.4 and 966.4 m/z, respectively).

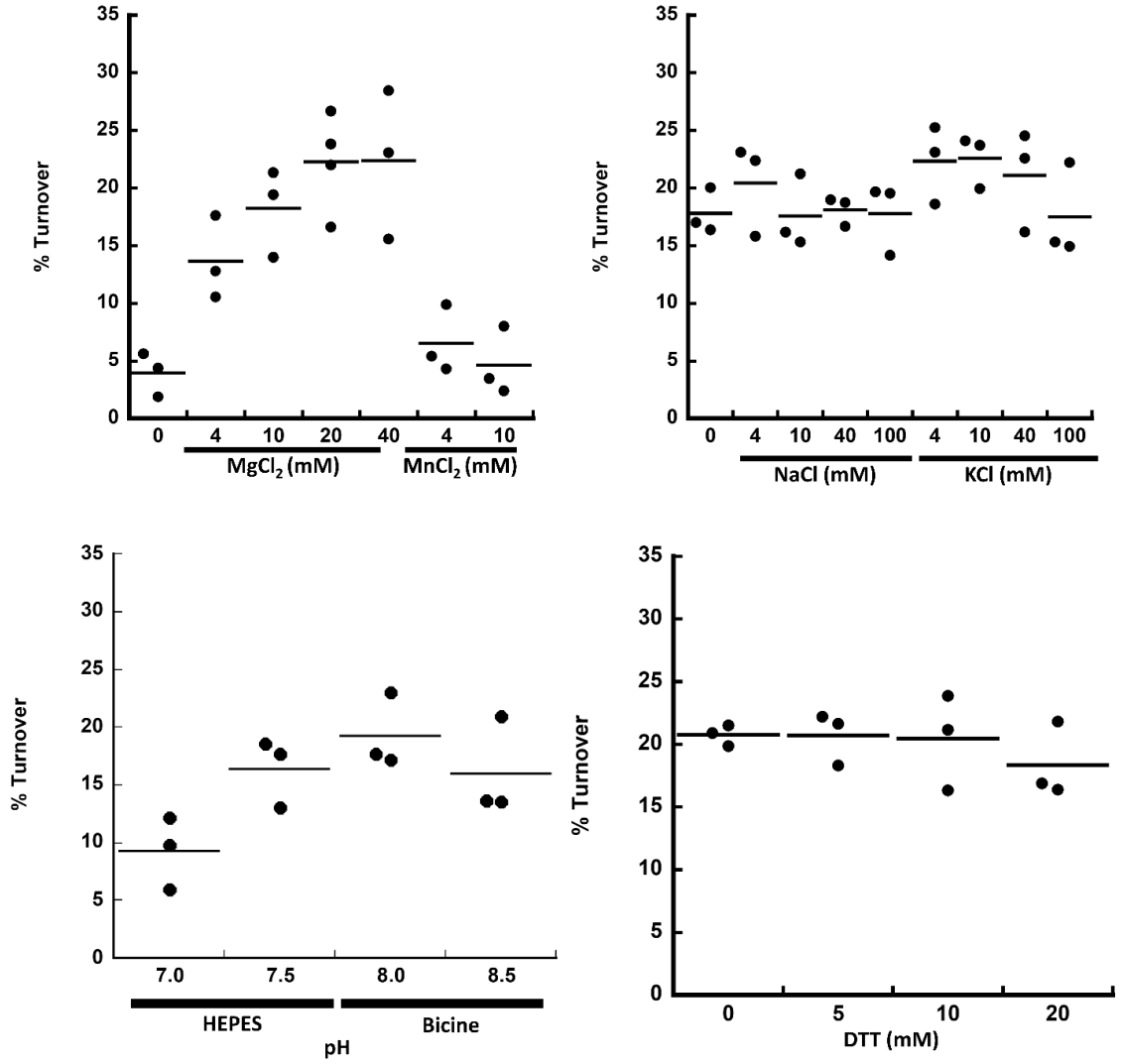

Figure A7. Optimization of WecP

When not varied, standard conditions included the following: 10 mM $MgCl_2$, 10 mM KCl, 200 mM Bicine (pH 8.0), 4 uM 2CN-B(*7Z*)P with 2% n-propanol, 216 uM UDP-GlcNAc, 20 mM DTT, 2.08 ug/mL WecP, and 0.0192% (2.4 xCMC) DDM. Reactions were quenched after 20 minutes and analyzed by fluorescence HPLC for total product turnover.

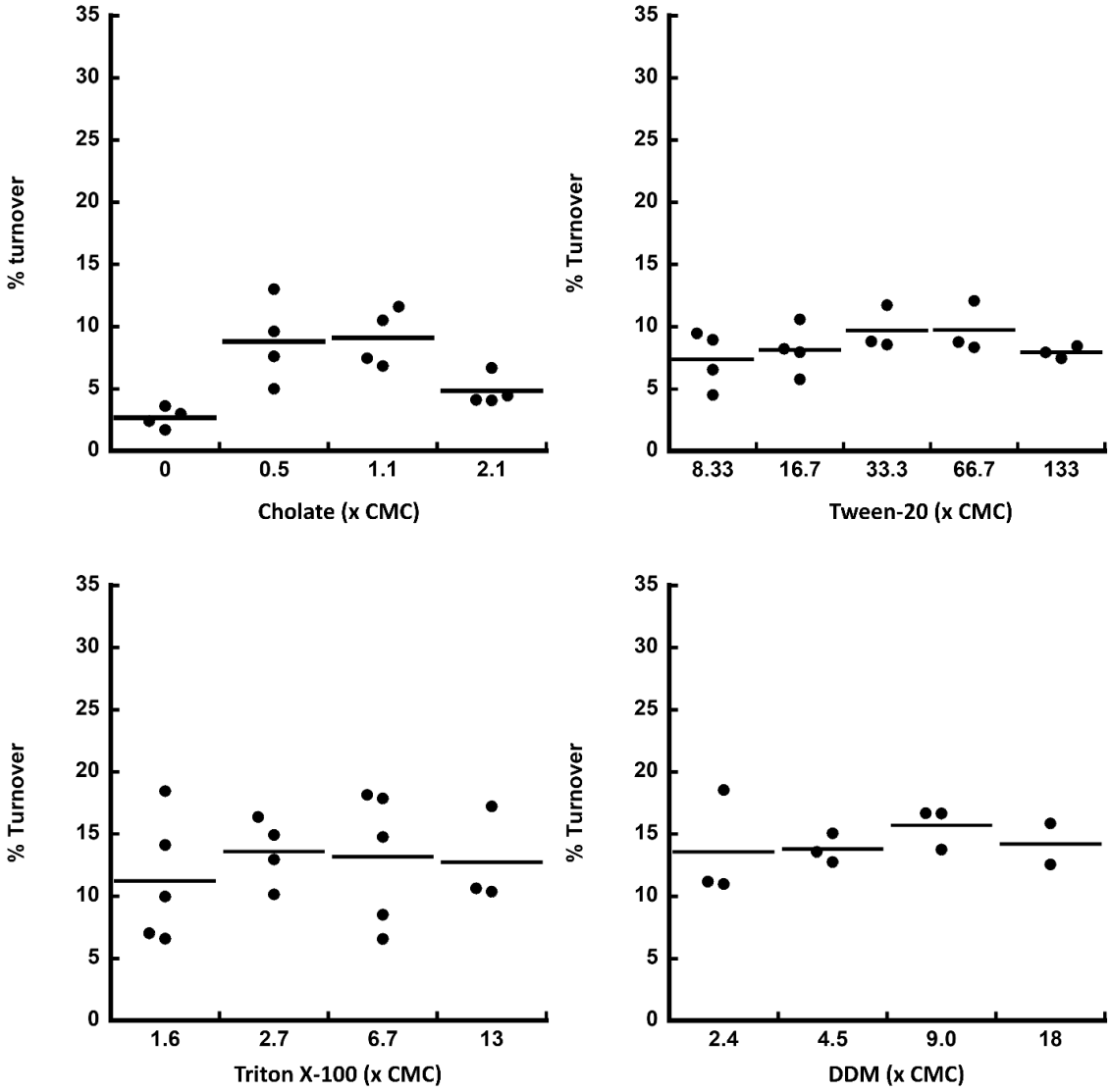

Figure A8. **Optimization of surfactant choice on WecP activity.**
When not varied, standard conditions included the following: 10 mM $MgCl_2$, 10 mM KCl, 200 mM Bicine (pH 8.0), 4 uM 2CN-B(*7Z*)P with 2% n-propanol, 216 uM UDP-GlcNAc, 20 mM DTT, 2.08 µg/mL WecP, and 0.0192% (2.4 xCMC) DDM. Reactions were quenched and analyzed as in Figure S7.

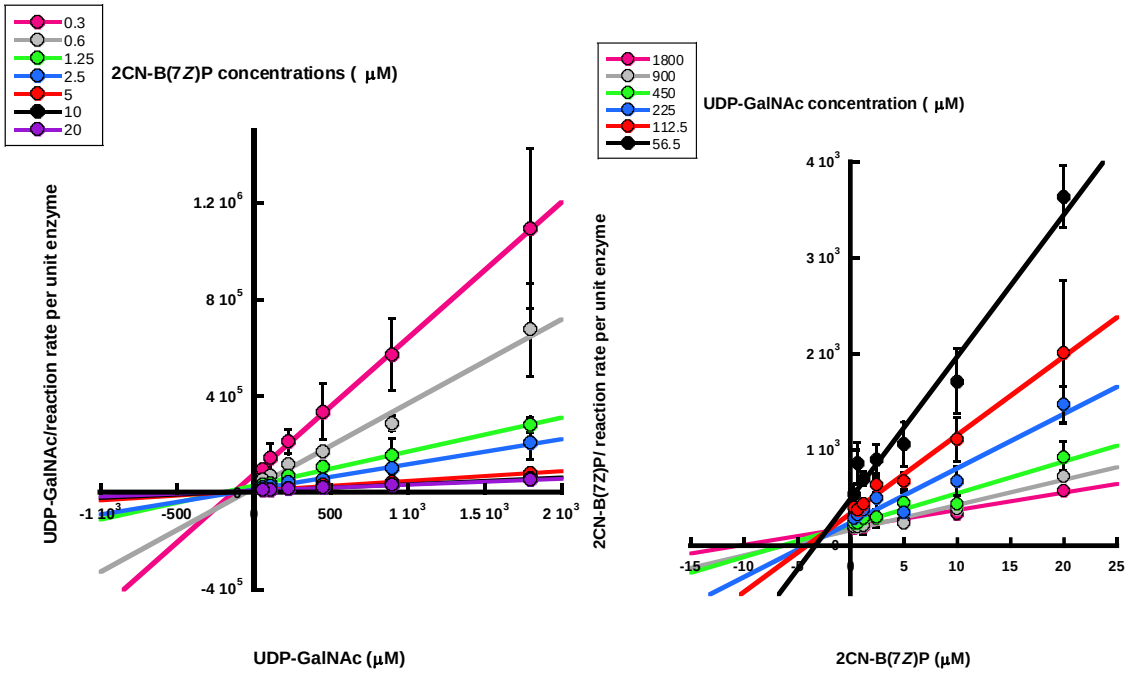

Constant component	Concentration of constant component (µM)	R^2
UDP-GalNAc	56.5	0.9698
	112.5	0.9908
	225	0.9254
	450	0.9463
	900	0.9535
	1800	0.9470
Isoprenoid	0.3	0.9995
	0.6	0.9872
	1.25	0.9935
	2.5	0.9941
	5	0.9768
	10	0.9980
	20	0.9941

Figure A9. Hanes-Woolf plot of WecP
Kinetic analyses of 2CN-7Z-BP holding isoprenoid constant (left) or UDP-GlaNAc constant (right) with varying concentrations of the other substrate. Reactions were prepared and sampled as described in materials and methods. Fit statistics for each plot is provided in the table.

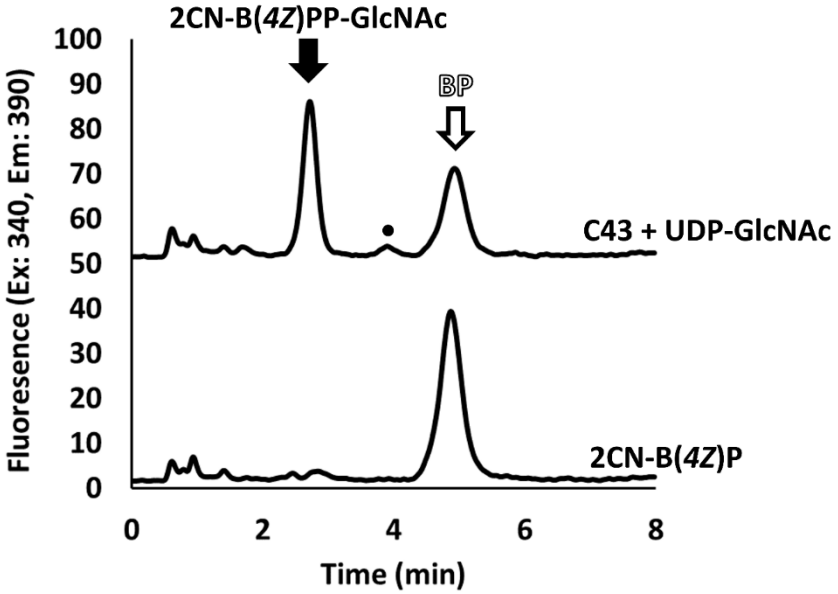

Figure A10. Endogenous WecA activity in cef.
The native *E. coli* protein WecA catalyzes the formation of fl-BPP-GlcNAc in the presence of 1 mM UDP-GlcNAc, independent of overexpression.

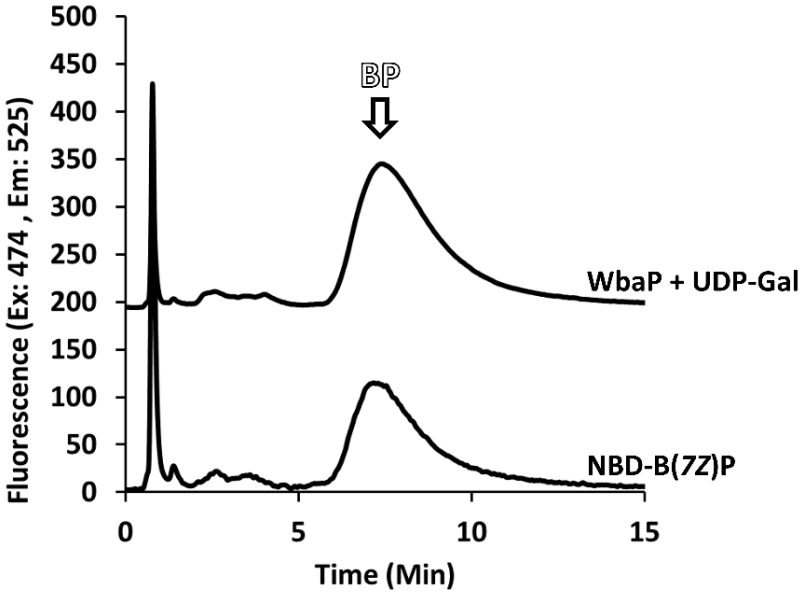

Figure A11. WbaP inactivity with NBD-B(7Z)P.
Longer polyisoprenoids of NBD do not result in transferase activity with WbaP in the presence of cholate.

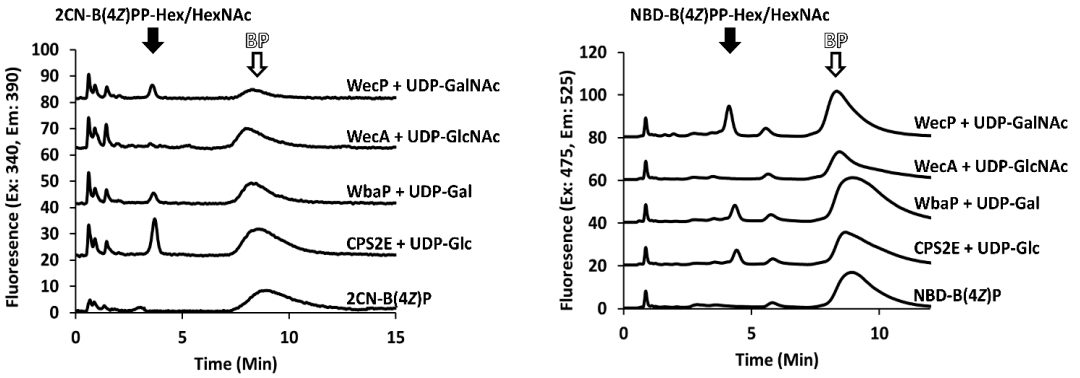

Figure A12. PGT inactivity with n-propanol addition. PGT reactions were supplemented with 5% *n*-propanol in the absence of cholate. PGT activity is poor in all cases when propanol is not added with fl-BPs.

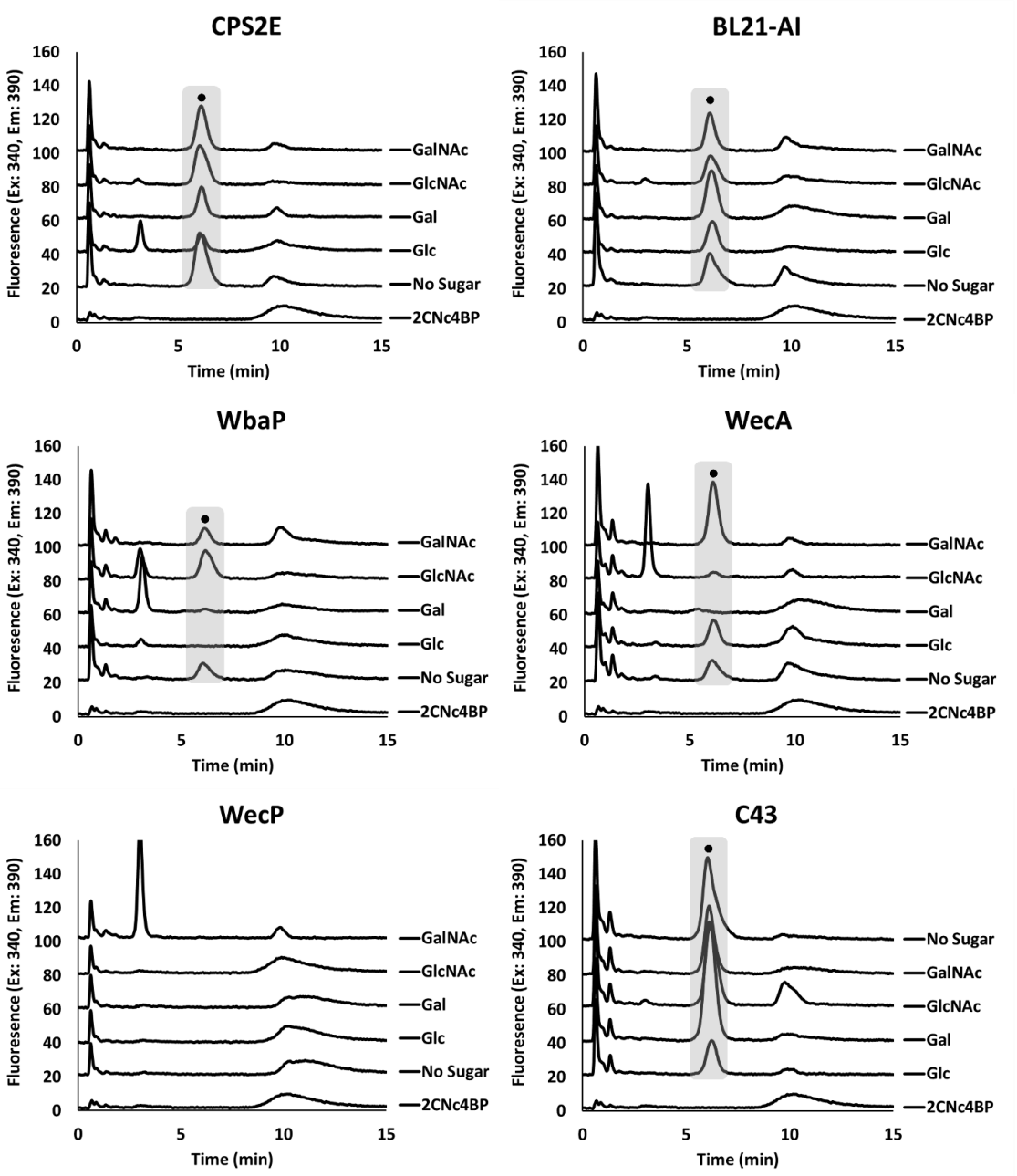

Figure A13. Full glycan donor substrates specificity analysis with 2CN.
An additional fluorescence peak (•) is observed at 6.2 min and appears independent of UDP-sugar addition. Injection quantities of each reaction were 40 pmol for 2CN. A co-eluting contaminant is present in the 2CN-B(*4Z*)P standard, which appears at 10 min only after utilization by these enzymes.

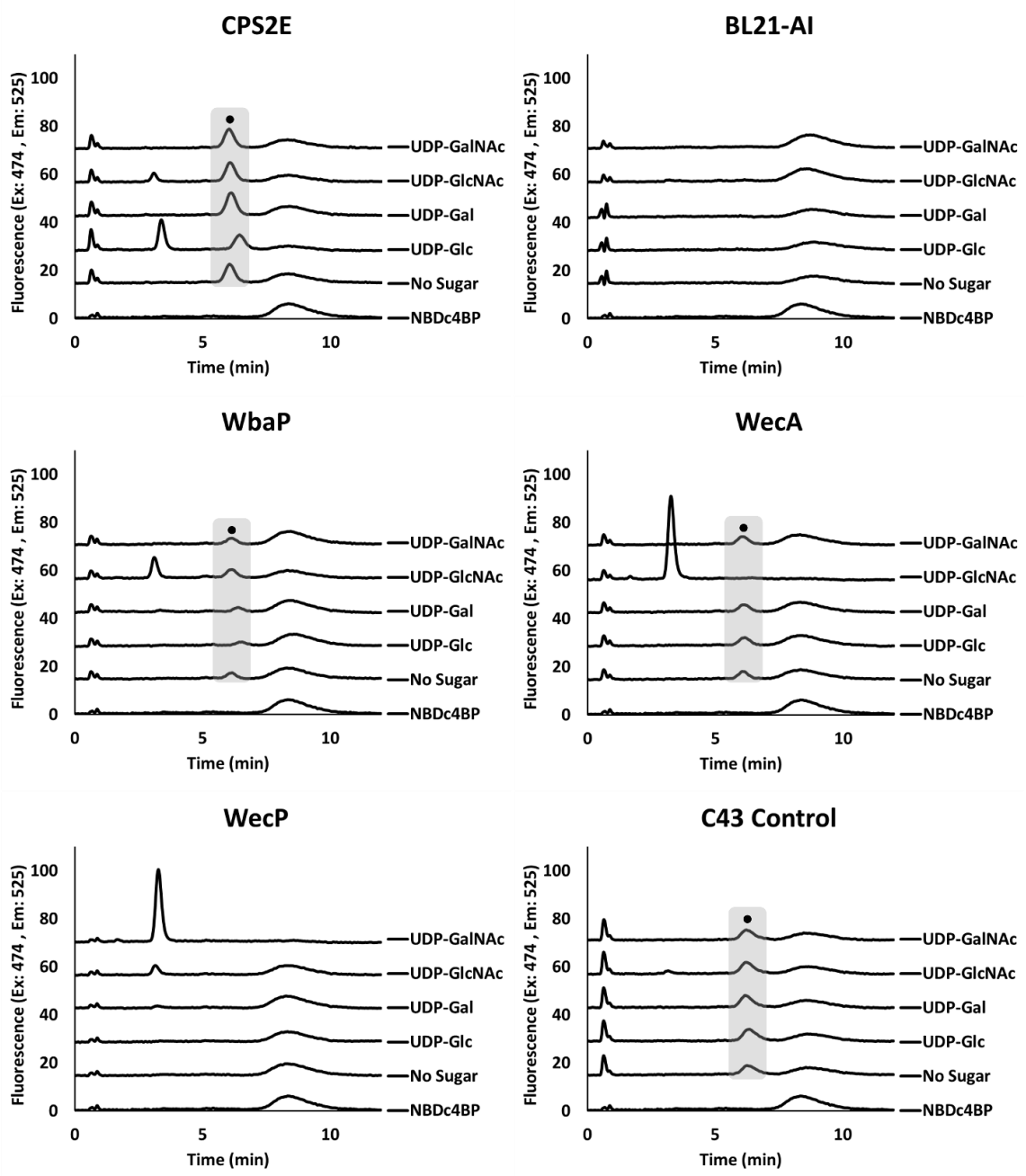

Figure A 14. Full glycan donor substrates specificity analysis with NBD.
An additional fluorescence peak (•) is observed at 6.4 min and appears independent of UDP-sugar addition. Injection quantities of each reaction were 10 pmol.

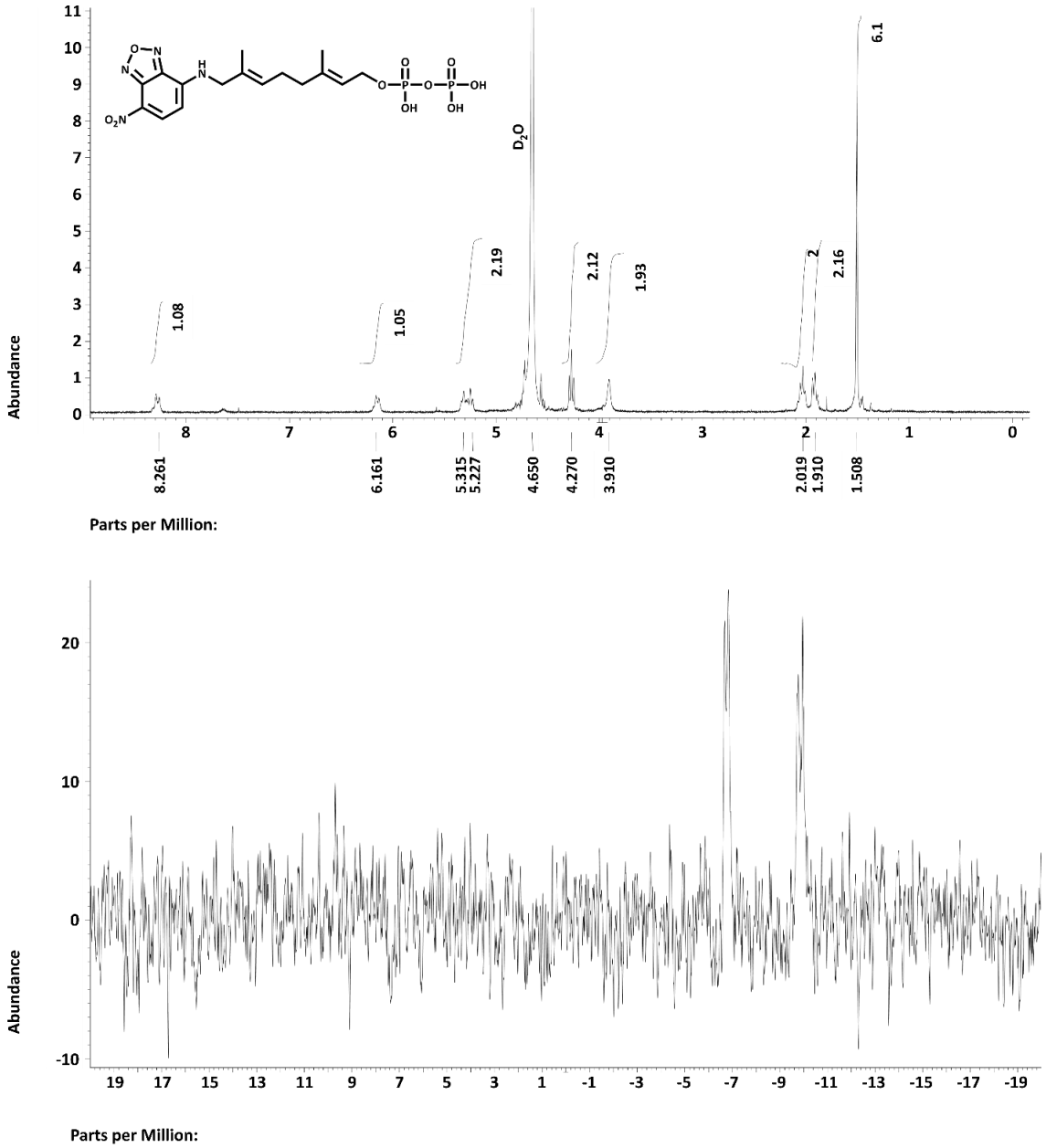

Figure A 15. NBD-GPP 1H and 31P NMR.

Table A1. Primer sequences used for ΔwecA mutants.

WecA pRED Forward	TGCACAGGACTGGTGGGTTTGGAACGGACTTTCCCTTCTG AATAAAGGTCAATTAACCCTCACTAAAGGGCGG
WecA pRED Reverse	TTATTTGGTTAAATTGGGGCTGCCACCACGATTTCTACGCA GTCTGCGTTTAATACGACTCACTATAGGGCTCG
WecA_ck_Rev	CCCATGCCAATAATCCATAGC

CHAPTER 3: CLICK-ENABLED IMMOBILIZATION OF POLYISOPRENOID SUBSTRATES FOR A SURFACE PRESENTING BACTERIAL OLIGOSACCHARIDE IN *CAMPYLOBACTER JEJUNI*

Author Contributions: Manuscript figures, protein purification, data acquisition and interpretation were performed by Amanda Reid. Kate Erickson aided in preparing isoprenoids and glycans used in this work. Joe Hazel performed molecular cloning and developed conditions for expression of WbpP. Vinita Lukose supplied the plasmids needed to produce all other proteins used in this work. Early conceptualization of the project design were carried out by Phillip Scott. The manuscript was written by Amanda Reid, and reviewed by Jerry Troutman and Colleen Eade.

Overview

Click-enabled azide and alkyne-linked sugar analogues have proven to be powerful tools among a wide range of biologically important fields. The exceptional utility of these glycan probes has also enhanced our understanding of the bacterial cell wall. An immense diversity in sugar composition exists throughout bacteria and has been the primary challenge in generating a comprehensive toolbox to include this wide variety of surface glycans. Herein, we address the need for accessible and cost-conscious bioorthogonal tools by instead incorporating an azido modification to an essential polyisoprenoid lipid carrier central to early stages of surface glycan bioassembly. An azido-modified neryl scaffold was found to be an effective substrate replacement for assembling an oligosaccharide important for virulence in the food pathogen *Campylobacter jejuni*. This finding addresses a persistent problem with insoluble polyisoprenoid substrates and simplifies *in vitro* recapitulation of these important structures. We also demonstrate covalent immobilization of this lipid-linked oligosaccharide on click-functionalized magnetic beads. Altogether, this work aims to develop tools for future applications toward novel affinity-based assays to detect pathogens in therapeutic settings. Importantly, because the isoprenoid and not glycan, features the modification, this tool may be broadly applied to a variety of polysaccharide synthesizing components.

Introduction

Advances in chemical tools have highlighted the role of bacterial surface glycans in pathogenicity, cell surface adhesion, and biofilm formation.[32, 81] Click-enabled glycan probes, in particular, have had an extraordinary impact on our fundamental understanding of cell wall formation.[82] The extension of these glycan-based probes to a broader array of surface polysaccharides requires dedicated synthetic efforts given the wide breadth of glycan diversity and the lack of commercial sources of rare bacterial glycans.[33, 83] The presence of these unique glycans highlights a fundamental difference in mammalian and bacterial biology that is a largely unexploited area of health care. Tools that can facilitate robust progress towards cheap and scalable glycan-specific targets are first needed.

Akin to a fingerprint, the extensive glycan diversity is one method to differentiate bacterial sub-species. Pathogenicity is sometimes determined by the presence or absence of certain surface glycans. The food borne pathogen *Campylobacter jejuni*, for instance, can be attenuated by the absence of a well-characterized N-linked heptasaccharide present on cell surface proteins.[84-86] This protein glycosylation (Pgl) heptasaccharide has been identified as an attractive target for vaccine development and is one possible alternative to replace or reduce traditional broad-spectrum antibiotic use.[87] Characteristic oligosaccharides, like Pgl, could also be used to identify *C. jejuni* infections in point-of-care testing. Developing biological sensors for these materials often depends on immobilization of target glycoconjugates to enrich for high affinity ligands. Chemical derivatization of glycans is needed to generate sites for immobilization. These include common bioconjugation methods, such as reductive amination, malamide, or hydrazine formation to an anomeric carbon.[88, 89] Preserving the unmodified structure of the glycan, however, is critical for conserving the bimolecular interaction needed for ligand recognition.[88, 90]

Complete characterization and *in vitro* recapitulation of the enzymes involved in Pgl heptasaccharide formation have been well described in the literature.[41, 50, 84, 91-101] The biosynthesis begins with the universal lipid carrier, bactoprenyl phosphate (**BP**, also called Und-P) (**Figure 3.1**). The tendency for BP to aggregate in aqueous environments has prompted inquiries into the minimum lipid scaffold size required for enzyme activity for Pgl and other bacterial surface glycans. At least one cis-isoprene is important for substrate recognition of Pgl and other glycosyltransferases, but preferentially several.[71, 76] Chemoenzymatic and semi-synthetic strategies to introduce non-native tags on the distal ω-isoprenoid on polyisoprenoids can also enhance solubility to a small extent.[40, 102] A two-step chemoenzymatic approach has been employed by our group previously to generate shorten isoprenoids with ω-fluorescent tags.[102] These isoprenoid probes have permitted facile detection of enzymatic roles during *in vitro* polysaccharide.[26, 27] We wondered if shortened isoprenoid probes could also be used to build immobilized glycoconjugates for future sensing applications of the Pgl heptasaccharide. This would also retain the native glycan structure and could serve as a model for other glycan assembling systems that rely on BP.

Herein, we identify two azido- tagged polyisoprenoids that are suitable substrate replacements for recapitulating the Pgl heptasaccharide from *C. jejuni* (**Figure 3.1)**. Utilizing smaller isoprenoid sizes results in milligram yields and enhanced solubility over native BP, thereby overcoming a persistent problem with using these hydrophobic substrates for *in vitro* recapitulation of bacterial glycans. We also characterize activity from a putative epimerase to reduce the cost of producing the Pgl heptasaccharide. Lastly, we immobilize the heptasaccharide onto magnetic resin and demonstrate affinity of that conjugate towards a GalNAc-specific lectin. Altogether, this work

provides a model towards the future development of functional assays to detect pathogens, or perhaps even prophylactic platforms such as glycoconjugate.[87, 103]

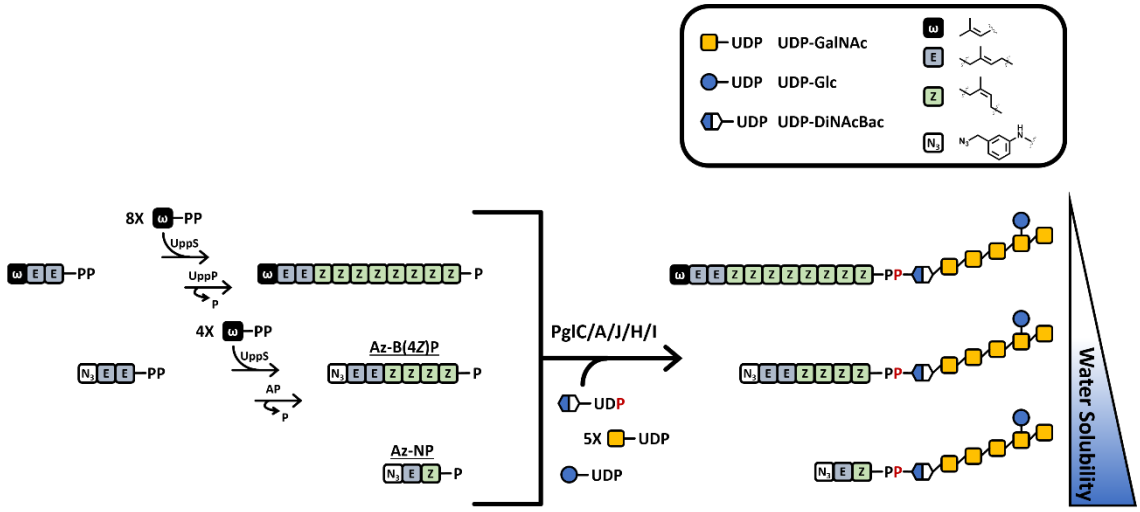

Figure 3.1. Assembly of pgl oligosaccharide from *C. jejuni* with native BP and isoprenoid tags.
Native BP is produced from eight cis condensation reactions of isopentenyl diphosphate to farnesyl diphosphate by Undecaprenyl diphosphate synthase (UppS) and subsequent dephosphorylation by Undecaprenyl diphosphate phosphatase (UppP). Polyisoprenoid tags are prepared by a similar route by tuning the length and utilizing potato acid phosphatase (AP). Alternatively, a two-isoprene monophosphate probe was synthesized directly. Sequential glycan addition is achieved by the transferase enzymes PglC, A, J, H, and I from the *C. jejuni* Pgl pathway with their respective sugar substrates as described in the literature. Figure legend adapted from Liu et al.[41]

Results and Discussion

HPLC Monitoring of the Enzymatic Synthesis of UDP-DiNAcBac

The first glycan of pgl assembly utilizes the rare sugar UDP-N,N-diacetylbacillosamine (UDP-DiNAcBac) which is not commercially available. Methodologies for monitoring glycan modifications commonly employ capillary electrophoresis or NMR.[94, 99, 104] Since HPLC analysis has already been reported with PglF and a homolog of PglE, we chose this high-throughput technique for monitoring successive product formation by sequential addition of enzymes (**Figure 3.2**).[105] First, UDP-GlcNAc (retention time 9.3 min) was converted to the 4-keto product by a truncated PglF which produced a slight shift to 9.9 min. PglE then produced the 4-amino product with a new retention time of 3.7 min, consistent with our previous observations of similar aminotransferase enzymes.[105] Full turnover of the 4-keto product by PglE was typically not observed until the addition of PglD, which resulted in complete conversion of the 4-amino sugar

to UDP-DiNAcBac giving an HPLC retention time of 11.2 min. The crude reaction was used as the UDP-DiNAcBac donor for subsequent Pgl heptasaccharide formation to avoid losses from HPLC purification.

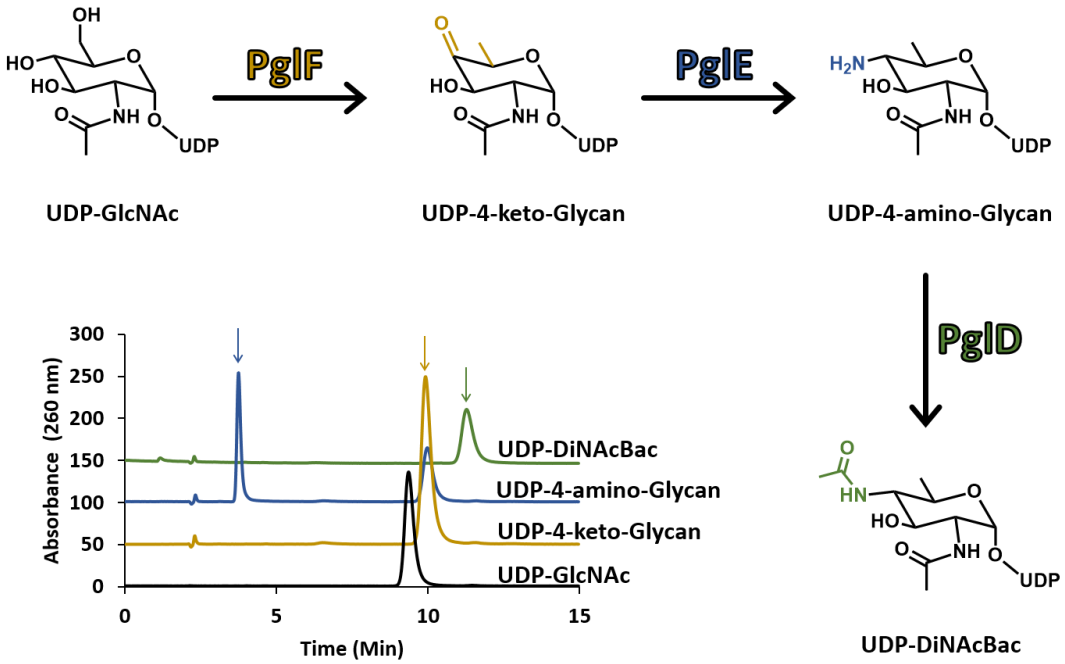

Figure 3.2. HPLC analysis of UDP-DiNAcBac formation with sequential addition of PglF, E, and D. Arrows indicate the elution of respective products. Samples were blanked with a water injection and the chromatograms were offset along the y-axis by 50 abs units for each reaction.

ω-Azido Bactoprenyl Phosphate Biosynthesis by UppS and Acid Phosphatase Treatment

We first prepared click-enabled BP using chemoenzymatic strategies similar to our previous reports.[102] The geranyl diphosphate analogue with a ω-benzyl azide moiety was then incorporated into bactoprenyl diphosphate (Az-BPP) with previously described methods.[102, 106] Dephosphorylation was achieved by extracting Az-BPP products with *n*-butanol and cleaving with potato acid phosphatase to produce Az-BP. Lengths of formed products (*Z*4-6) and enzyme conversion from BPP to BP were confirmed by LC-MS analysis for both steps (Figure B1). In addition, we sought to develop an alternative detection method complimentary to HPLC. To overcome the low molar absorptivity associated with this compound, we appended TAMRA-DBCO to monitor product formation by fluorescence.[54, 55] HPLC analysis of new fluorescent

materials appeared at retention times corresponding to the major BPP or BP products, *Z*4 (*) and *Z*5 (**) respectively, for each enzymatic step (**Figure 3.3**). The minor product, *Z*6, was less evident following acid phosphatase treatment due to characteristically broad peaks following phosphate cleavage.

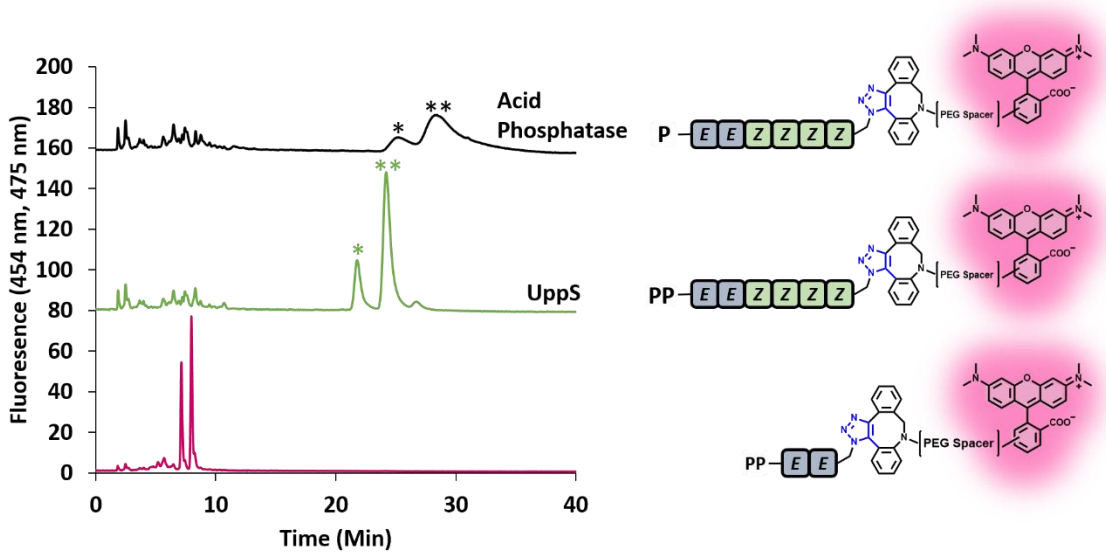

Figure 3.3. Az-BP formation from UppS$_{Sa}$ and potato acid phosphatase reactions
Azido isoprenoid products were reacted to DBCO-TAMRA for fluorescence monitoring after respective enzymatic reactions. Two isomers of TAMRA are apparent in the bottom chromatogram which are present in commercial sources of DBCO-TAMRA. TAMRA isomers in BPP and BP appear to co-elute as each peak represents a different size isoprenoid. Samples were blanked with a water injection and the chromatograms were offset along the y-axis by 80 fluorescent units for each sample.

Building the Pgl Heptasaccharide on Click-Enabled Bactoprenyl Diphosphate

With purified Az-B(4*Z*)P in hand, we next assembled the Pgl heptasaccharide by supplying 2-fold excess glycan substrates followed by sequential addition of each enzyme. Membrane associated proteins PglC, A, J, H, and I were prepared as enriched membrane fractions as described in the methods and materials (Figure B2).[91, 93, 97, 107, 108] Samples were analyzed by ESI-LC-MS in scanning ion mode monitoring for $[M-H]^{-1}$ and $[M-2H]^{-2}$ ion species. Each glycan addition from Pgl heptasaccharide formation (2-6) resulted in products with a shorter retention time, eluting at 9.99, 9.85, 9.80, 9.72, and 9.73 respectively (**Figure 3.4**). Both the anticipated product and the

starting material were monitored in separate SIM channels to prevent co-detection of unreacted material (**Figure 3.4**). In each case, near complete depletion of the starting material was observed. Additionally, total ion plots were generated over the full elution range (9.5-10.5 min) in scanning mode to confirm the presence of enzyme product formation.

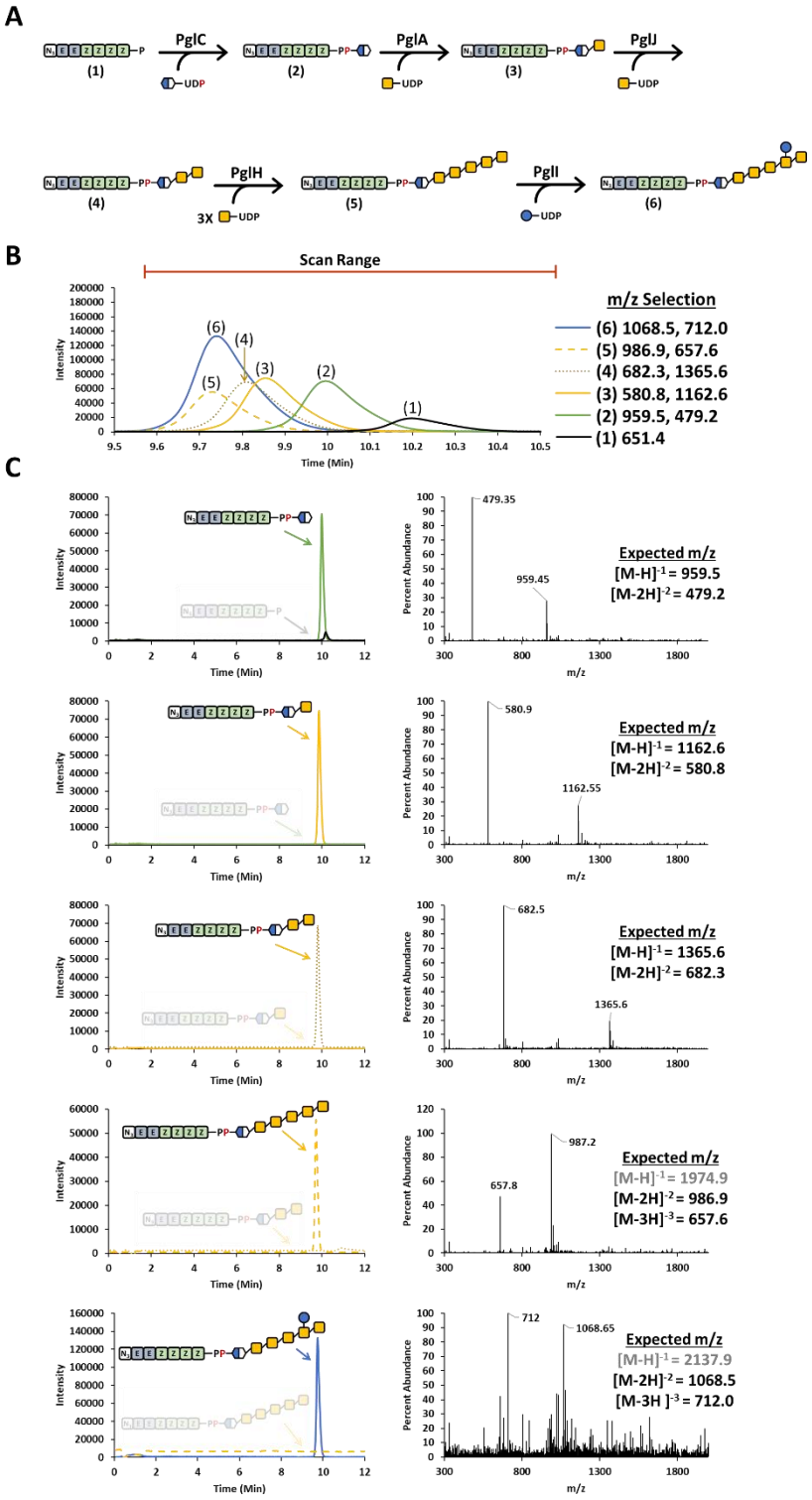

Figure 3.4. LC-MS analysis of sequential Pgl oligosaccharide formation on Az-B(4*Z*)P.
(A) Biosynthetic scheme associated with pgl heptasaccharide formation on Az-B(4Z)P. (B) Combined SIM chromatograms for each oligosaccharide product overlaid over the elution time 9.5-10.5 minutes. (C) Sequential enzymatic reactions tracking product formation and starting material disappearance by SIM. Total ion plots were acquired from scanning mode over the entire range of product elution (range indicated in B). Structures and mass to charge ratio are provided for each expected product.

Az-Neryl Monophosphate is a Substrate for Pgl Assembly

Naturally abundant *E*/*Z* isoprenoids, such as nerol, have been used for bacterial glycan production with varying degrees of success.[41, 109, 110] We wondered if the limited successes of neryl probes in these instances could be solved by the addition of the benzyl azide tag (Az-NP).[106] Notably, the monophosphate was synthesized directly omitting the need for both enzymatic steps, UppS and acid phosphatase. We then evaluated the assembly of the Pgl oligosaccharide with Az-NP as a replacement substrate. The formation of the Pgl oligosaccharide on Az-NP was monitored by ESI-LC-MS by stepwise addition of Pgl enzymes (**Figure 3.5**). The first phosphoglycan addition resulted in a later retention time shift from 7.11 to 8.21 min for Az-NP and the PglC product (8), respectively. This aberrant retention time shift led us to further evaluate if differing column chemistries could explain this observation and was indeed found to be the case (Figure B4). Each new product thereafter afforded a retention time shift earlier than the previous, at 8.41, 8.23, 8.10, 8.18, and 8.03 min for subsequent (9-12) Pgl enzyme products. As described for Az-B(4*Z*)P, SIM was carried out for targeted masses of the starting material and product for each enzyme to ensure complete conversion (**Figure 3.5**).

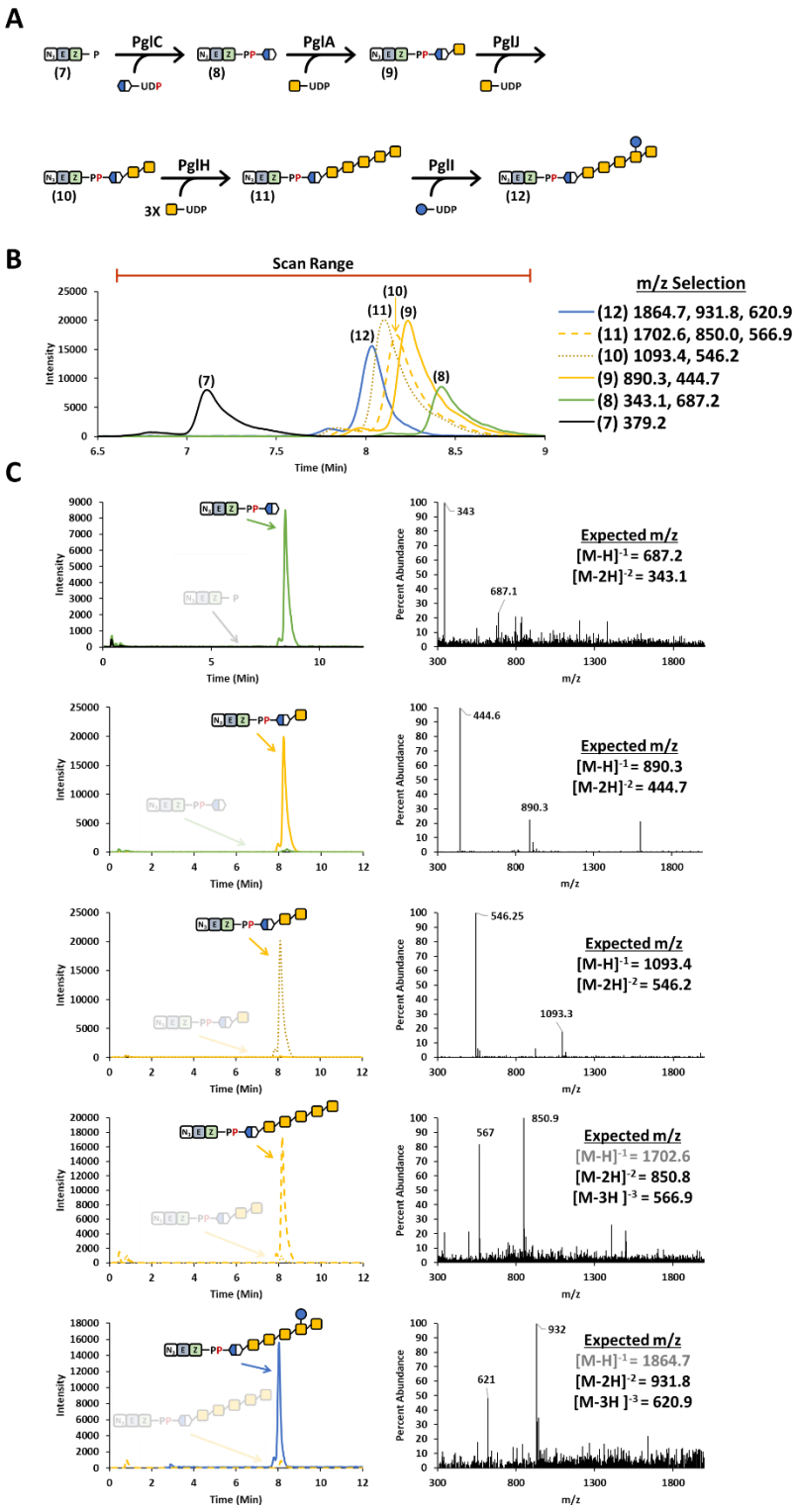

Figure 3.5 Pgl oligosaccharide assembly on Az-NP.
(A) Biosynthetic scheme associated with pgl heptasaccharide formation on Az-NP. (B) Combined SIM chromatograms for each oligosaccharide product overlaid over the elution time 6.5-9.5 minutes. (C) Sequential enzymatic reactions tracking product formation and starting material disappearance by SIM. Total ion plots were acquired from scanning mode over the entire range of product elution (range indicated in B). Samples were blanked with a water injection.

We attribute Az-NP activity with Pgl enzymes to locking of the internal isoprenoid in the *E*-orientation. It would be interesting to see if the addition of the ω-benzyl azide tag could resolve the inactivity associated with other glycan synthesizing enzymes previously reported.[41, 46, 50, 71, 76] Furthermore, direct synthesis efforts afforded milligram quantities of Az-NP and addresses a common issue with isoprenoid insolubility and tendency to aggregate in aqueous environments.[71, 76, 111] Indeed, a considerable amount of effort has been put forth to identify the smallest isoprenoid that retains activity for glycan assembly while also avoiding various problems related to polyisoprenoid substrate low solubility.[41, 45, 46, 50, 76, 109, 112] However, we also recognize the possibility that water miscible or immiscible isoprenoid scaffolds may better serve various purposes depending on the application.

In situ UDP-GlcNAc Epimerization by WbpP from Vibrio vulnificus

High costs are associated with some commercially available UDP-linked glycans. UDP-GlcNAc, for example, is more than ten times the cost of UDP-GalNAc. We wondered if a general epimerase could be exploited to produce UDP-GalNAc from UDP-GlcNAc at a lower cost. We cloned the *Vibrio vulnificus* putative HexNAc epimerase *wbpP*, which derives its name from homologues of this enzyme class (Table B1).[113] In the presence of UDP-GlcNAc, purified WbpP afforded a product with an identical retention time as UDP-GalNAc at 9.6 min by normal phase HPLC (**Figure 3.6**). The equilibrium of an overnight epimerase reaction yielded an approximate product ratio of 30:70 (UDP-GalNAc:UDP-GlcNAc) in conditions used for Pgl production. Although UDP-GlcNAc was the major product of WbpP, we hypothesized that *in situ* UDP-GalNAc production could be driven by the depletion of the nucleotide sugar as the Pgl heptasaccharide is assembled.

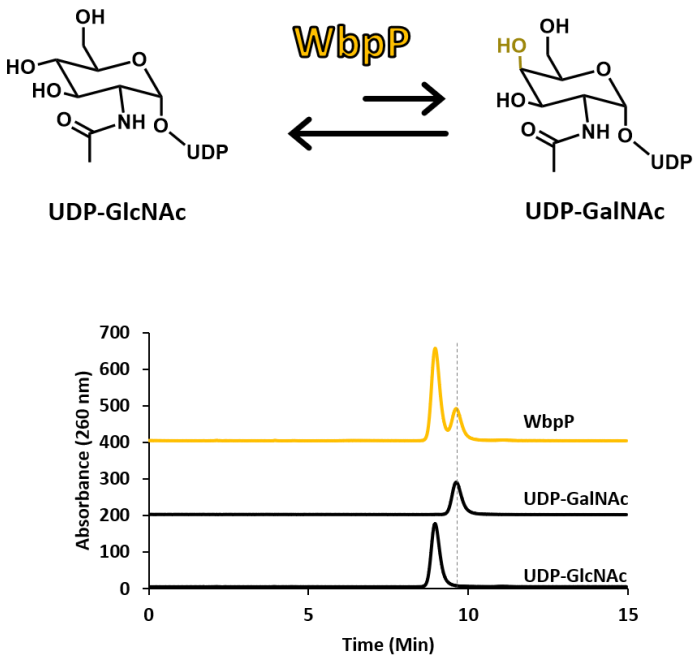

Figure 3.6 Az-B(Z4)P oligosaccharide assembly with *in situ* generation of UDP-GlcNAc.
Overnight activity of the putative epimerase WbpP producing a mixture of UDP- GalNAc and -GlcNAc (30:70). Chromatograms were offset along the y-axis by 200 units.

Next, we addressed whether Pgl HexNAc transferases A, J, or H could also utilize UDP-GlcNAc as a substrate. Both HexNAc products have identical m/z values and are therefore indistinguishable from one another by mass spectrometry. Additionally, a slight excess of UDP-GalNAc was found to be optimal for A, J, and H product formation. Using excess sugar could further confound which HexNAc product was being formed, if indeed both glycan substrates could be incorporated into the heptasaccharide. To overcome these challenges, we selected Az-B(4*Z*)P which is *n*-butanol miscible and thus easily extracted away from excess UDP-sugars to assess downstream HexNAc specificity. Since Az-NP was not *n*-butanol miscible (data not shown), this highlights one unique advantage of aqueous miscible and immiscible polyisoprenoids. First, we prepared (2) since PglC has demonstrated cross-reactivity for UDP-GlcNAc and likewise PglA for BPP-GlcNAc.[98] The subsequent activity of PglA, J, H, and I were individually assessed with their respective oligosaccharide intermediate in the presence of UDP-GlcNAc and no additional activity towards this sugar was observed (Figure B5). Pgl assembly was only possible in the presence of

WbpP, demonstrating specificity for UDP-GalNAc, over -GlcNAc (**Figure 3.7**). The limited water solubility of elongated isoprenoids is generally problematic for aqueous conditions needed for recapitulation of bacterial glycans. Extracting intermediates for quick sample cleanup is one unique advantage of these relatively hydrophobic isoprenoids like Az-B(4*Z*)P over Az-NP. Longer isoprenoids have been reported as the preferred substrate for processive glycan polymerization *in vitro*.[110]

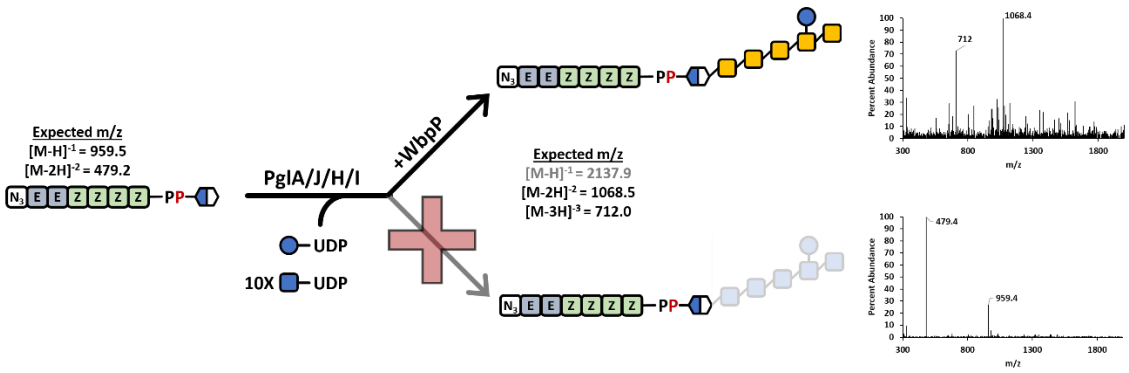

Figure 3.7. Glycan assembly with *in situ* generation of UDP-GalNAc.
Pgl heptasaccharide formation only occurs with the addition of WbpP as PglA, J, and H lack activity with UDP-GlcNAc.

Magnetic Bead Immobilization and Detection of Neryl Tagged Pgl Heptasaccharide

With the development of future downstream affinity assays in mind, we next scaled up Pgl heptasaccharide production. Typical synthesis of Az-NP yielded hundreds of micromoles and required two fewer steps for synthesis, whereas purified Az-B(4*Z*)P yielded just tens of nanomoles per round of HPLC purification. Combining Az-NP with *in situ* GalNAc production with WbpP, a robust and cost-conscious method for assembling the Pgl heptasaccharide was achieved. With the pgl heptasaccharide in hand, we then selected magnetic beads as the immobilizing resin for ease of recovery. Surface functionalization with dibenzocyclooctyne groups provided the click-partner for copper-less Huisgen cycloaddition of the azido- modified neryl scaffold. Unpurified reactions containing (**12**) were used directly for click-addition producing Pgl@MB. Similarly, a control was prepared from Az-NP in water (Az-NP@MB). The supernatant was decanted and

analyzed by LC-MS to monitor for unbound oligosaccharide before and after incubation (**Figure 3.8**). The absence of either material in the supernatant following incubation suggested complete click-addition to the magnetic bead surface. Next, we sought to test if the Pgl heptasaccharide was indeed exposed on the MB surface and could be used for affinity assays. To do this, we employed a fluorescently conjugated lectin used to detect Pgl, which has a high affinity and specificity for GalNAc, Soybean Agglutinin.[24, 84, 114, 115] A dot blot was performed with Pgl@MB and Az-NP@MB coincubated with 488-Soybean Agglutinin and were subsequently imaged (**Figure 3.8**). A bright fluorescent signal was observed at the spot containing Pgl@MB, but not Az-NP@MB, consistent with the presence of GalNAc moieties present in the Pgl heptasaccharide.

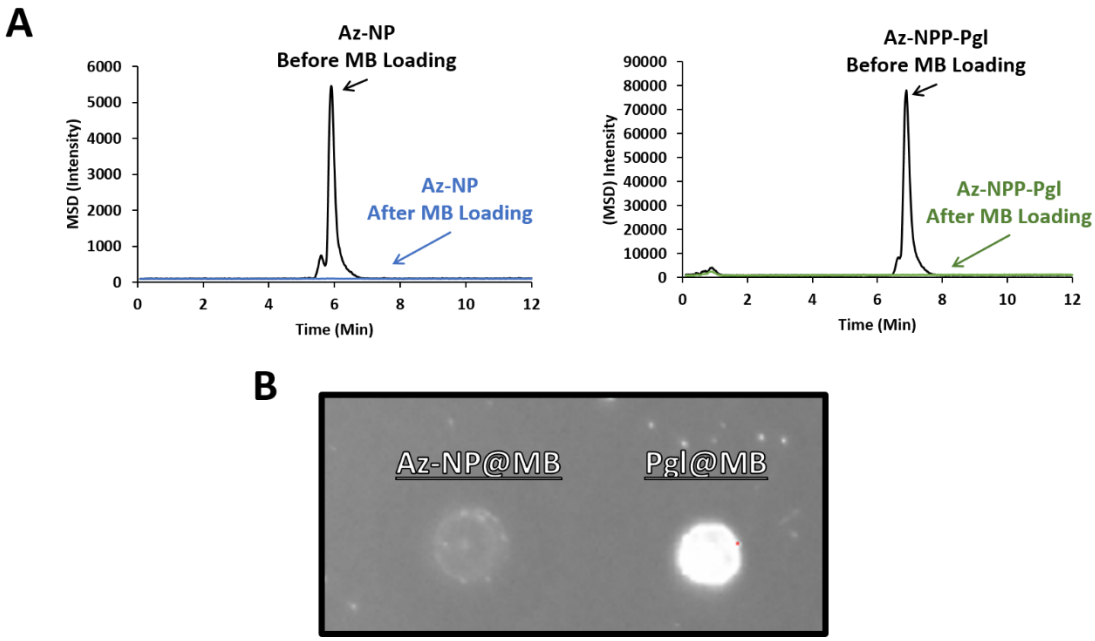

Figure 3.8. Pgl heptasaccharide immobilization onto magnetic nanoparticles.
(A) LC-MS analysis of Pgl oligosaccharide on Az-NP present in the supernatant before and after introducing DBCO coated magnetic beads. (B) Soybean Agglutinin lectin blot assay with Az-NP@MB verses Pgl@MB.

Conclusion

Fluorescent isoprenoid probes have aided in the identification of sequential enzyme roles during polysaccharide biosynthesis for two oligosaccharides.[26, 27] Here, we expand the functionality of isoprenoid-based probes by appending a bioorthagonal handle, which greatly

enhances the range of subsequent downstream applications beyond fundamental characterization. To illustrate this, a well-characterized N-linked heptasaccharide important for virulence in the human pathogen *C. jejuni* was recapitulated on an azido-modified isoprenoid scaffold. Further, the size of the isoprenoid was reduced to the commercially available nerol, thereby affording a more direct synthesis and higher overall yield compared with the elongated isoprenoid counterpart. The addition of a neryl probe greatly streamlines isoprenoid tag development since it can be synthesized directly, thus eliminating the need for enzymatic preparation and purification of mixed polyisoprenoids.

Ultimately, both lipid scaffolds were effective substrate replacements for assembling the Pgl heptasaccharide. The water soluble neryl scaffold omitted carryover of co-solvents (e.g. DMSO, triton, etc.) into reaction conditions, can sometimes inhibit enzyme activity.[45, 102] In contrast, the elongated polyisoprenoid substrate, while lower in yield, was complimentary to *n*-butanol extraction needed to quickly change reaction conditions. This was especially advantageous during Pgl sugar specificity analysis, where Az-NPP oligosaccharides would require iterative purification at each step. Biological activity downstream of glycosyltransferase activity may also be impacted from scaffold size. Longer isoprenoid substrates, for instance, are proposed to be essential for oligosaccharides that undergo polymerization.[110] Therefore, both scaffolds have distinct benefits depending on the application.

Lastly, the azido-modified neryl scaffold was used to demonstrate immobilization and subsequent detection of the Pgl with a GalNAc specific lectin. Similar approaches have been undertaken with the native glycoprotein in *Escherichia coli* that have been engineered to produce Pgl.[87] Building the Pgl heptasaccharide on a modified lipid scaffold opens up the potential for tailoring the lipid linker to suit a wide variety of solid support surfaces. Broadly, this work

extends the utility of isoprenoid-based tools by appending a click-enabled moiety for a wider range of downstream applications that can be applied to affinity-based assays such as glycoarrays or perhaps aptamer development. Importantly, this approach preserves the native identity of the oligosaccharide, unlike methods that immobilize via chemical attachments through glycans.

of this lipid-linked oligosaccharide on click-functionalized magnetic beads. Altogether, this work aims to develop tools for future applications toward novel affinity-based assays to detect pathogens in therapeutic settings. Importantly, because the isoprenoid and not glycan, features the modification, this tool may be broadly applied to a variety of polysaccharide synthesizing components.

Experimental Procedures

General

Azido labeled isoprenoids were synthesized following procedures from Labadie et al.[106] Targeted formation of Az-B(4*Z*)P was prepared as previously reported by our group.[55, 102] All reagents were ACS grade or higher. TAMRA DBCO (Sigma-Aldrich 760773), DBCO Magnetic Beads (Jena Bioscience CLK-1037-1), and Soybean Agglutinin 594-Conjugate (Thermo Fisher L32462) were purchased from indicated suppliers.

Huisgen-Cycloaddition of Azido Isoprenoids

Azido modified isoprenoids (neryl, geranyl, or BP/BPP) were labeled with one equivalent of TAMRA-DBCO (100 µM) in either water or UppS/acid phosphatase reaction conditions directly. Reactions were typically complete in under 60 min. Products were analyzed after this time on an Agilent 1100 HPLC system (Agilent Eclipse XBD-C18, 3.5 µM, 4.6 x 50 mm) monitoring for the TAMRA fluorophore (454/525 ex/em). A gradient method was used to separate BPPs and BPs with 100 mM ammonium bicarbonate (A) and *n*-propanol (B). Line B was increased from 15% to 95% over 36.9 min, then held at 95% until 42 min, then decreased to

15% until 45 min. LC-MS analysis of non-conjugated azide materials was performed on an Agilent 1260 LC and 6,000 series ESI-MS single quad with four channels for monitoring ions (Waters XBridge Peptide BEH C18, 3.5µM, 4.6 x 50 mm). *n*-Propanol was increased at a rate of 4% per min, starting at 20% with 80% of a 0.1% ammonium hydroxide solution as the co-solvent. Mass values for Az-BP's (*Z*1-*Z*10) were scanned following acid phosphatase treatment (Figure B1).

Sugar Modifying Enzyme Preparation and Analysis

The Pgl sugar modifying enzymes PglF, E, and D were prepared identically to previous reports, without the addition of Triton X-100.[94] The preparation of UDP-DiNAcBac was performed in a total volume of 4 mL with 50 mM Tris-Acetate pH 7.5, 50 mM NaCl, 5 mM UDP-GlcNAc, 4.0 µM PLP, 15 mM L-glutamate, and 6 mM acetyl coenzyme A. PglF, E, and D (25 µm each) were added sequentially and an aliquot taken for HPLC analysis after incubation at 37 °C for 1h. The reaction mixture was then filtered (30K MWCO) and dried under vacuum in a centrifugal evaporator. This crude solution was then resuspended in 400 µL water and used as the sugar donor source for subsequent Pgl assembly.

WbpP was cloned from *Vibrio vulnificus* MO6-24 into a pET-24a vector with primers outlined in Table B1. An overnight culture of BL21-RP transformants was used to inoculate 0.5 mL of TB (10 g tryptone, 12 g yeast extract, 2 mL glycerol). The culture was grown at 37 °C with shaking until the OD reached 0.6, then the temperature was dropped to 25 °C . IPTG (1 mM) was added at this time and the culture was allowed to induce for 4 h or overnight. Pelleted cells were lysed in WbpP-Buffer (50 mM Tris-HCl pH 8, 200 mM NaCl) with 20 mM imidazole and the viscous liquid was pelleted at 10,000 RCF for 30 min at 4 °C. The supernatant was then passed through 2 mL Ni-NTA agarose and washed in WbpP-Buffer with 50 mM imidazole, and

finally eluted in WbpP-Buffer with 500 mM imidazole. Elutions containing protein were collected and dialyzed three times in WbpP-Buffer.

HPLC analysis of all sugar modification reactions occurred on an Agilent 1100 monitoring at an absorbance of 260 nm (Agilent Zorbax NH_2, 5 µm, 4.6 x 250 mm). Buffer A was prepared by titrating 250 mM ammonium acetate solution with acetic acid to pH 4.5, ultimately producing 685 mM Acetate-NH_4. All sugar modifying reactions were monitored with an isocratic method containing 80% A and 20% B (water).

Protein Expression of Pgl Transferase Enzymes

A series of DE3 cell lines were assessed for protein expression in autoinduction media with P-buffer (Figure B3).[116] BL21-Star cells were used for protein expression herein. Overnight cultures were used to inoculate 0.5 L autoinduction media (10 g tryptone, 12 g yeast extract, 2 mM $MgSO_4$, 2.5 mL glycerol, 0.25 g glucose, 1 g lactose, 100 mM phosphate buffer pH 7.4) with 100 µg/mL kanamycin. Cultures were grown at 37 °C with generous shaking at 300 rpm for 4 h, then the temperature reduced to 20 °C for 24 h. The expression of PglI, specifically, was enhanced by the addition of 3% ethanol in growth media (data not shown).[117] Pelleted cultures were then lysed and purified under identical conditions to previous reports.[93, 97]

Pgl N-linked oligosaccharide bioassembly on Azido linked Isoprenoids

The reactions were set up in a total volume of 40 µL with 50 mM Tris-Acetate pH 7.5, 1 mM $MgCl_2$, and 100 µM of tagged isoprenoid (Az-B(4*Z*)P or Az-NP). Glycans were then added at a final concentration of 200 µM UDP-DiNAcBac, 2 mM UDP-GalNAc, and 1 mM UDP-Glc. Triton extracted Pgl enzymes (8 µg/mL each) were added sequentially and no additional triton was added (a final concentration of 0.2% accounting for carryover). The reaction was proportionally scaled up to 500 µL and filtered (MWCO 10,000) prior to magnetic bead immobilization. When WbpP was used for *in situ* generation of UDP-GalNAc, reactions

contained 1 µM enzyme and 5-fold excess UDP-GlcNAc. Enzyme activity was monitored by LC-MS on an Agilent 1260 LC and 6,000 series ESI-MS single quad with four channels for monitoring ions. The column (Waters XBridge Peptide BEH C18, 3.5µM, 4.6 x 50 mm) was either connected to the MSD, for azide tagged materials, or the column eluent was split with a TEE connector between the MSD and FLD (2:1 split), for TAMRA tagged materials. A gradient method was used with 0.1% ammonium hydroxide (A) and *n*-propanol (B). For Az-NP, line B was increased from 5 to 15% over 10 min, then reduced to 5% until 12 min. For Az-B(4*Z*)P, line B was increased from 15 to 30% over 10 min, then reduced to 15% until 12 min.

PglA, J, H, and I Glycan Specificity Assay

Pgl intermediates were produced as described in the previous section with Az-B(4*Z*)P as the substrate. Overnight reactions were extracted in an equal volume of *n*-butanol three times and dried under a gentle stream of air to prepare intermediates for subsequent reactions. Dried material was resuspended in Pgl reaction buffer, as described above, with 5 mM UDP-GlcNAc in place of -GalNAc. Prepared reactions for *in situ* generation of UDP-GalNAc additionally contained 1 µM WbpP.

DBCO Magnetic Bead Surface Modification and Detection

Magnetic beads (0.8 mg) functionalized with DBCO were washed with water three times. A crude reaction mixture containing either Pgl heptasaccharide or Az-NP (40 nmol each) was added to the washed beads. The mixture was incubated at room temperature overnight with gentle agitation. The magnetic resin was magnetically decanted and the supernatant reserved for LC-MS analysis. The Pgl functionalized beads were then washed with water three times, resuspended at 1 mg/mL then stored at 4 °C. For lectin affinity assays, 5 µL modified beads were blocked with 3% BSA for 30 min, then washed with water. The beads were then resuspended in 200 µL of 0.1 µg/mL of Soybean Agglutinin 594-conjugate for two hours prior to three water

washes, 5 min each. All steps occurred with spinning on an end-over-end rotator at room temperature. The beads were magnetically decanted, then briefly spun and reconstituted in the residual water following centrifugation (~ 5 µL). The solution was transferred to dry nitrocellulose square and immediately imaged.

Appendix B: Supplemental Information

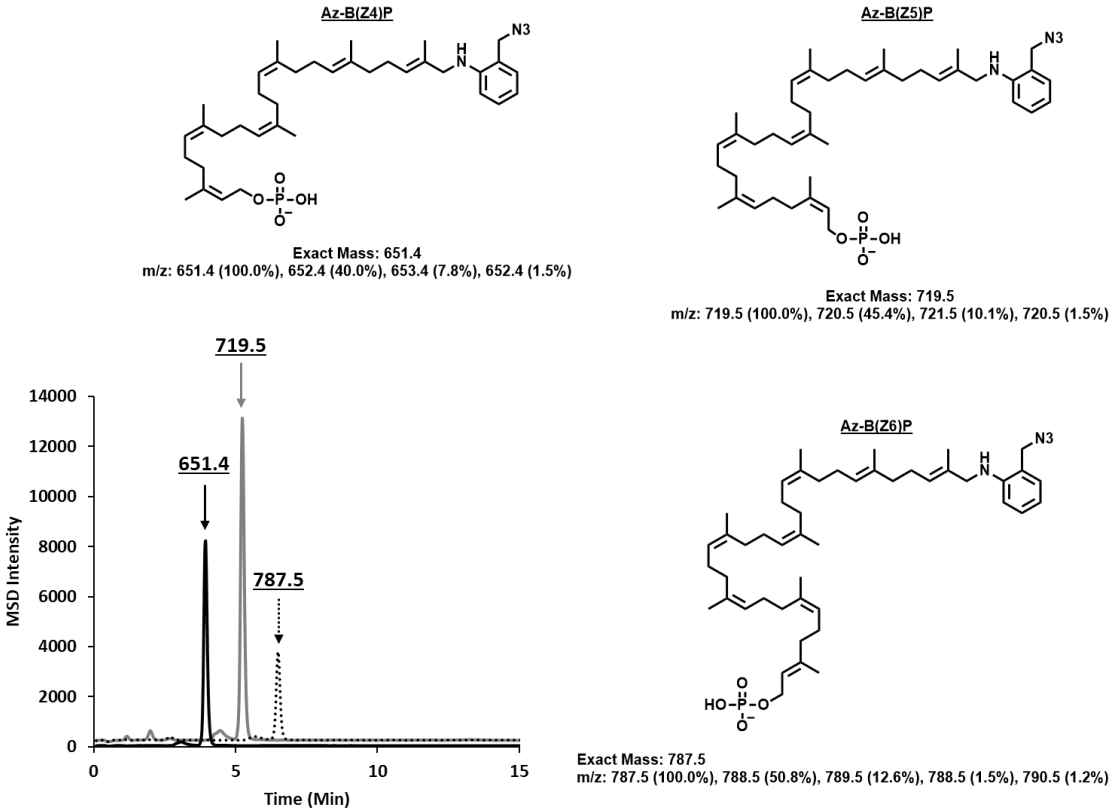

Figure B1. LCMS of Az-BP product formation by UppS and acid phosphatase.
SIM analysis of $[M\text{-}1H]^{-1}$ ion species in separate channels corresponding to Az-BPs from *Z*4-6 (651.4, 719.5, and 787.5 m/z respectively).

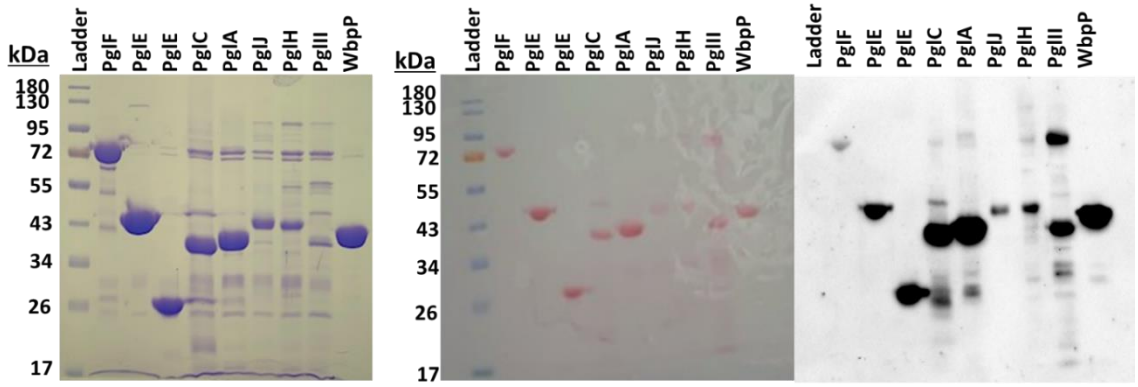

Figure B2. SDS-PAGE, Ponceau Staining, and Western blot of proteins used in this work. SDS-PAGE gels were stained with coomassie. Nitrocellulose blots were stained first in ponceau to confirm successful transfer. Western blots were treated with primary mouse anti-His (1:10,000 dilution) followed by anti-mouse conjugated HRP (1:20,000 dilution). Staining occurred with a chemiluminscent substrate and an exposure time of 30s. All Pgl expressions were carried out in BL21-Star cells and PglI cultures contained 3% ethanol.

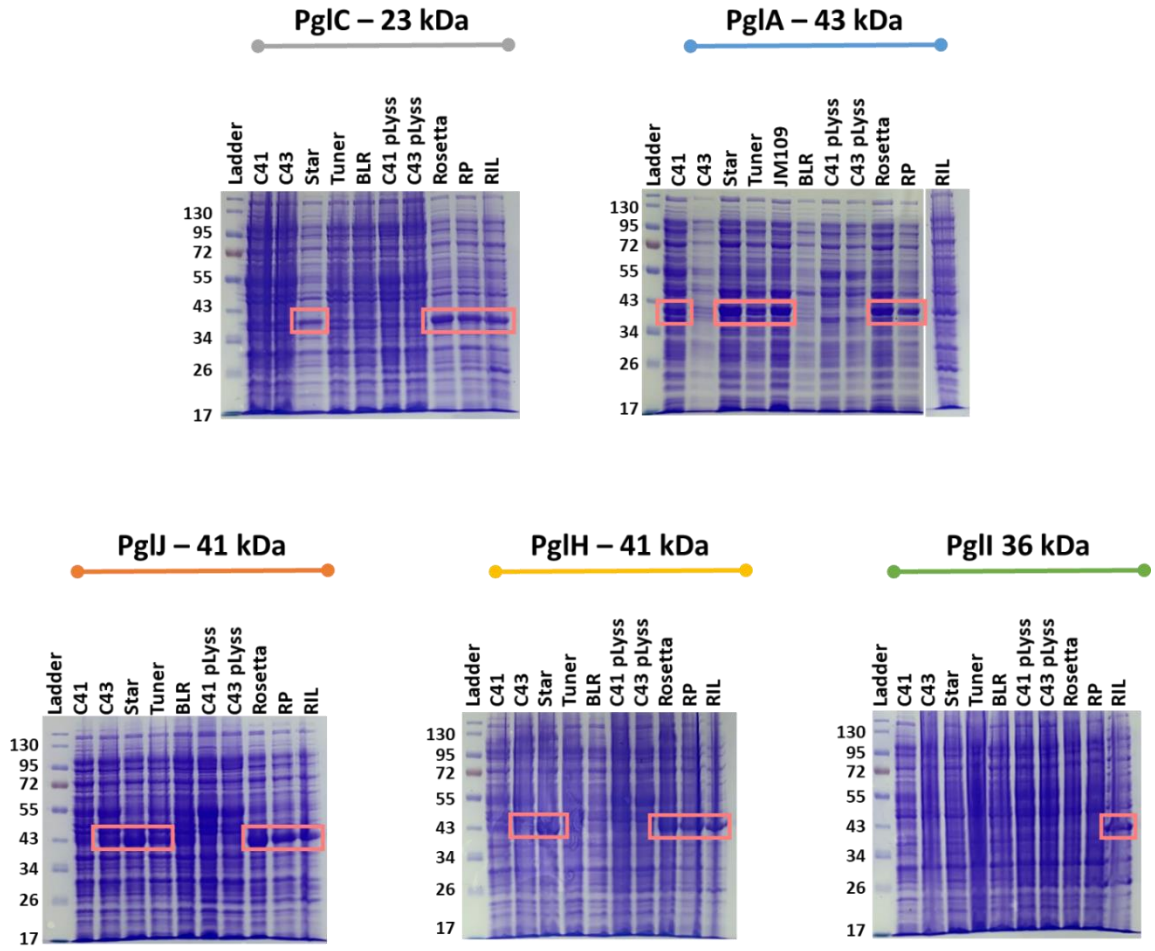

Figure B3. Pgl Expression Cell Line Comparison.
Whole cell lysates on SDS-PAGE of respective transferase enzymes in different cell backgrounds. PglC and PglI appear heavier than their anticipated protein size, which is not unusual for membrane associated proteins.[118] PglI expression was carried out in the absence of 3% ethanol.

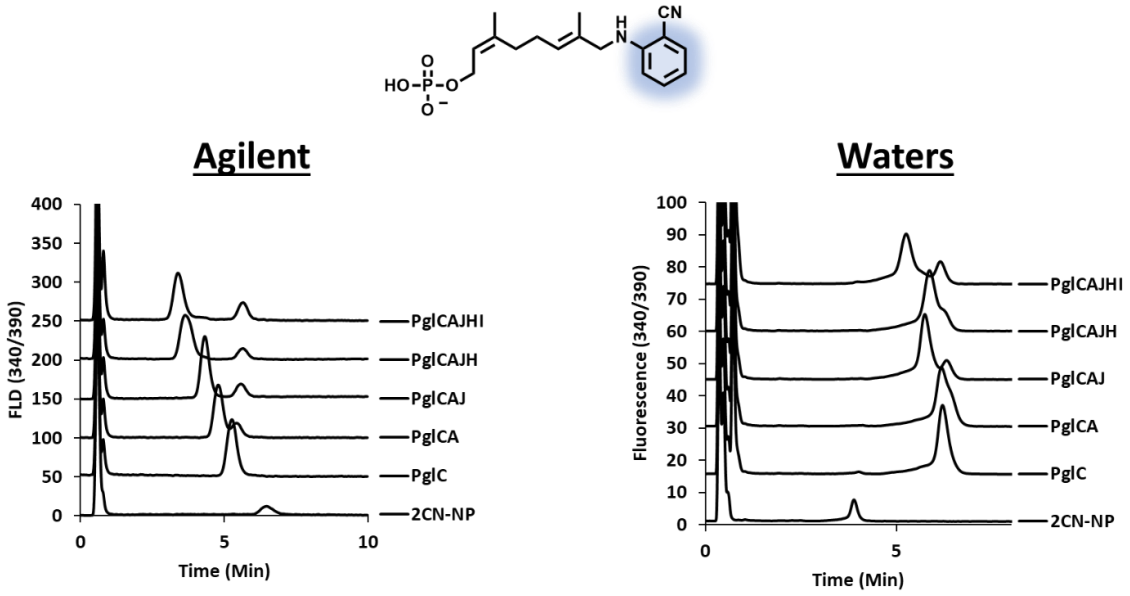

Figure B4. Comparison of Waters XBridge BEH C18 and Agilent C18 Elution Patterns.
A fluorescent nerol monophosphate substrate (2CN-NP) was used to evaluate the elution behavior of pgl formation with two different C18 columns. The same sample and injection volume was used to perform this analysis. The Agilent column (PN: 935967-902) produced an oligosaccharide product that eluted faster, which is the anticipated behavior from the addition of glycans. The Waters column (PN: 186003611) produced a notable later elution upon the first glycan addition by PglC. Small decreases in retention were noted, except for the PglCAJH product which produced a slightly later shift than the corresponding J product. This discrepancy is likely due to secondary column interactions associated with the Waters XBridge BEH C18.

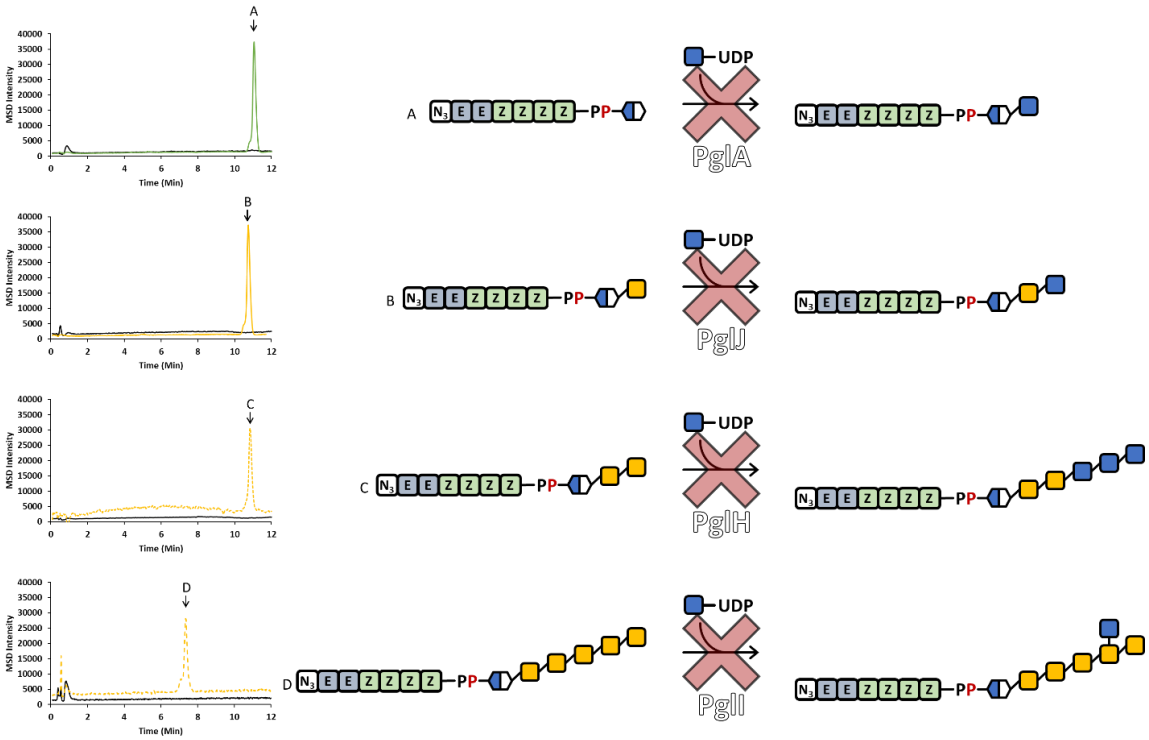

Figure B5. Pgl HexNAc Specificity.
Sugar specificity with pgl enzymes and their respective substrate with UDP-GlcNAc in which no transferase activity is observed.

Table B1. Primers for *wbpP* PCR amplification

Forward	CGACGGATCCACCAAATACGAAAAAATCCAACAAG
Reverse	CCACTCTCGAGTTTTTTATCATTTATAAAGCTTATATACCATGGC

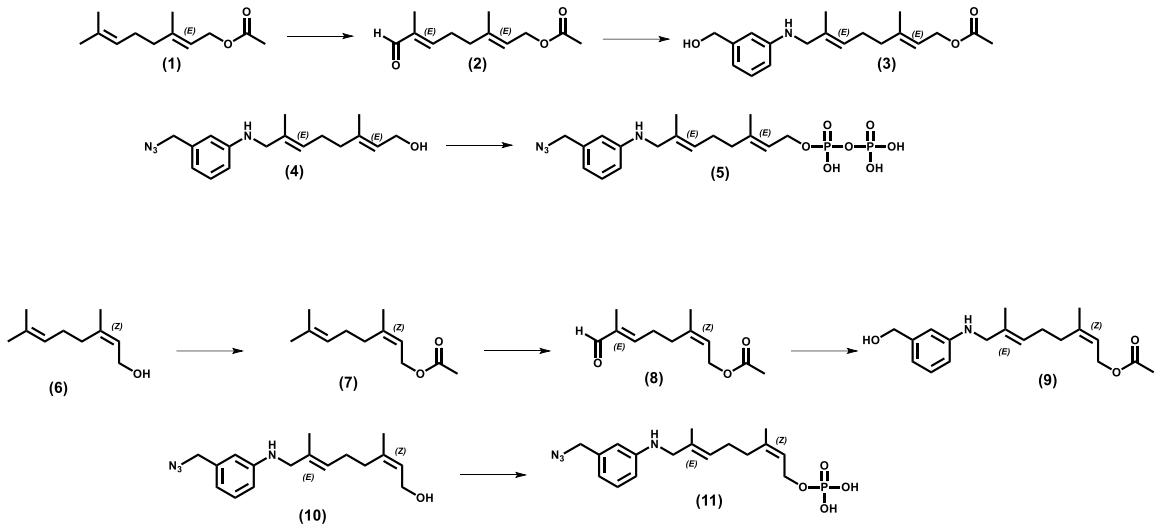

Synthesis Reaction Scheme

The synthesis protocol for azido- modified geranyl diphosphate and neryl monophosphate analogues have been adapted from Chehade *et. al* and Labadie *et. Al*. [119, 120]

Synthesis of neryl acetate (7)

Nerol (5 g, 32.4 mmoles), excess pyridine (10 mL) and acetic anhydride (10 mL) were added to a round bottom flask. The reaction was allowed to stir at room temperature overnight and then diluted with ether. The crude product was washed with saturated sodium bicarbonate (2x), water, then brine. The organic layer was dried with $MgSO_4$ and the solvent removed by rotary evaporation. The resulting oil was used directly for subsequent allylic oxidation without further purification. ^{1}H NMR (7) (500 MHz, $CDCl_3$, δ): 5.26 (q, *J* = 7.1, 1H), 5.00 (q, *J* = 6.2, 1H), 4.46 (d, *J* = 7.6, 2H), 2.04-1.95 (m, 4H), 1.67 (s, 3H), 1.59 (s, 3H), 1.51 (s, 3H). Yield = Theoretical.

Synthesis of 3,7-Dimethyl-1-acetoxy-2,6-octadien-8-al (2 or 8)

Excess CH_2Cl_2, 0.283 g SeO_2 (2.55 mmols), 0.354 g salicylic acid (2.56 mmols) and 70% tert-butyl hydroperoxide (13.1 mL, 135 mmols) were added to a round bottom flask and placed in an ice bath. Once the mixture was homogeneous, the acetate (1 or 7) was added (5 g, 25.47 mmols) and the reaction was left stirring overnight. The reaction was diluted with ether and extracted in a separatory funnel with the following: 5% $NaHCO_3$, saturated $CuSO_4$, saturated $Na_2S_2O_3$ twice, and 0.9% NaCl. The organic layer was dried with anhydrous $MgSO_4$ and the solvent was removed by reverse pressure. The remaining oil was purified using silica flash chromatography using a 5% (v/v) EtOAc/Hexanes solution. Typical yields of the aldehyde product were between 15-35%. ^{1}H NMR (8) (500 MHz, $CDCl_3$, δ): 9.36 (s, 1H), 6.45 (q, *J* = 7.3, 1H), 5.40 (q, *J* = 6.3, 1H), 4.53 (d, *J* = 7.8, 2H), 2.44 (q, *J* = 5.6, 2H), 2.29 (q, *J* = 7.6, 2H), 1.67 (s, 3H), 2.02 (s, 3H), 1.77 (s, 3H), 1.72 (s, 3H). ^{1}H NMR of (2) has been previously published by our group.

Synthesis of 8-N-m-benzyl alcohol-amino-3,7-dimethyl-2,6 octadien-1-ol (3 or 9)

A round bottom flask was flame-dried under argon gas to remove any moisture. Once

cooled, excess CH_2Cl_2, 1.3 g of 3-aminobenzyl alcohol (10.56 mmols) and 2.0 g (9.5 mmols) of the aldehyde (2 or 8) were added to the flask followed by 0.75 mL glacial acetic acid (13.11 mmols) and 3.0 g of $Na(OAc)_3BH$ (14.15 mmols). The reaction was left overnight and extracted with chloroform the following day. The product was purified using 30% EtOAc/Hexanes to isolate the desired product. A contaminate with an R_f value similar to the desired compound was co-purified, and did not affect downstream synthesis. All attempts to mitigate this contaminate by using less ethyl acetate during purification resulted in significant losses of the desired compound. ^{1}H NMR (3) (300 MHz, $CDCl_3$, δ): 7.14 (t, *J* = 7.2, 1H), 6.66-6.52 (m, 3H), 5.39 (t, *J* = 6.9, 1H), 5.34 (t, *J* = 6.9, 1H), 4.59 (s, 2H), 4.57 (d, *J* = 7.5, 2H), 3.63 (s, 2H), 2.19-2.08 (m, 4H), 2.03 (s, 3H), 1.72 (s, 3H), 1.68 (s, 3H). ^{1}H NMR (9) (500 MHz, $CDCl_3$, δ): 7.11 (t, *J* = 7.9, 1H), 6.50-6.59 (m, 2H), 6.49 (d, *J* = 5.2, 1H), 5.31 (m, 2H), 4.56 (s, 2H), 4.46 (d, *J* = 3.9, 2H), 4.08 (d, *J* = 5.4, 2H), 3.6 (s, 2H), 2.12 (s, 3H), 2.09-1.98 (m, 4H), 1.75 (s, 3H), 1.67 (s, 3H).

Synthesis of 8-N-m-benzyl azido-amino-3,7-dimethyl-2,6 octadien-1-ol (4 or 10)

The reductive amination products (*3* or *9*) were then dissolved in toluene with 2.1 mL of DPPA (2.68 g, 9.74 mmols) and 2.6 g of benzylic alcohol geranyl acetate (8.2 mmols) were added and cooled to 0 °C. Then, 1.5 mL of DBU (1.53 g, 2.91 mmols) was added and allowed to stirred on ice for 2 hours. The reaction was then left at room temperature overnight and quenched with the addition of an equal volume of water. The reaction was diluted with ethyl acetate. The organic layer was dried with $MgSO_4$ and the solvent removed under reduced pressure. Without further purification, the crude product (theoretical yield of 8.2 mmol) was deacylated in the same flask. Methanol (40 mL) and 4.7 g of K_2CO_3 (34 mmol) dissolved in 5 mL of water, then was added to the flask and left at room temperature overnight. Pure 8-N-m-benzyl alcohol-amino-3,7-dimethyl-2,6 octadien-1-ol was obtained with 40% EtOAc/Hexanes (R_f = 0.3 in 30% EtOAc/Hexanes). ^{1}H NMR (4) (300 MHz, $CDCl_3$, δ): 7.14 (t, *J* = 7.8, 1H), 6.60-6.51 (m, 3H), 5.36 (q, *J* = 6.5, 2H), 4.18 (s, 2H), 4.08 (d, *J* = 7.0, 2H), 3.60 (s, 2H), 2.14-2.02 (m, 4H), 1.64 (m, 6H). ^{1}H NMR (4) (300 MHz, $CDCl_3$, δ): 7.14 (t, *J* = 7.8, 1H), 6.60-6.51 (m, 3H), 5.36 (q, *J* = 6.5, 2H), 4.18 (s, 2H), 4.08 (d, *J* = 7.0, 2H), 3.60 (s, 2H), 2.14-2.02 (m, 4H), 1.64 (m, 6H).

Synthesis of (E, E,)-8-N-m-benzyl azido-amino-3,7-dimethyl-2,6 octadiene diphosphate (5)

Next, the benzyl azido geranyl alcohol (*4*) was brominated followed by subsequent diphosphorylation. To a flame dried flask, 1 mL of a 100 mg/mL solution in CH_2Cl_2 of 8-N-m-benzyl alcohol-amino-3,7-dimethyl-2,6 octadien-1-ol (333 µmol) was added upon cooling to room temperature under argon. From a 1 M solution, 0.17 mL of PBr_3 in Cl_3CH (170 µmol) was then added to the flask, without further addition of solvent. Bromination occurred almost instantaneously, and was checked by TLC. Without further purification, 1.8 mL of tris tetra n-butyl ammonium diphosphate in acetonitrile (0.5 mg/mL) was added and the reaction (999 µmol) and was left at room temperature for no longer than 2h. The solvent was removed under reduced pressure without heat. The resulting viscous solution was resuspended in minimal 25 mM ammonium bicarbonate (generally less than 0.5 mL). The crude reaction was then placed directly on NH_4^+ charged cation exchange resin and eluted with the same buffer. The compound was then frozen and lyophilized prior to purification by HPLC. ^{1}H NMR of (5) (500 MHz, D_2O, δ): 7.13 (t, *J* = 7.64, 1H), 6.66 (m, 3H), 5.30 (q, *J* = 5.97, 2H), 4.36 (t, *J* = 6.59, 2H), 4.17 (s, 2H), 3.54 (s, 2H), 2.06 (m, 2H) 1.97 (m, 2H), 1.58 (s, 3H), 1.51 (s, 3H). ^{31}P (D_2O, δ): -6.30 (1P), -9.83 (1P). Expected m/z 459.1, obtained 459.3 m/z; Extinction coefficient ε= 4,345 M^{-1} cm^{-1} at 260 nm; Typical yield =25-35%

Synthesis of (Z, E)-8-N-m-benzyl azido-amino-3,7-dimethyl-2,6 octadiene monophosphate (11)

To a flame dried flask, 1 mL of a 100 mg/mL solution in CH_2Cl_2 of (*10*) (333 μmol) and excess trichloroacetonitrile (217 μL, 2.2 mmol) was added under argon. Solid tetra-n-butylammonium dihyrogen phosphate (226 mg, 6.7 mmol) was added next, prepared from the lyophilized product after titrating phosphoric acid.[121] The reaction was stirred for 10 min and the solvent removed. The viscous solution was resuspended in an equilibrated mixture of THF (2 mL) with 25% (v/v) ammonium hydroxide (0.2 mL) and stirred for 30 min. Next, a 5 mL of a toluene:methanol mixture (1:1) was added for an additional 20 min. The resulting precipitate was removed by filtration and the solvent removed. The crude reaction was resuspended in minimal 25 mM ammonium bicarbonate with 10% isopropanol (generally less than 0.5 mL) and placed directly on NH_4^+ charged cation exchange resin and eluted with buffer. The compound was then frozen and lyophilized prior to purification by HPLC purification. Purified fractions were dried down under vacuum. ^{1}H NMR of (10) (500 MHz, D_2O, δ): 7.00 (t, *J* = 7.64 1H), 6.47 (m, 3H), 5.36 (t, *J* = 6.81, 2H), 5.26 (t, *J* = 6.54, 1H), 4.33 (t, *J* = 6.75, 2H), 3.99 (s, 2H), 3.67 (s, 2H), 1.99 (s, 4H), 1.60 (s, 3H), 1.49 (s, 3H). ^{31}P (D_2O, δ): 1.46 (1P). Expected m/z 379.2, obtained 379.0 m/z; Typical yield ~ 50%

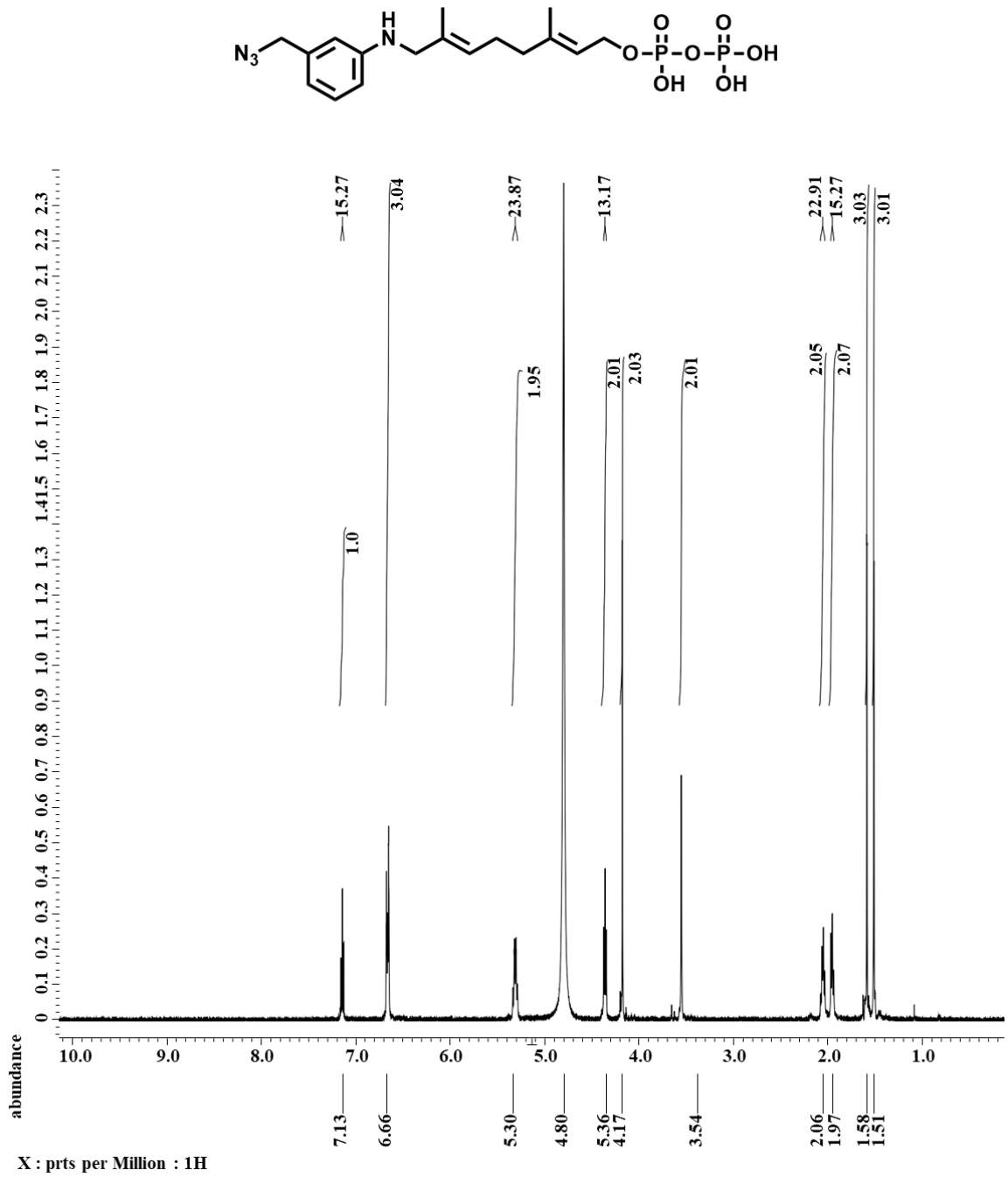

^{1}H NMR of Az-GPP (5)

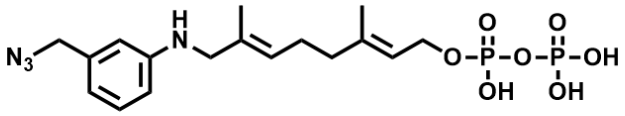

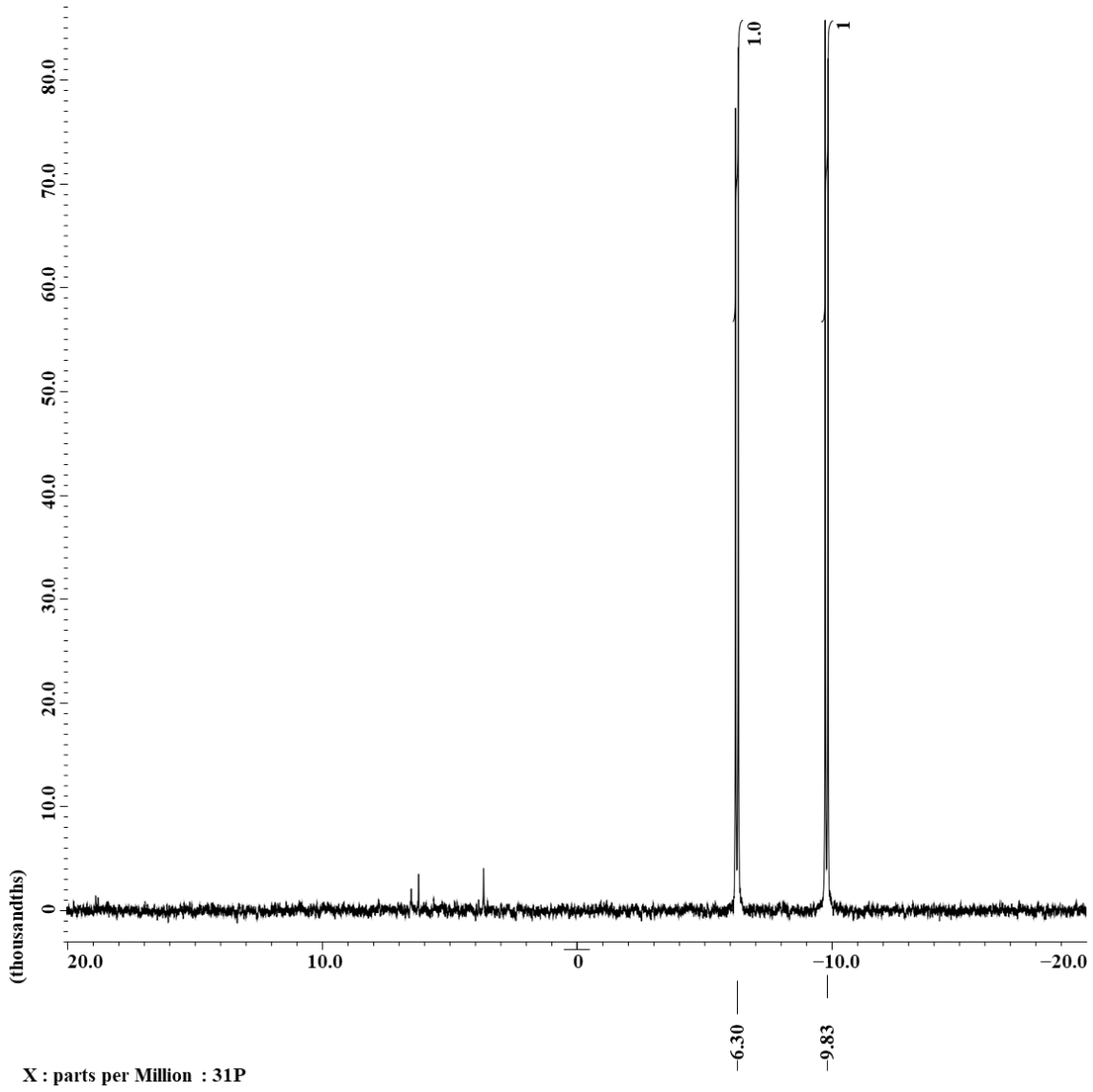

^{31}P NMR of Az-GPP (5)

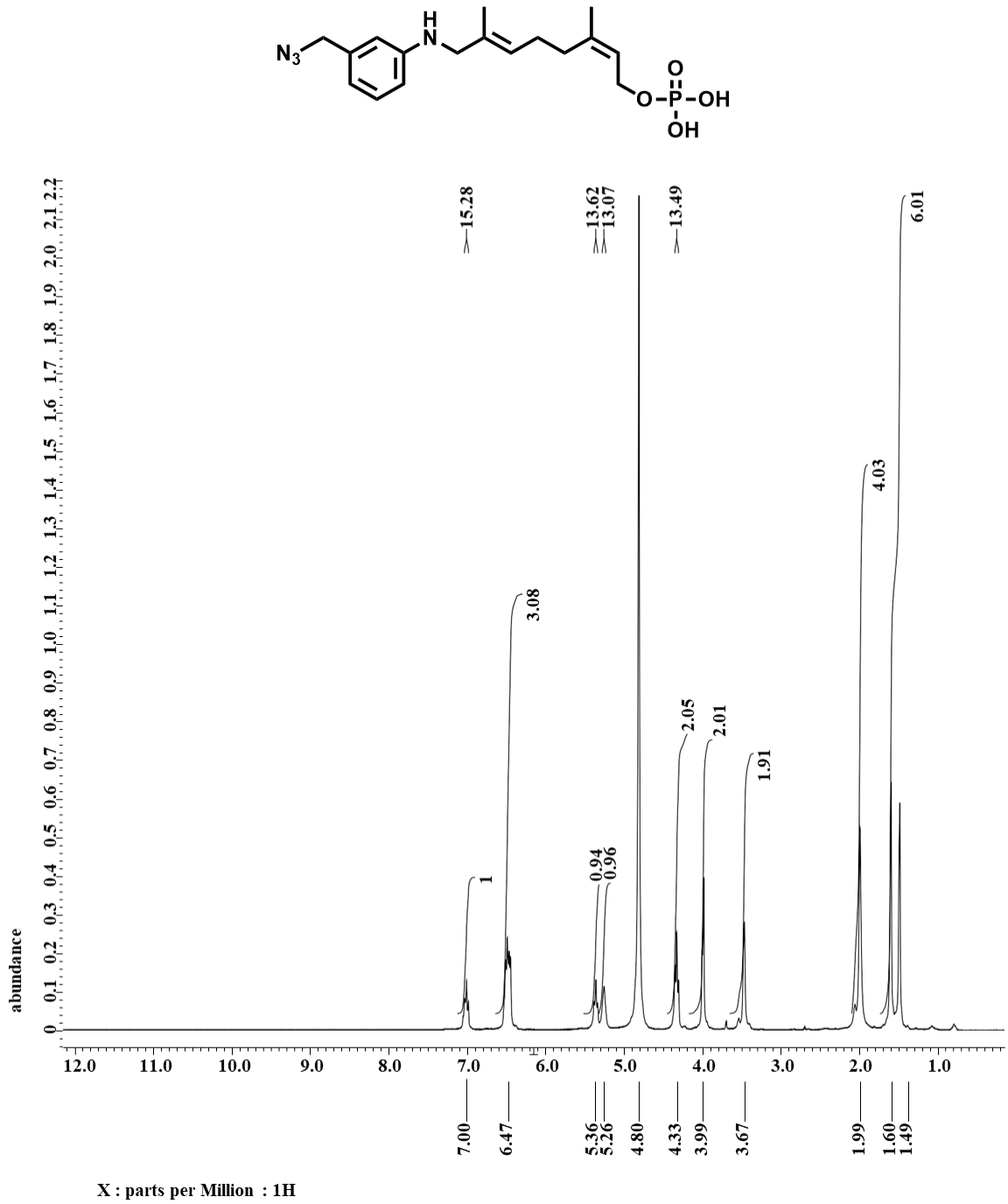

^{1}H NMR of Az-NP (11)

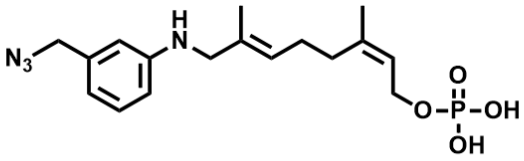

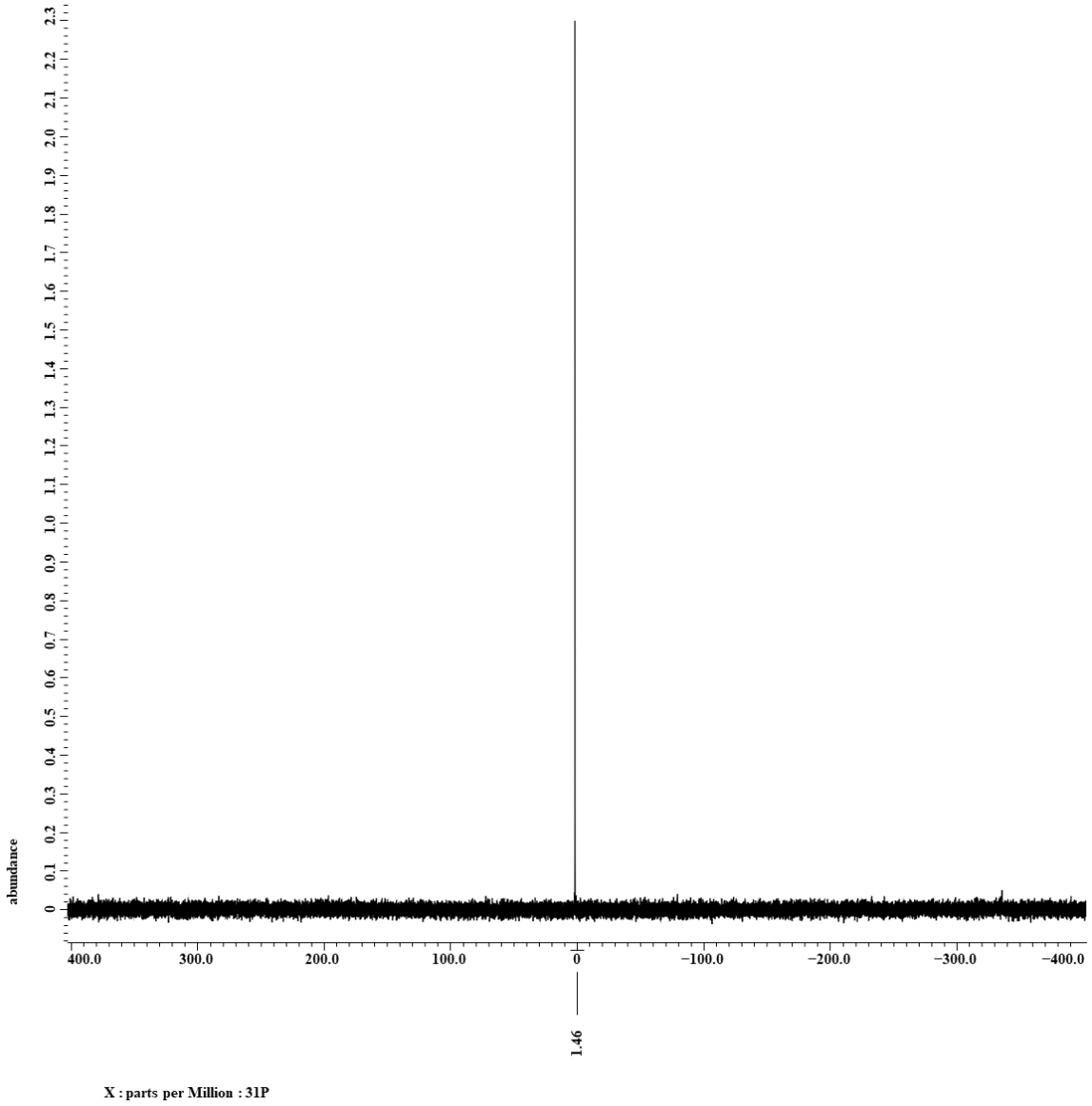

^{31}P NMR of Az-NP (11)

CHAPTER 4: TRACKING COLANIC ACID PYRUVYLATED HEXASACCHARIDE FORMATION FROM STEPWISE BIOSYNTHESIS INACTIVATION IN ESCHERICHA COLI

Author Contributions: Data acquisition, manuscript figures, and methodology were developed by Amanda Reid, Kyle Jones, and Matthew Jorgenson. Dr. Colleen Eade performed genetic work to produce rcsA mutants. Colanic acid single deletion mutants were prepared by Matthew Jorgenson. The manuscript was prepared by Amanda, and reviewed by all authors. We would like to thank Dr. Kevin Young and Dr. Dev Ranjit for suppling some of the strains used in this work.

Overview

Colanic acid is a glycopolymer loosely associated with the outer membrane of *Escherichia coli* that plays a role in pathogen survival. For nearly six decades since its discovery, the functional identities of the enzymes necessary to synthesize colanic acid have yet to be assessed in full. Herein, we developed a method to detect the lipid-linked intermediates from each step of colanic acid biosynthesis in *E. coli*. The accumulation of each enzyme product was made possible by inactivating sequential genes involved in colanic acid biosynthesis. Upregulating the colanic acid operon by inducing *rcsA* transcription was required to detect the buildup of intermediates. LC-MS analysis revealed that these accumulated materials were consistent with the well-documented composition analysis. Recapitulating the native bioassembly of colanic acid enabled us to identify the functional roles of the last two enzymes associated with the hexa- and pyruvlated hexasaccharide for the first time. These findings provide insight toward the development of methods for the identification of enzyme functions during cell envelope synthesis.

Introduction

The bacterial cell envelope is a formidable barrier providing protection from numerous environmental stressors, antimicrobials, and host immune systems. Surface polysaccharides comprise a major component of the cell envelope and play specific roles in mediating cell

adhesion, immune system evasion, and biofilm formation, among other important physiological functions that are central to bacterial proliferation.[122] The exopolysaccharide colanic acid, for example, confers protection to members of the *Enterobacteriaceae* family such as *Escherichia coli* while in inhospitable environments.[123-125] Colanic acid may also act as a scaffold for biofilm formation.[126] First reported nearly 60 years ago, all but the last two steps associated with colanic acid production have been elucidated to date.[26, 127] Corroborating genetic predictions with biosynthetic function is important not only to characterize enzymatic activity, but also to identify conditions in which colanic acid can be produced in controlled environments.

The colanic acid operon contains genes encoding six glycosyltransferases and three sugar modifying enzymes that lead to the production of the repeating unit pyruvylated hexasaccharide (**Figure 1**).[128] Like many bacterial surface glycans, colanic acid is produced on the isoprenoid scaffold bactoprenyl phosphate (**BP**). The identification of the first six enzymatic roles associated with early stages of colanic acid bioassembly were previously identified with a nonnative fluorescently-modified polyisoprenoid.[26] *In vitro* reconstitution revealed that sequential glycosylation and modification of the polyisoprenoid led to the formation of the diacetylated pentasaccharide. The putative galactose transferase, WcaL, and subsequent pyruvylation by WcaK remain unconfirmed *in vitro* to date. It is not clear whether the inactivity of these last two steps was due to the unnatural lipid substrate used to characterize each step, or perhaps other reasons associated with glycan bioassembly *in vitro*.

A number of superfluous artifacts can arise during *in vitro* bioassays. Relaxed substrate specificity of glycans has been observed with some glycosyltransferases.[98, 102, 129] For instance, the initiating phosphoglycosyltransferase WbaP from *Salmonella enterica* transfers phospho-glucose, a non-native substrate, *in vitro* but does not extensively catalyze this reaction *in vivo*.[29, 102]

Membrane-associated proteins are notoriously difficult to express and purify for a variety of reasons that include unstable plasmids, toxic proteins, low yields, and inclusion body formation (i.e., misfolded proteins).[130, 131] Similarly, obtaining naturally occurring lipid-linked intermediates from live cells is challenging due to competition for BP and the lack of methods available to detect these materials.[132] Some essential cell envelope intermediates are present in detectable quantities but it is not known if non-essential surface glycans like colanic acid are also sequentially accumulated.[132, 133] Increasing capsule production by modifying regulatory genes has been shown to enhance mucoid phenotypes associated with colanic acid production.[29, 134-136] However, genetic disruption of exopolysaccharide biosynthesis negatively affects cell physiology.[59, 137] This is explained by sequestration of BP in the form of over-accumulation of dead-end intermediates and also the reduction of free BP for peptidoglycan cell wall synthesis, an essential component of the cell envelope.

Methods for detecting lipid-linked oligosaccharide intermediates have recently been reported by our group. Enterobacterial Common Antigen was elucidated by coupling deletion mutants with LC-MS detection.[138] Therefore, we hypothesized that it might also be possible to detect colanic acid intermediates by utilizing a similar approach. Lipid-linked oligosaccharides were extracted from cells containing a single deletion of each gene involved in colanic acid synthesis. These were compared to *in vitro* synthesized intermediates which served as standards for comparison.[26] Lastly, we sought to corroborate the *in vitro* activity of the last two steps of colanic acid biosynthesis with genetic analysis. This could address whether or not isolated enzymes could indeed use native substrates, or if other problems were present with substrate recognition. Our findings provide methods to reconstruct early stages of non-essential surface glycan synthesis as they exist in nature.

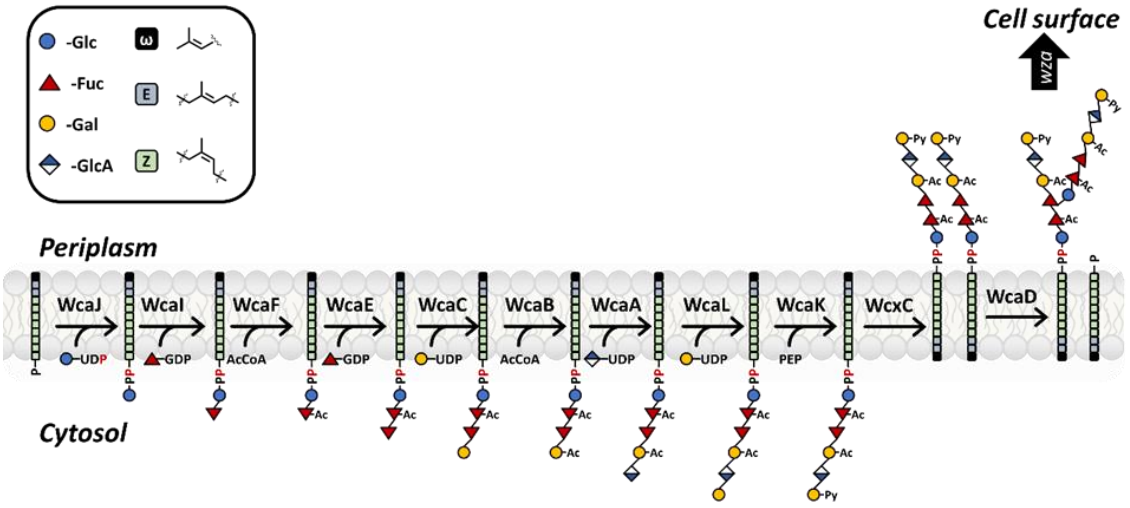

Figure 4.1. Bioassembly of the colanic acid repeating unit.
Bactoprenyl monophosphate, a common lipid carrier, is comprised of five-carbon isoprenoid building blocks (either *E* or *Z* double bond configuration). The colanic acid repeating unit is assembled on bactoprenyl phosphate and is comprised of glucose, two fucoses, two galactoses, and a glucuronic acid. Nine membrane-associated glycosyltransferases or glycan-modifying enzymes have been implicated in the production of the pyruvylated hexasaccharide. The repeating unit is flipped by WzxC to the periplasm and polymerized by WcaD before exportation to the cell surface by a Wza transporter.

Results and Discussion

In vitro Preparation of Colanic Acid Pentasaccharide

Previous work from our group has demonstrated the *in vitro* preparation of the colanic acid pentasaccharide on a fluorescent analogue of BP.[26] In order to analyze the cellular production of colanic acid intermediates, we first assembled a set of standards to later compare to cell-derived materials. To do this, we used the same set of proteins described previously to prepare the pentasaccharide on native bactoprenyl phosphate.[102] A two-step procedure was used to prepare polyisoprenoid diphosphates with UppS and the native substrate, farnesyl diphosphate. Subsequent extraction and acid phosphatase treatment then generated the corresponding BP. Product formation was monitored in selected ion monitoring (SIM) mode for all *Z*1-10 isoprenoid monophosphates, where *Z* represents the number of *Z*-configuration isoprene units incorporated by UppS (**Figure 4.2**). Mass to charge ratios corresponding to the *Z*6-9 products were observed. Unlike with

fluorescent polyisoprenoids, BPs eluted with a retention time approximately 0.5 min earlier than BPPs (**Figure C1**).

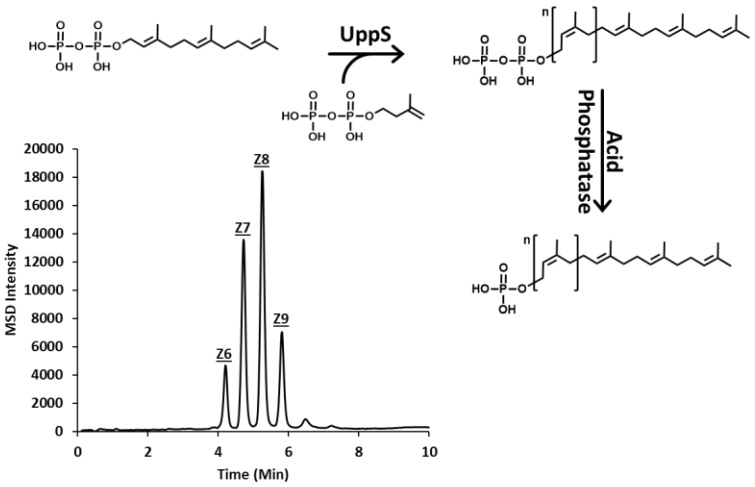

Figure 4.2. Production of bactoprenyl monophosphates.
Elongation of bactoprenyl monophosphate occurs by sequential condensation of eight isopentenyl diphosphates (IPP) to a single farnesyl diphosphate (FPP). Monophosphates were prepared by UppS and subsequent acid phosphatase treatment. LC-MS analysis of acid phosphatase products showed the presence of *Z*n (n=6-9) BPs, where n is the number of *Z* configuration isoprene units added by UppS *in vitro*.

The colanic acid pentasaccharide was then assembled on purified B(*Z*8)P (native BP) with established methods.[26] Colanic acid intermediate formation was monitored in SIM with the indicated mass to charge ratios selected individually for each intermediate, with indicated ion species (**Figure 4.3A**). This resulted in a unique SIM chromatogram corresponding to stepwise enzyme product formation for each intermediate numbered 1-10 (**Figure 4.3B**). Retention time shifts of -0.1 min occurred after each glycan addition for the mono-, di-, tri-, and tetrasaccharide products. Retention shifts were absent with acetyl modifications of the di- and tetrasaccharide. These results are consistent with previous observations when utilizing fluorescent BP analogues. A notable shift of -1.1 min was seen for the pentasaccharide after the addition of glucuronic acid.[26] Inactivity of WcaL prevented us from acquiring the hexasaccharide and subsequent pyruvlated

hexasaccharide, which was reported for the fluorescent substrate as well.[26]

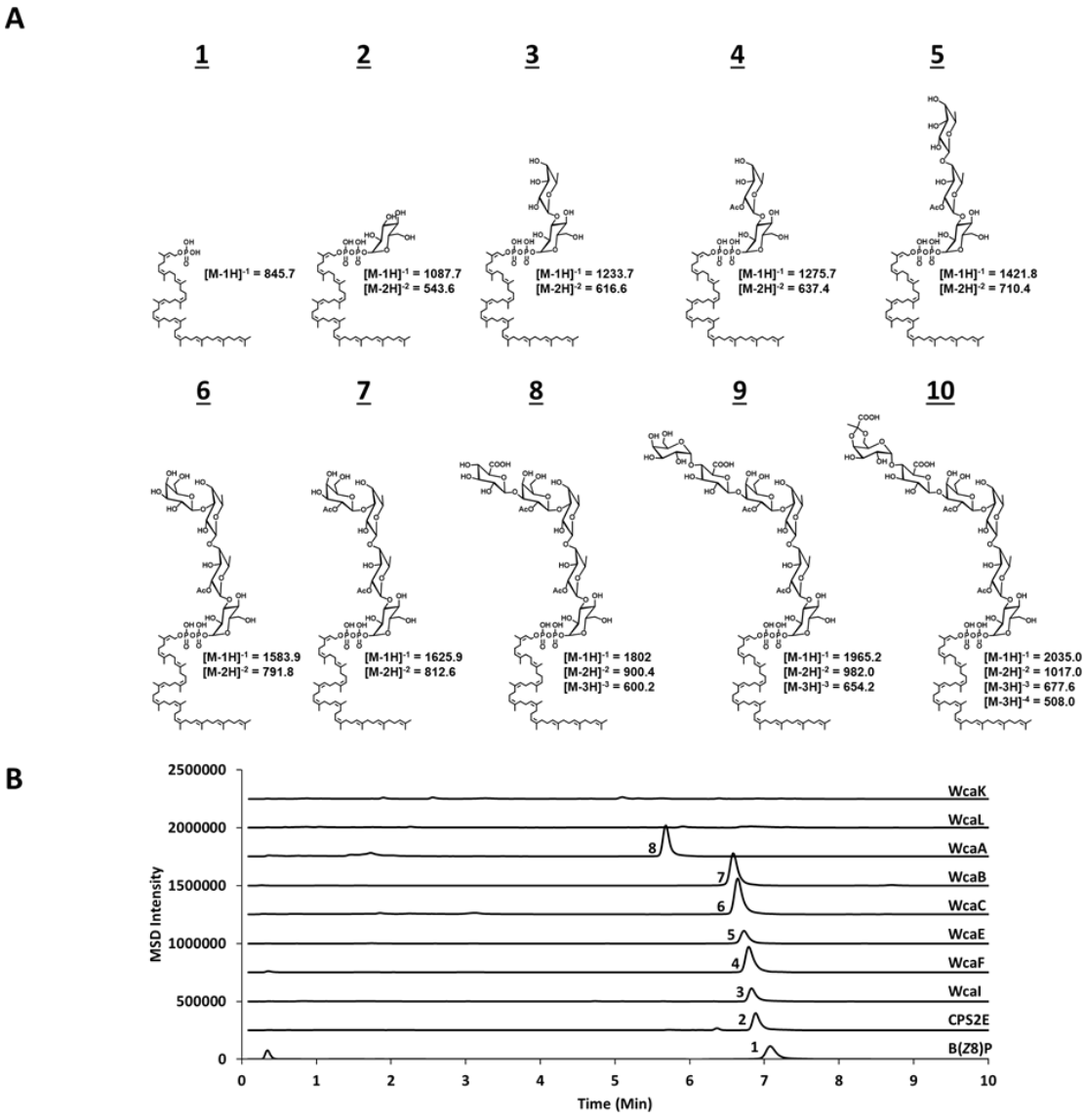

Figure 4.3. LCMS of *in vitro* produced standards of colanic acid intermediates.
(A) Structures of colanic acid enzyme products starting with bactoprenyl phosphate. Indicated mass to charge ratios of charged intermediate species were used for selected ion monitoring in the subsequent detection of colanic acid intermediates. (B) Preparation of the colanic acid pentasaccharide with indicated glycosyltransferase enzymes. Eluted products were observed at 7.1, 6.9, 6.8, 6.8, 6.7, 6.6, 6.6, and 5.7 min for 1-8, respectively. WcaL activity could not be reconstituted in vitro, therefore both the final reactions with WcaL and WcaK showed no product formation.

Colanic Acid Intermediates do not Accumulate in Single Deletion Mutants

To test whether inactivation of sequential transferase or glycan modifying enzymes could lead to the accumulation of colanic acid intermediates *in vivo*, single genes associated with colanic

acid synthesis were individually deleted in *E. coli* to produce null mutants used in this work (**Table C1**). Cells were grown at 25 °C to promote formation of colanic acid and extracts were prepared for LC-MS as described in the methods and materials.[126 139, 140] Each sample was analyzed in selected ion mode for the presence of m/z values corresponding to BP, isoprenoid-linked oligosaccharide intermediates, or the colanic acid repeating unit (**Figure 4.4**). BP (solid black chromatogram) was eluted at an identical retention time as *in vitro* synthesized materials at 7.1 min. The wild-type (WT) parent strain (MG1655) and a complete deletion of the colanic acid operon (ΔCA) acted as controls for comparison. Background cell material eluted at 3.3 min and was present in both the WT and ΔCA strains. However, no intermediates were detected utilizing this method, suggesting either they do not accumulate or accumulate below our limit of detection (**Figure C2**). Herein, this unrelated material has been denoted by a gray arrow.

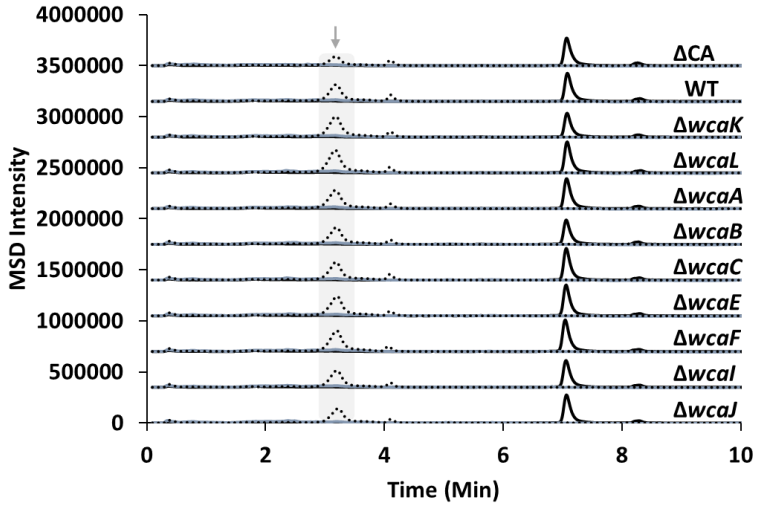

Figure 4.4. Bactoprenyl monophosphate is observed in colanic acid deletion mutants.
Bactoprenyl monophosphate (solid black), oligosaccharide intermediates (solid blue), and colanic acid (dashed black) in selected ion mode. Detectable quantities of bactoprenyl monophosphate, but not lipid-linked oligosaccharides, were observed. Background cellular material eluting at 3.8 min (gray arrow) was not associated with colanic acid production. Mass to charge ratios used for detection were the same as in Figure 3.

It was surprising that intermediate accumulation was absent in these cells despite detectable quantities of BP. The native BP pool was therefore not a limiting factor for intermediate accumulation with these cells. Transcription of the colanic acid operon is induced by the regulators of capsule synthesis (Rcs) signaling pathway.[136, 141] Environmental (e.g. low pH or high salt) or cell envelope stressors activate this cascade terminating at the positive regulator of colanic acid synthesis, RcsA.[142, 143] Conversely, protease degradation of RcsA limits the production of colanic acid.[144] Regulation of Rcs may therefore account for either the lack of intermediate accumulation, or accumulation that lies below our LC-MS detection limit.

Increasing rcsA Expression Promotes Colanic Acid Intermediate Accumulation

We next examined if promoting transcriptional production of the Rcs system could increase the accumulation of colanic acid intermediates. To do this, we incorporated a tetracycline inducible promoter upstream of *rcsA* which, when induced by tetracycline, prompted cells to produce a thick mucoid layer that was absent from ΔCA cells (**Figure C3**). To further promote the possibility of detecting colanic acid intermediates, we supplemented cells with a plasmid encoding IPTG-inducible *uppS* to bolster native BP levels.[138] Cells induced with tetracycline and IPTG were then lysed under identical conditions as the original mutants and were found to accumulate intermediates detectable under identical conditions as *in vitro* synthesized materials (**Figure 4.5**). A total ion scan was performed for each sample and total ion counts generated to demonstrate the presence of all anticipated ion species (**Figure C4**). Each glycan addition produced an analyte with an earlier retention time consistent with *in vitro* colanic acid intermediates. In addition, cell extracts were analyzed for all other intermediates, which demonstrated the presence of only the anticipated intermediate (**Figure C5**). The WT parent and complete colanic acid deletion (ΔCA) strains were also analyzed in SIM for all intermediate ion species (1-9).

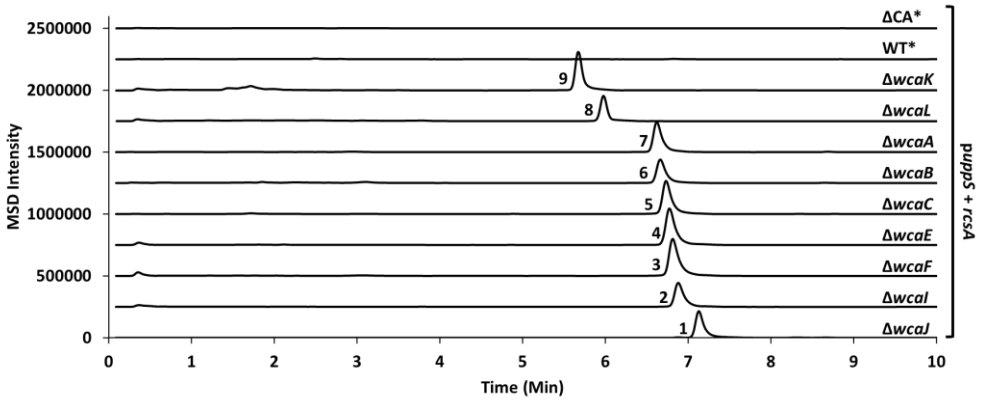

Figure 4.5. LC-MS detection of colanic acid intermediate accumulation.
Indicated single deletion mutants containing tetracycline- and IPTG-inducible *rcsA* and *uppS*, respectively, were lysed and analyzed by SIM in negative mode. Selected mass to charge ratios were identical to *in vitro* synthesized materials in Figure 3. *Indicates that all ion species were selected during SIM monitoring.

These results demonstrate that *rcsA* induction is required to detect colanic acid intermediates. Yet, even with induction, intermediates were not observed in the WT strain. Thus, gene inactivation is required to observe the accumulation of lipid-linked colanic acid intermediates. Deletion of *wcaM*, a gene without a proposed function, did not lead to detectable intermediate formation (**Figure C5**). This was not surprising since loss of WcaM does not affect colanic acid production in *E. coli*.[128, 145] Curiously, mutants accumulating early colanic acid intermediates, corresponding to materials 1-9, produced normally shaped cells (**Figure C6**). This is presumably because sufficient levels of BP were being produced by *uppS* overexpression to meet the demand for peptidoglycan synthesis.

Under typical conditions, RcsA is readily degraded by the Lon protease, which acts to modulate capsular polysaccharide synthesis, among other numerous housekeeping functions.[134, 135] Overexpressing *rcsA* or deleting *lon* is a common strategy for inducing colanic acid production (i.e., mucoidy) in *E. coli*.[29, 146] During our efforts to overproduce colanic acid, we constructed strains with *lon* deleted, which produced a noticeable mucoid layer (**Figure C3**). However, *rcsA* overexpression was preferentially chosen to induce colanic acid production since deleting *lon* is

otherwise deleterious.[135, 147] Mucoid colonies were not observed when tetracycline was used to induce *rcsA* in cells that were grown at 37 °C, likely because RcsA is less stable at temperatures above 30 °C.[148, 149]

Pyruvlated Hexasaccharide Accumulates in Polymerase and Flippase Deficient Mutants but Not Transporter Deficient Mutants

We next sought to accumulate the pyruvlated hexasaccharide repeating unit by removing later enzymes involved in colanic acid biosynthesis, such as the flippase (WzxC), polymerase (WcaD), or exporter (Wza). Mutants lacking these factors were grown and lysed; cell extracts were then analyzed by LC-MS monitoring for the most abundant ion species typically $[M-3H]^{-3}$, of the repeating unit (**Figure 4.6A**). Pyruvlated hexasaccharide was observed in the polymerase mutant (Δ*wcaD*) with apparent ions from the $[M-2H]^{-2}$, $[M-3H]^{-3}$, $[M-4H]^{-4}$ charged species observed (**Figure 4.6B**). Deletion of the colanic acid exporter (*wza*) did not result in the formation of detectable quantities of intermediates nor the colanic acid repeating unit. We reasoned that the formation of polymerized colanic acid may account for the lack of repeating unit accumulation in exporter deficient cells.

Whereas disrupting earlier stages in colanic acid assembly had no appreciable effect on cell shape, mutants lacking the colanic acid exporter (*wza*) or polymerase (*wcaD*) grew as misshapen rods and spheres despite *uppS* overexpression (**Figure 4.6C**). These findings suggests that BP levels are limiting in mutants lacking Wza or WcaD. Though these cells appeared similar, we expected more severe phenotype defects with the polymerase mutant than those of the exporter mutant since the latter should titrate less BP because of polymerization. One possible explanation why Δ*wcaD* cells did not appear worse was offloading of the repeating unit, but not polymerized intermediate, onto lipopolysaccharide by the WaaL ligase.[150] A greater amount of available BP, and thus lower cell rounding, could be expected from liberating colanic acid in this way. Indeed,

deleting *waaL* from cells lacking WcaD resulted in extensive cell lysis when *rcsA* was induced (**Figure 4.6D**). Thus, promiscuous activity by WaaL suppresses defects in the colanic acid polymerase (and probably other BP-related polymerases).

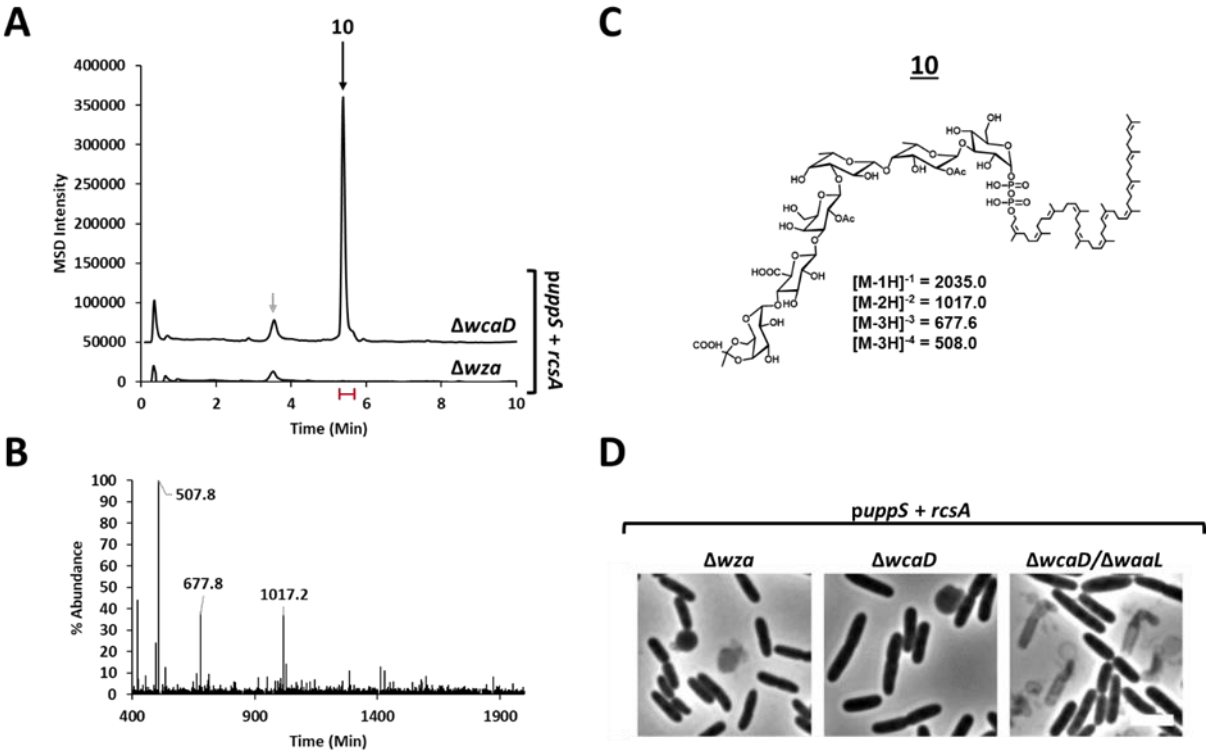

Figure 4.6 Full length colanic acid repeating unit is formed in *wcaD* but not *wza* deficient cells.
(A) SIM chromatograms of the $[M-3H]^{-3}$ ion species for the Δ*wcaD* and Δ*wcaD* mutants. (B) A section of the total ion scan corresponding to the elution of the colanic acid pyruvlated hexasaccharide demonstrating the presence of the $[M-2H]^{-2}$, $[M-3H]^{-3}$, $[M-4H]^{-4}$. (C) The colanic acid repeating unit with anticipated mass to charge ratios. (D) Morphological phenotypes produced by mutants with the indicated genotypes. Background cellular material eluting at 3.8 min (gray arrow) not associated with colanic acid production from both strains. The white bar represents 3 μm.

A previously reported flippase (*wzxC*) mutant produced a product consistent with the formation of a tetrasaccharide intermediate rather than the pyruvylated hexasaccharide repeating unit (**Figure C7**).[59] Surprisingly, the lack of pyruvlated hexasaccharide accumulation in flippase deficient cells was reproducible and led us to initially consider the possibility of co-regulation. However, *wcaA* is directly downstream of *wzxC*, and tetrasaccharide accumulation could instead be the result of a polar mutation. With this in mind, primers were redesigned for this gene and a

non-polar *wzxC* deletion mutant revealed the anticipated accumulation of the colanic acid repeat unit (**Figure 4.7A and B**). These cells demonstrated cell rounding and lysis similar to Δ*wza* and Δ*wcaD* cells (**Figure 7C**). Both of these findings corroborate observations on the stringent substrate specificity of flippases.[151]

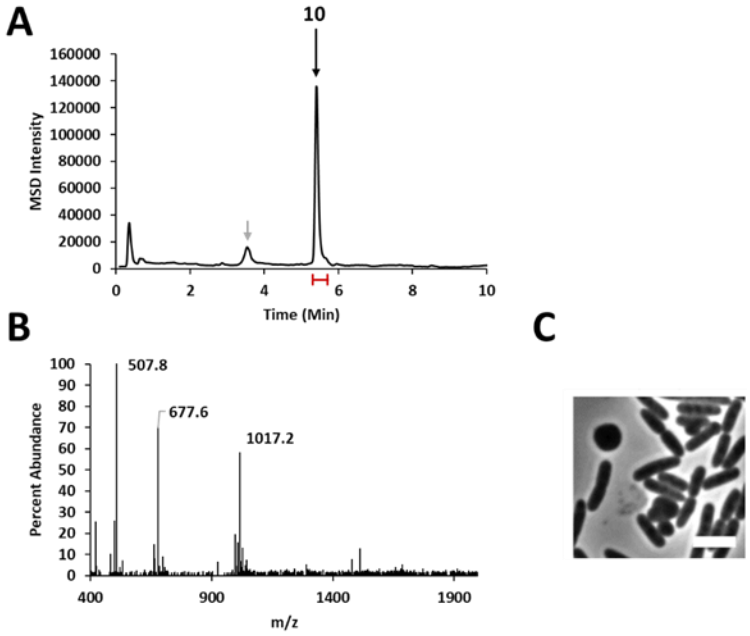

Figure 4.7. Pyruvlated hexasaccharide accumulation in a *wzxC* deficient mutant.
(A) A SIM chromatogram of the $[M-3H]^{-3}$ ion species. (B) A section of the total ion scan corresponding to the elution of the colanic acid pyruvlated hexasaccharide repeating unit demonstrating the presence of the $[M-2H]^{-2}$, $[M-3H]^{-3}$, $[M-4H]^{-4}$. (C) Morphological phenotypes produced by Δ*wzxC* cells with pUppS and *rcsA* induction. Background cellular material eluting at 3.8 min (gray arrow) not associated with colanic acid production. The white bar represents 3 µm.

In vitro Evidence for WcaK Activity, but not WcaL

Lack of recombinant WcaL activity prevented our group from tracking the *in vitro* formation of the hexasaccharide. Subsequently, it was also not possible to evaluate WcaK activity without WcaL product in hand. Some radiolabeling assays have successfully used endogenous BP as the lipid donor source for *in vitro* reactions.[146, 152, 153] We therefore wondered if supplying the crude cell extract from intermediate accumulating mutants could provide the needed substrate instead. Both WcaL and WcaK were expressed and purified as previously described, and then incubated with crude cell extracts containing accumulated penta- or hexasaccharide, respectively.[26] In

agreement with our previous observations, WcaL failed to catalyze the formation of the hexasaccharide when supplied Δ*wcaL* extract and UDP-galactose (**Figure 4.8A**). However, WcaK produced the pyruvyl modification when given Δ*wcaK* lipid extract and phosphoenolpyruvate (**Figure 4.8B**).

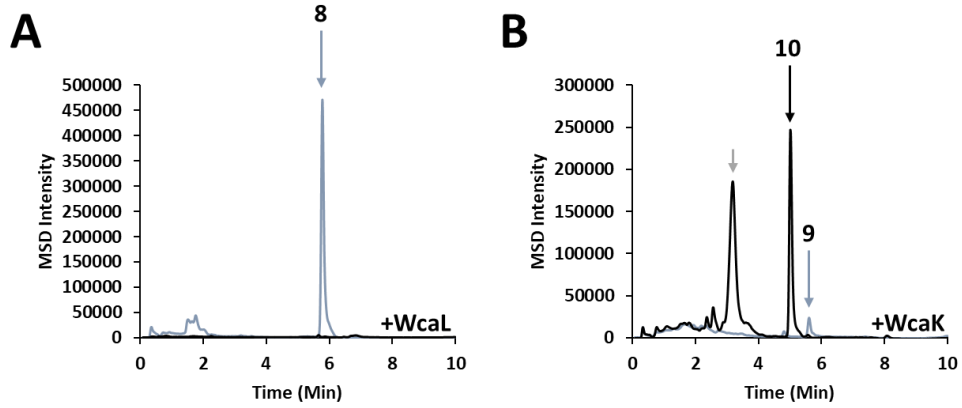

Figure 4.8. *In vitro* functional assays of WcaL and WcaK with intermediate extracts.
(A) Isolated WcaL did not catalyze the formation of the hexasaccharide with extracted pentasaccharide from Δ*wcaL* cells. (B) Conversion of the hexasaccharide to a m/z consistent with a pyruvlated product occurs in the presence of WcaK and extracted hexasaccharide from Δ*wcaK* cells. Background cellular material eluting at 3.8 min (gray arrow) not associated with colanic acid production.

The absence of WcaL activity after the addition of endogenous material demonstrates that even the native acceptor substrate was insufficient for turnover. Analysis on the chemical composition of colanic acid strongly suggests that galactose is present in the pentasaccharide.[28, 154 127, 155] Indeed, our analysis of the Δ*wcaK* mutant confirms the mass associated with a hexose in the hexasaccharide. Instead, we ascribe the lack of WcaL activity to problems associated with the recombinant protein expression, resulting in loss of downstream activity. The rate of transcription/translation, lysis conditions, and buffer composition can all contribute to failed enzyme activity.[130] WcaL is not predicted to contain transmembrane domains, however we observed consistent localization in the membrane fraction of our protein preparations (see SI material in Scott, PM et al).[26] This aberrant solubility may further indicate protein aggregation. However, it cannot yet be ruled out that a different sugar than galactose is incorporated by WcaL

and the stereochemistry is then altered by the activity of WcaK to give galactose. Attempts to utilize UDP-Glucose as an alternative substrate for WcaL also failed though.

Partitioning of Colanic Acid Intermediates

Two-phase Bligh and Dyer mixtures are commonly employed to extract polyprenyl linked glycans into the organic phase. We wondered if certain glycan lengths might be sufficient to solubilize BPP-oligosaccharides into the non-buffered aqueous or organic phase. A two-phase Bligh and Dyer system was used to assess this, followed by a secondary extraction with *n*-butanol of the aqueous layer (**Figure 4.9**). All intermediates including BP up until the pentasaccharide were chloroform miscible. Penta-, hexa- and pyruvlated hexasaccharide were aqueous-miscible with marginal solubility in *n*-butanol at neutral pH. Surprisingly, just five glycan moieties can overcome the hydrophobicity of the polyisoprenoid chain. It should be noted that the pentasaccharide contains a negatively charge glucuronic acid moiety at neutral pH unlike earlier oligosaccharide intermediates. The increasing polarity and introduction of a charged species may contribute to this unexpected shift in hydrophobicity of later intermediates.

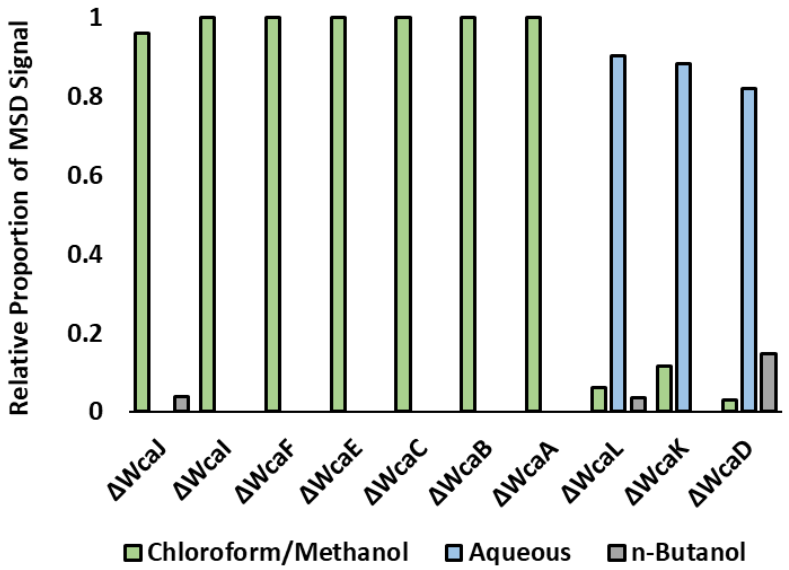

Figure 4.9. Partitioning of colanic acid intermediates in different solvents.
Intermediates containing four or fewer glycans were primarily present in the organic layer of the two-phase Bligh and Dyer extraction. Penta- and hexasaccharide intermediates were primarily present in the water after a secondary extraction in *n*-butanol. Relative signals are reported as the area under of curve of the chromatogram peak of the most abundant ion species.

Conclusion

A method for tracking the *in vivo* formation of colanic acid biosynthesis with single deletion mutants is herein reported. Accumulation of detectable quantities of intermediates ultimately required upregulation of Rcs translation of the colanic acid operon. It has been proposed that this stress response is one possible mechanism by which BP utilization is modulated.[156] Presumably essential cell well features, such as peptidoglycan, are prioritized first given the limited BP pool. However, whether peptidoglycan synthesis is prioritized over other surface glycans is not known. It is interesting to consider if the accumulation of colanic acid intermediates in this case might further incite this response due to changes in membrane composition. This could explain why mutants without RcsA induction did not produce detectable quantities of oligosaccharides despite the presence of BP. Reconstituting colanic acid synthesis by accumulating stepwise intermediates provided a full map of the functional roles associated with

producing this exopolysaccharide. Our efforts highlight the need to establish alternative methods for evaluating bacterial surface glycans as they occur in nature.

Experimental Procedures

Standard Growth and Lysis of Mutants

A single colony selected from agar plates incubated overnight at 37 °C was used to inoculate 5 mL of modified TB media.[116] The media composition included: 2.4% yeast extract, 2.0% tryptone, 0.5% glycerol, 100 mM phosphate buffer pH 7.4, 2 mM $MgCl_2$, 1 mM IPTG, and 10 μg/mL tetracycline. Cultures were incubated at 25 °C with shaking (300 rpm) for 22 h and then harvested with centrifugation. Cell pellets were washed with 0.9% NaCl after which the centrifuged supernatant was decanted and excess wash removed by pipette. Cells were then resuspended in 700 μL water (approx. total volume ~800 μL) and transferred to glass tubes with 3 mL of Methanol:Chloroform (2:1) for 20 min to ensure complete lysis. Glass tubes were then placed in a CentriVap with an appropriate adapter and allowed to centrifuge for an additional 20 min without vacuum. The soluble supernatant was then transferred to new glass tubes and placed at -80 °C until a slurry formed. Tubes were then placed back on the CentriVap with vacuum and dried to completion. The crude cell lysate was then stored in 200 μL of *n*-propanol and 0.1% ammonium hydroxide (1:3) at - 20 °C for up to one month.

Two Phase Extraction of Crude Cell Lysates

To assess partition of colonic acid intermediates, cells were grown and lysed as described above. Additional water and chloroform was added to induce a two phase mixture (1.8:2:2 total Water: Methanol:Chloroform). The phases where placed in a CentriVap for 20 min and the upper methanol/aqueous phase was transferred to a new glass tubes and then dried to completion. The aqueous fractions were then resuspended in 2 mL water and extracted with an equal volume of *n*-butanol in a second step. The resulting emulsion was placed on a CentriVap for 20 min and the

upper organic phase was transferred to a new glass tube. All dried down fractions (Chloroform, Aqueous, and n-Butanol) were stored in in 500 µL of *n*-propanol and 1% ammonium hydroxide (1:3) at - 20 °C.

LC-MS Analysis of Cell Lysates and in vitro Materials

Samples were analyzed on an Agilent 1260 Infinity II system equipped with a single quadrupole electrospray ionization MS detector. A high-pH stable Waters Xbridge Peptide BEH C18 column (4.6 x 50 mm with 2.5 µM particle size) was used. The mobile phases used included 0.1% Ammonium Hydroxide (A) and *n*-propanol (B), unless otherwise stated. A gradient was used to separate oligosaccharides starting at 5% B which was increased to 65% over 10 min at 1 mL/min. All LC-MS runs were performed in negative ion mode with a peak width of 0.1 min. Samples were analyzed in both scanning mode (500-2,000 m/z) as well as selection ion mode (SIM) for either the $[M-1H]^{-1}$ or $[M-2H]^{-2}$ ion species as indicated. The highest peak in the SIM chromatogram was then used to identify the time in the scan used for extracted ion counts and to monitor for other ion species. A fragmentor voltage of 240 V was used for BPP or BP, and 100 V for oligosaccharide intermediates and during the scan. Unless otherwise stated, 5 µL of each sample following resuspension was injected.

In vitro Activity Assays with Cell Extracts

A 20 µL aliquot of the cell extract was dried under a gentle stream of air. The crude cell material was resuspended in 100 mM Bicine (pH 8), 2.5 mM $MgCl_2$, and 1% Triton X-100 then sonicated briefly. The enzyme, WcaL or WcaK, was added at 10 µg total protein with either 5 mM UDP-Gal or 10 mM PEP, respectively. The total volume for each reaction was 40 µL. Reactions were left overnight at room temperature and analyzed following the described LC-MS methods.

Morphological analysis of colanic acid deletion mutants

Overnight cultures were diluted 1:200 in TB media containing carbenicillin (to select for p*uppS*), 1 mM IPTG (to induce *uppS* expression), and tetracycline (to induce *rcsA* expression), and grown at 25 °C for 5 h. Live cells were spotted on 1% agarose pads and imaged by phase-contrast microscopy using an Olympus BX51 microscope fitted with an XM10 monochrome camera.

Appendix C: Supplemental Information

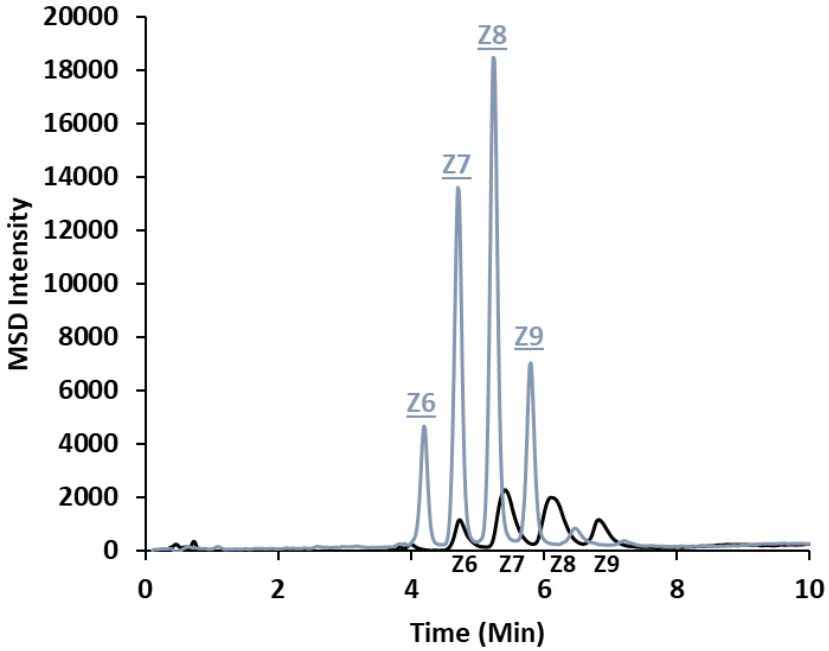

Figure C1. Retention time differences of BPP and BP.
BPPs (solid black) have an apparent ~0.5 min later retention time than corresponding BPs (solid blue).

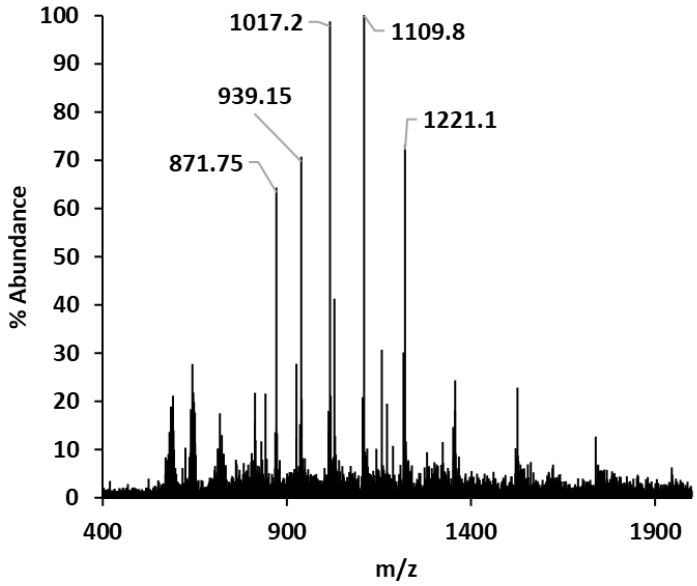

Figure C2. Total ion count of background ion scanning colanic acid repeating unit mass-to-charge ratio.
The 1017.2 m/z ion was present in a cellular background contaminate eluting at 3.3 min in all cell strains, including a complete deletion of colanic acid. This material has been noted with a gray arrow when colanic acid was selected in SIM chromatograms.

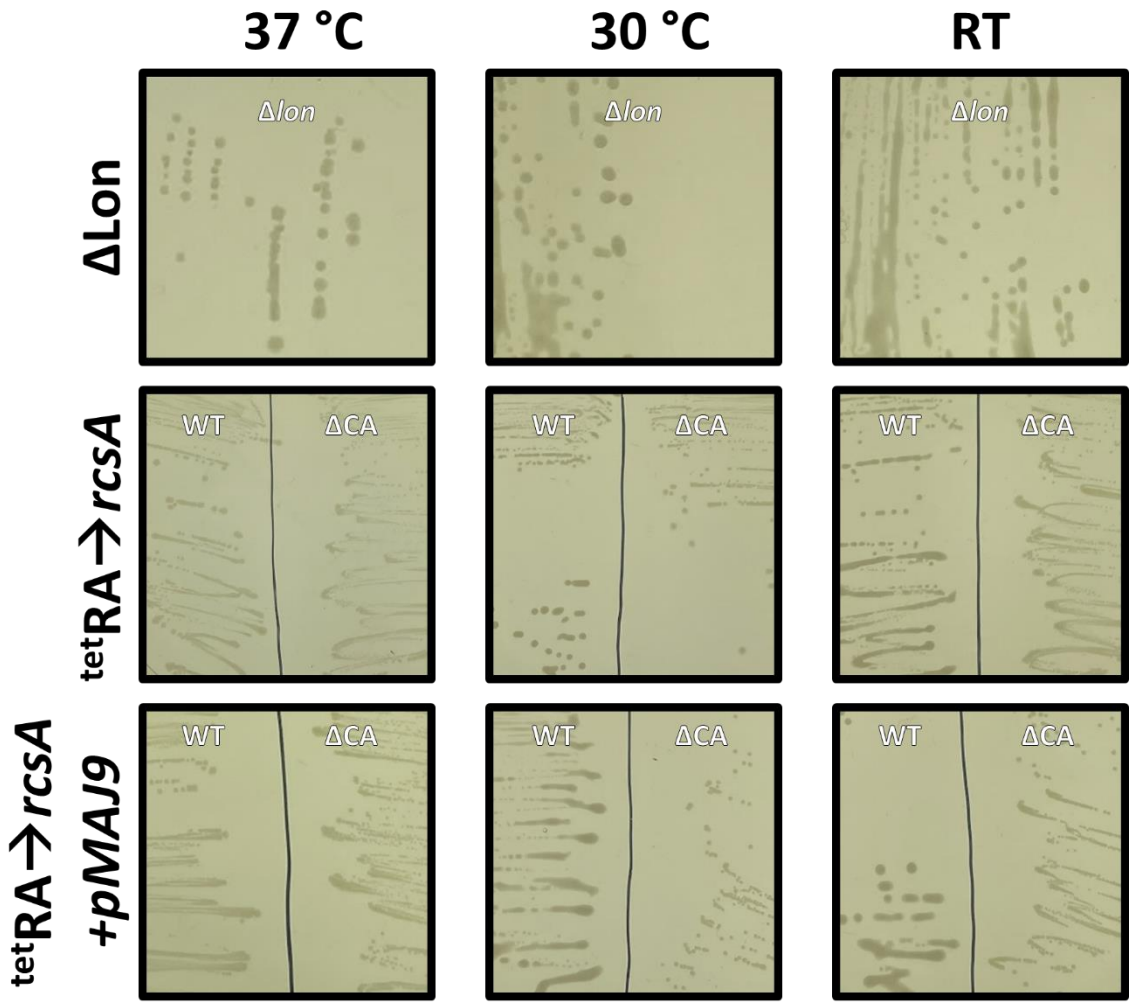

Figure C3. Mucoid Production.
Strains with the indicated genotypes were struck onto LB and grown at 37 °C, 30 °C, and RT for 48 h. A mutant lacking the Lon protease (Δ*lon*) or cells overexpressing *rcsA* produce mucoid colonies when grown at 30 °C or RT. Cells lacking the colanic acid operon (ΔCA) do not produce mucoid colonies when *rcsA* is overexpressed. Mucoid phenotype is not observed when cells are grown at 37 °C.

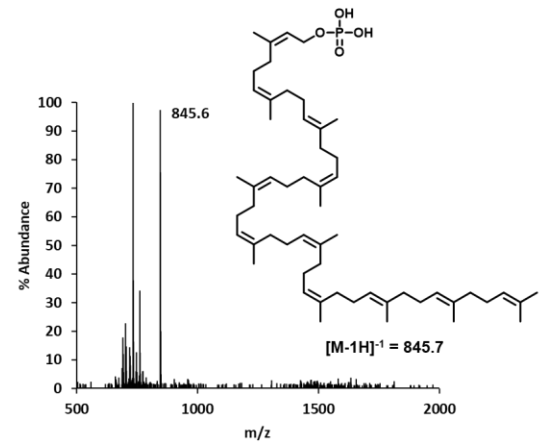
845.6
[M-1H]-1 = 845.7
% Abundance
m/z

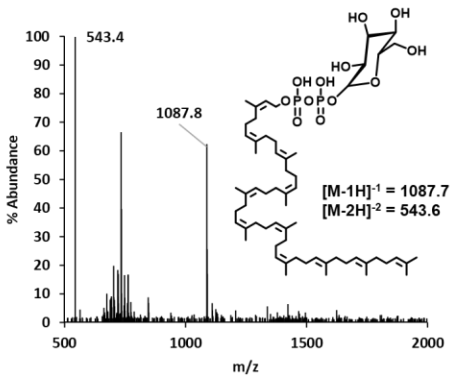
543.4
1087.8
[M-1H]-1 = 1087.7
[M-2H]-2 = 543.6
% Abundance
m/z

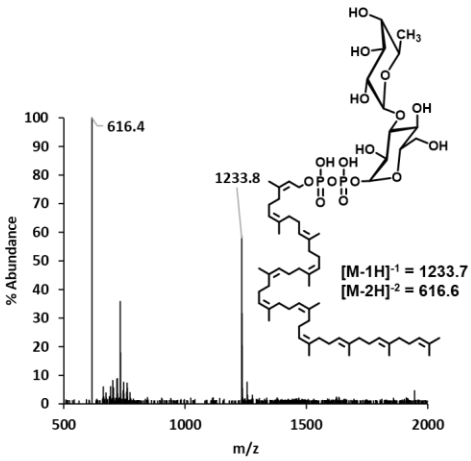
616.4
1233.8
[M-1H]-1 = 1233.7
[M-2H]-2 = 616.6
% Abundance
m/z

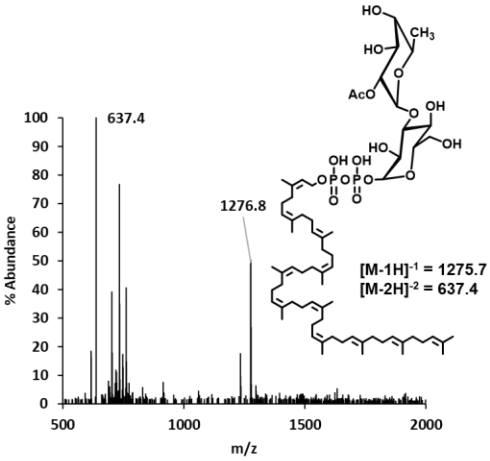
637.4
1276.8
[M-1H]-1 = 1275.7
[M-2H]-2 = 637.4
% Abundance
m/z

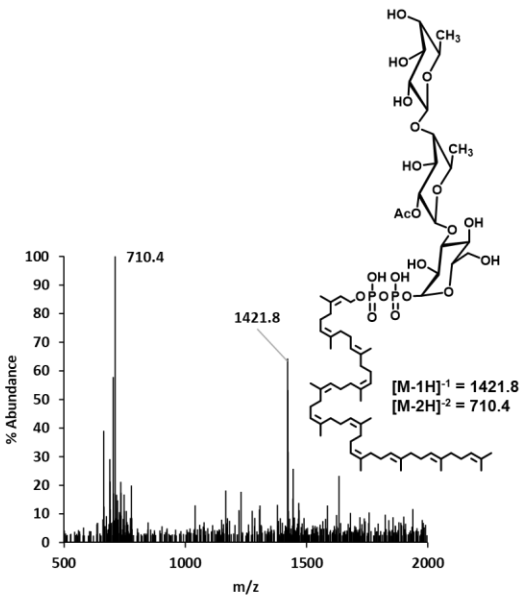
710.4
1421.8
[M-1H]-1 = 1421.8
[M-2H]-2 = 710.4
% Abundance
m/z

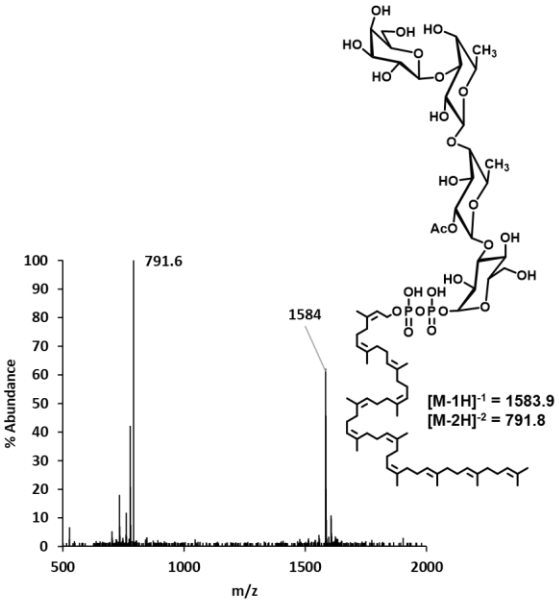
791.6
1584
[M-1H]-1 = 1583.9
[M-2H]-2 = 791.8
% Abundance
m/z

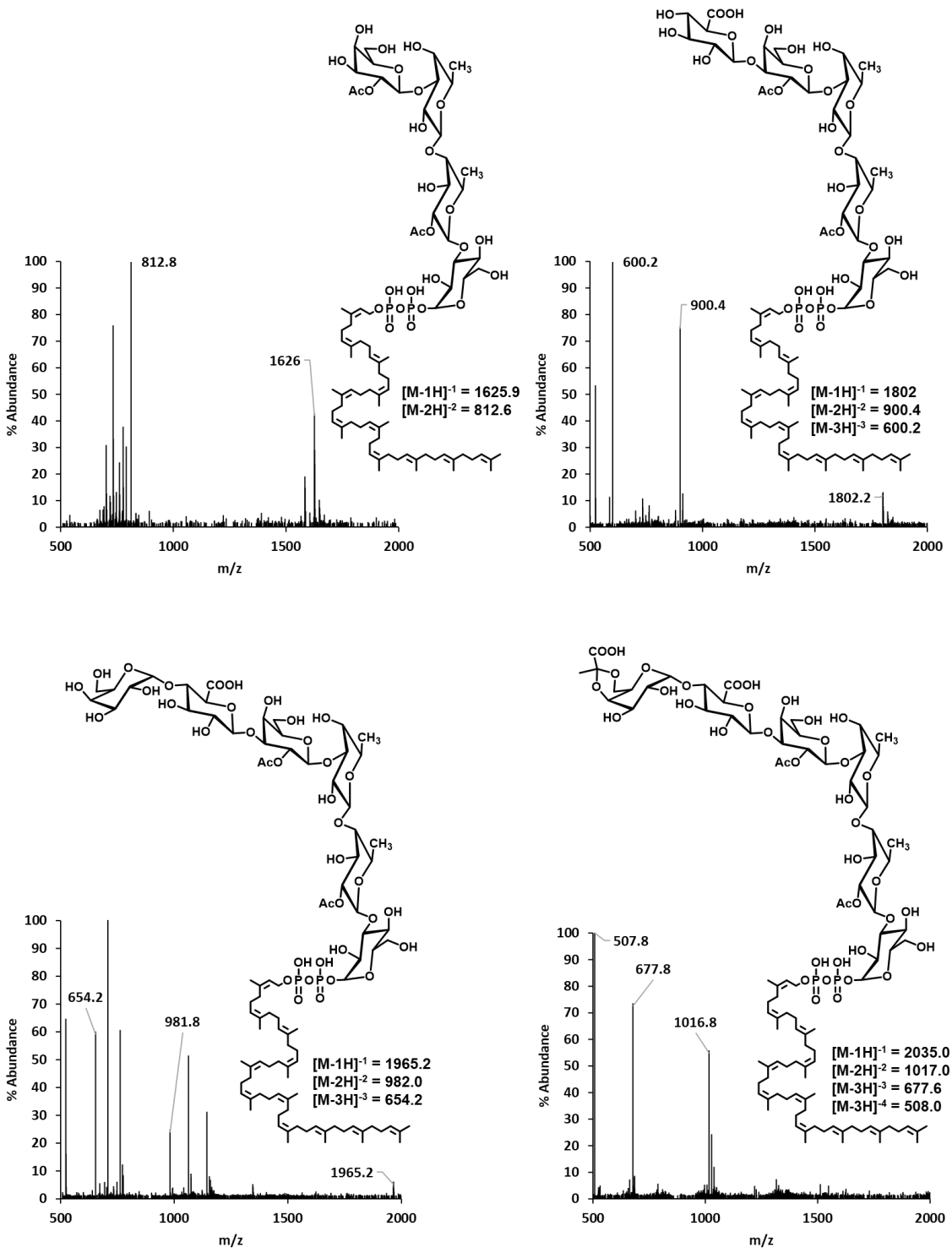

Figure C4. Total ion counts for colanic acid intermediates from cells.
Representative ion plots from a background scan (500-2,000 m/z) were acquired from peak maximums evident from the SIM chromatograms.

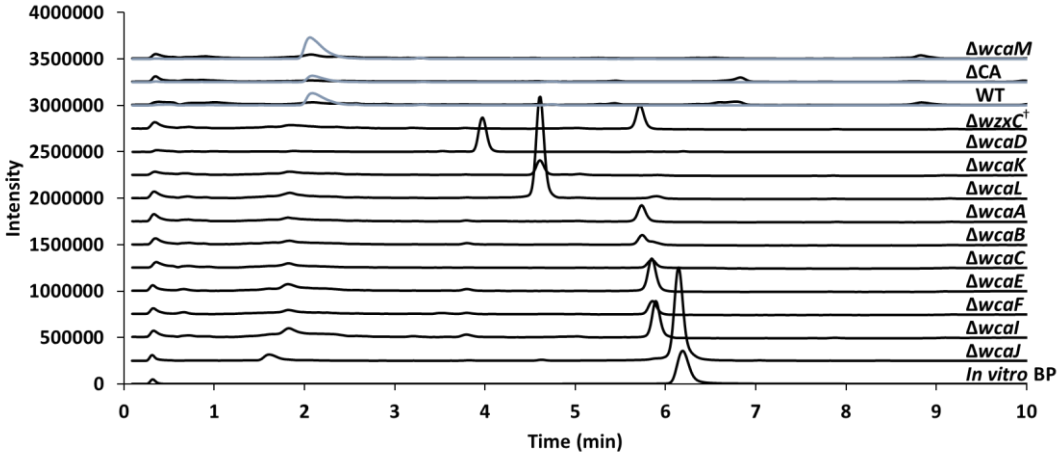

Figure C5. Screening for additional intermediate detection in mutant cell strains.
The mass to charge ratios of all intermediates (solid black) or colanic acid repeating unit (solid blue, WT, *Δ*CA, and *ΔwcaM*) were detected in SIM for each chromatogram. Only the anticipated intermediate was detected in each case. Solvent A was 1% ammonium hydroxide for all runs. The Δ*wzxC*† mutant shown here was prepared as previously described.[59]

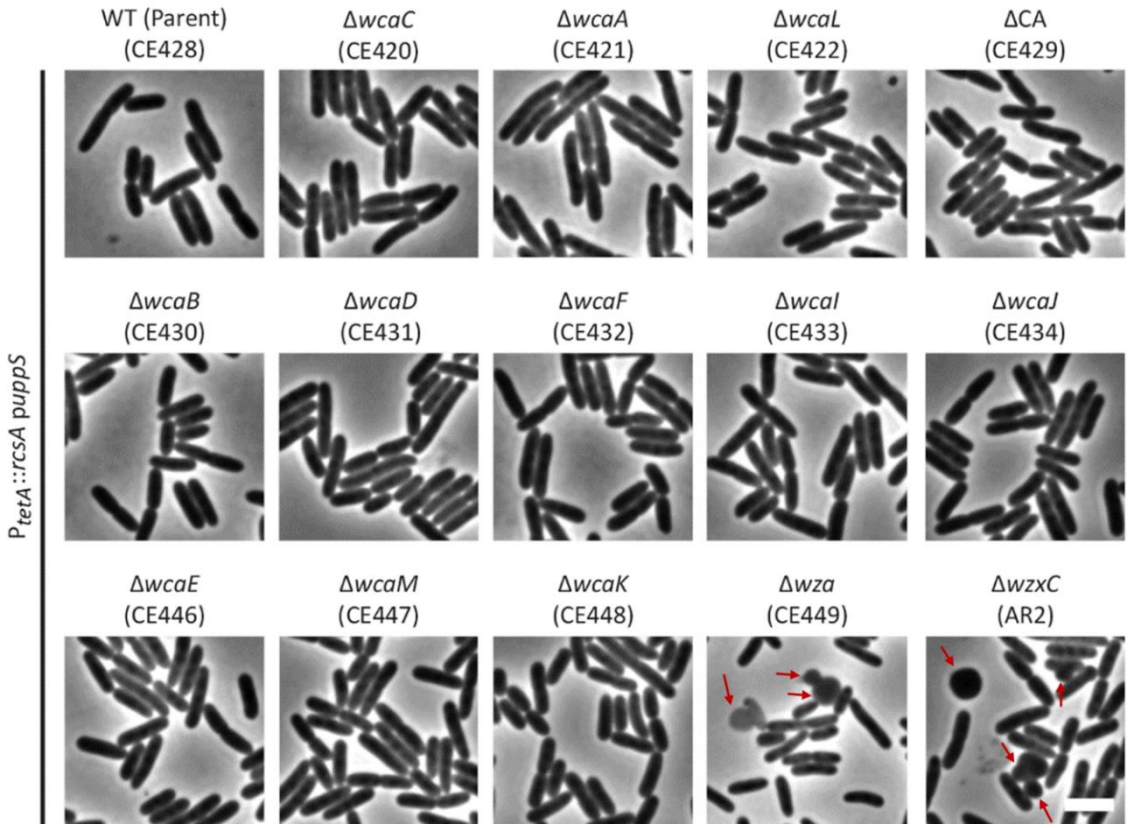

Figure C6. Morphologies produced by mutants accumulating colanic acid intermediates.
Micrographs of colanic acid mutants overexpressing rcsA and puppS. Note that mutants lacking Wza (exporter) or WzxC (flippase) grow as rods and spheres (red arrows). The white bar represents 3 µm.

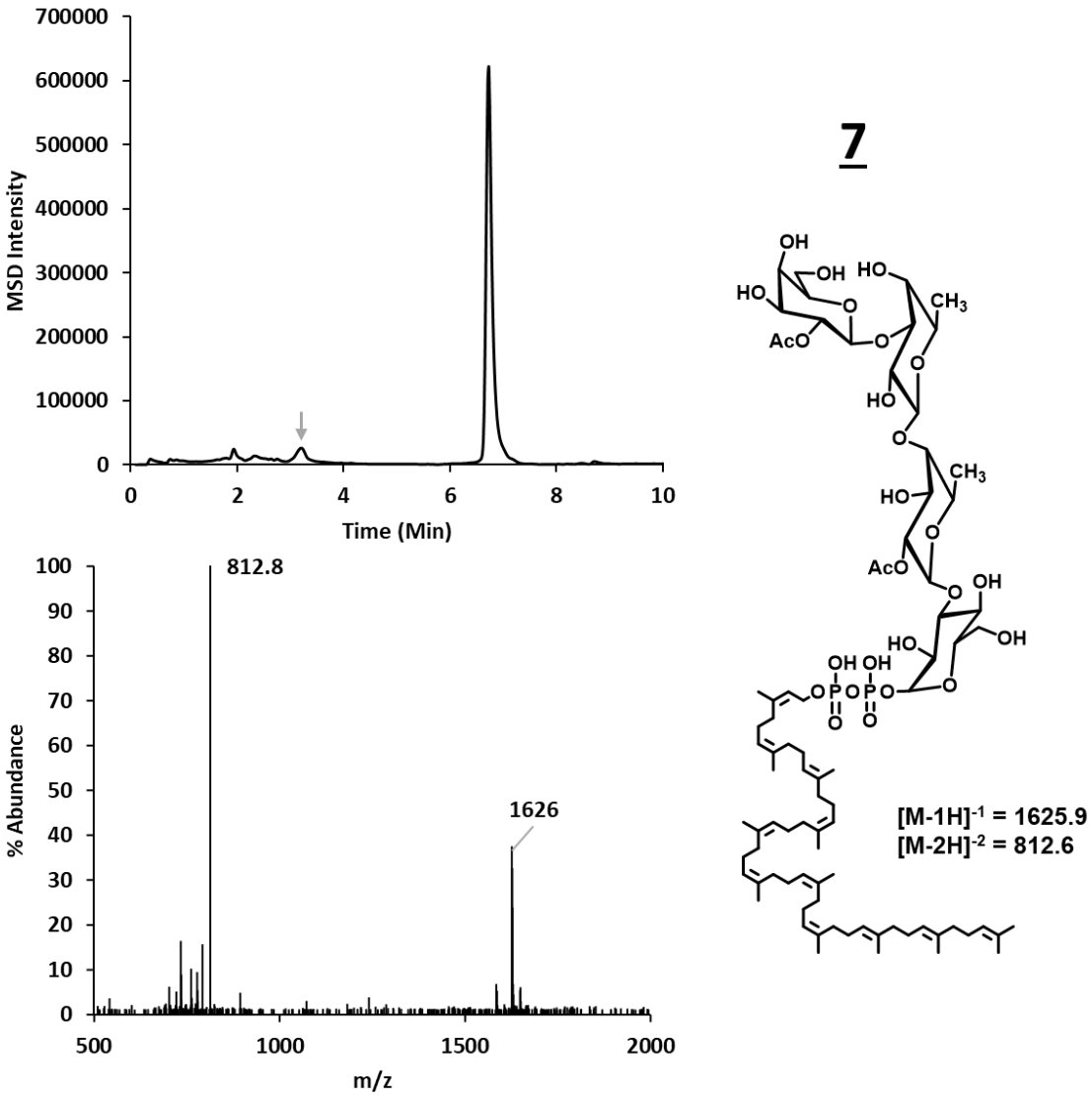

Figure C7. A previously reported ΔwzxC† mutant accumulated the tetrasaccharide intermediate. Total ion counts for colanic acid intermediates. Representative ion plots from a background scan (500-2,000 m/z) were acquired from peak maximums evident from the SIM chromatograms.

Table C1. Strains used in this work.

Strain	Abbreviation	Genotype	Source
MG1655	WT	MG1655 *wbbL*::IS*5*	Lab stock
DR35	Δ*wza*	MG1655 Δ*wza*::*kan*	[59]
DR38	ΔCA	MG1655 Δ[*wza-wcaM*]::*frt*	[59]
DR39	Δ*wcaD*	MG1655 Δ*wcaD*::*frt*	[59]
DR40	Δ*wzxC* †	MG1655 Δ*wzxC*::*frt*	[59]
DR46	Δ*wcaJ*	MG1655 Δ*wcaJ*::*frt*	[59]
MAJ878	Δ*wcaA*	MG1655 Δ*wcaA*::*cam*	This work
MAJ879	Δ*wcaB*	MG1655 Δ*wcaB*::*cam*	This work
MAJ880	Δ*wcaC*	MG1655 Δ*wcaC*::*cam*	This work
MAJ910	Δ*wcaL*	MG1655 Δ*wcaL*::*cam*	This work
MAJ911	Δ*wcaF*	MG1655 Δ*wcaF*::*cam*	This work
MAJ912	Δ*wcaI*	MG1655 Δ*wcaI*::*cam*	This work
MAJ1072	Δ*wcaE*	MG1655 Δ*wcaE*::*cam*	This work
MAJ1073	Δ*wcaM*	MG1655 Δ*wcaM*::*kan*	This work
MAJ1074	Δ*wcaK*	MG1655 Δ*wcaK*::*cam*	This work
MAJ1263	Δ*wzxC*	MG1655 Δ*wzxC*::*cam*	This work
MAJ1353	Δ*wcaD* Δ*waaL*	MG1655 ^{tet}RA→Δ*wcaD*::frt Δ*waaL*::*kan* pMAJ9^{carb}	This work
CE349	WT/Δ*lon*	MG1655 Δ*lon*::*kan*	This work
CE420	Δ*wcaC*/p*uppS*/*rcsA*	MAJ880* ^{tet}RA→*rcsA* pMAJ9^{carb}	This work
CE428	WT/p*uppS*/*rcsA*	^{tet}RA→*rcsA* pMAJ9^{carb}	This work
CE429	ΔCA/p*uppS*/*rcsA*	DR38 ^{tet}RA→*rcsA* pMAJ9^{carb}	This work
CE421	Δ*wcaA*/p*uppS*/*rcsA*	MAJ878* ^{tet}RA→*rcsA* pMAJ9^{carb}	This work
CE430	Δ*wcaB*/p*uppS*/*rcsA*	MAJ879* ^{tet}RA→*rcsA* pMAJ9^{carb}	This work
CE431	Δ*wcaD*/p*uppS*/*rcsA*	DR39 ^{tet}RA→*rcsA* pMAJ9^{carb}	This work
CE432	Δ*wcaF*/p*uppS*/*rcsA*	MAJ911* ^{tet}RA→*rcsA* pMAJ9^{carb}	This work
CE433	Δ*wcaI*/p*uppS*/*rcsA*	MAJ912* ^{tet}RA→*rcsA* pMAJ9^{carb}	This work
CE434	Δ*wcaJ*/p*uppS*/*rcsA*	DR46 ^{tet}RA→*rcsA* pMAJ9^{carb}	This work
CE422	Δ*wcaL*/p*uppS*/*rcsA*	MAJ910* ^{tet}RA→*rcsA* pMAJ9^{carb}	This work
CE411	Δ*wzxC*/p*uppS*/*rcsA*	DR40 ^{tet}RA→*rcsA* pMAJ9^{carb}	This work
CE446	Δ*wcaE*/p*uppS*/*rcsA*	MAJ1072* ^{tet}RA→*rcsA* pMAJ9^{carb}	This work

CE447	Δ*wcaM*/p*uppS*/*rcsA*	MAJ1073* ^{tet}RA→*rcsA* pMAJ9^{carb}	This work
CE448	Δ*wcaK*/p*uppS*/*rcsA*	MAJ1074* ^{tet}RA→*rcsA* pMAJ9^{carb}	This work
CE449	Δ*wza*/p*uppS*/*rcsA*	DR35 ^{tet}RA→*rcsA* pMAJ9^{carb}	This work
AR2	Δ*wzxC*/p*uppS*/*rcsA*	MAJ1263 ^{tet}RA→*rcsA* pMAJ9^{carb}	This work
Additional *E. coli* strains used as donors for P1 mediated transduction			
CE340	WT/*rcsA*	MG1655 ^{tet}RA→*rcsA*	This work

*Antibiotic marker evicted via pCP20

† Primer design as described in Ranjit DK. et al.[59]

Table C2. Primers used in this work

Δ*wcaA*-del-F	TCCGGCAAGCAAACCAGCTCATAAGCCGGGAGAACAACCTTGTAG GCTGGAGCTGCTTCG
Δ*wcaA*-del-R	ACGGGCGTAAACTCCAGCTGTTGGCGCGCAGATCTTCCAGCATAT GAATATCCTCCTTAG
Δ*wcaB*-del-F	ACGGCAAACGTCTGGCTGATGGTATTCGGGGGCGCTAAAGTGTAG GCTGGAGCTGCTTCG
Δ*wcaB*-del-R	CCCCGCCTTCCGCCAGTCGCACATTAAATTGCAAAATATTCATATG AATATCCTCCTTAG
Δ*wcaC*-del-F	CGCTGGTGGTGGGAGAAAAAGCGCGAGTGAAGGTAATTAATGTAG GCTGGAGCTGCTTCG
Δ*wcaC*-del-R	GCGGCAGCAACAGGTAGCTACAGATTCTGATAGAAGTTGACATAT GAATATCCTCCTTAG
Δ*wcaL*-del-F	AGATGGTGCAGTCTGTGCTTGAGCGCATCGGGGAGGTGAATGTAG GCTGGAGCTGCTTCG
Δ*wcaL*-del-R	TTGCCGTCAGGAACGTGCGTCGGGAGAGTTTTTTAAATGGCATATG AATATCCTCCTTAG
Δ*wcaE*-del-F	TTGCGAAAAGCGTTAAATATTACGAGGTAAGAATAAGAACTGTAG GCTGGAGCTGCTTCG
Δ*wcaE*-del-R	CCCGGAACCCTTTCGGCACCGAGAAACCGCTTAAATCTTGCATATG AATATCCTCCTTAG
Δ*wcaF*-del-F	GAAAGCCTTATATAACAAAGTCTGAATATAAGGAAAACCATGTAG GCTGGAGCTGCTTCG
Δ*wcaF*-del-R	CGTCTTGTCCGGTTACACCGGTGATGAGAGCGACTTTTGACATATG AATATCCTCCTTAG
Δ*wcaI*-del-F	CCTATTTTCTCGCTGAGAAGCGTACCGGAGTACCCGGATTTGTAGG CTGGAGCTGCTTCG
Δ*wcaI*-del-R	AGCCACCTGCCATCACAACTGGATAGAGTTTCGACTGCGCCATAT GAATATCCTCCTTAG
Δ*wcaM*-del-F	CTCGCCAGCTTGCTGCAGGCTTTATAGAGGAGAACGCATGTGTAG GCTGGAGCTGCTTCG

Δ*wcaM*-del-R	TCCAGGAATGGTCGCAAATCTACTCCCTCAGTTCCGGCAAATTCCG GGGATCCGTCGACC
Δ*wcaK*-del-F	ACGCAGCCTCACCTGGCATCAAATTTATGAGGAAAAAATGTGTAG GCTGGAGCTGCTTCG
Δ*wcaK*-del-R	CTGACGACAGCGGGAATTTCAGTAAAAAGAAGCCGACCTTCATAT GAATATCCTCCTTAG
Δ*wzxC*-del-F	GTGTTCAAAGGTTTCGTTAACAAAGCGGCATATTGATATGTGTAGG CTGGAGCTGCTTCG
Δ*wzxC*-del-R	CACGATTGCCGCAAGTGTGGTTGCCCAGAATAAGTAATTTCATATG AATATCCTCCTTAG
rcsA-tetF	TAAGACAATTCCAGGCAAATTATACAACACTTTACGGGATTAGGT GGGTACGTTGGAGC
rcsA-tetR	CCTAATGCGCCACTCTCGCGATTTTTCAGGCGGACTTACTCTAAGC ACTTGTCTCCTGTTTAC
rcsA-ck-F	CCTACGAACATCTTCCAGG

Chromosomal mutants were constructed by the methods of Datsenko and Wanner.[157] In brief, MG1655 *E. coli* harboring pKD46 were grown at 30 °C with ampicillin and arabinose to induce recombinase expression. Cells were washed 3 times in sterile, ice-cold 10% glycerol, then electroporated with the PCR products described below. After recovery, cells were grown on selective media at 37 °C to cure pKD46, and the correct insertion was verified by colony PCR using the primers listed above.

To construct the tetracycline-inducible *rcsA* strains, the *tetRA* locus was amplified off the chromosome of CE340 using primers rcsA_tetF and rcsA_tetR. The resulting amplicon was used to transform MG1655 cells as described above. Mutants were selected and purified on 10 μg/mL tetracycline, and the correct insertion was verified by colony PCR using the primers rcsA_ck_F and tetRAckR, which yielded a 312 bp amplicon for colonies with the appropriate chromosomal insertion.

CHAPTER 5: CONCLUSION

Overview

Bacterial surface glycans play a critical role in the host-microbe interactions which underlie both disease and commensalism. A great deal of variation exists in the glycan composition present throughout various microbes. This is even true of bacterial sub-species, making them excellent prophylactic, therapeutic, and detection targets. Yet, the challenge of studying these materials lies in this inherit complexity and extraordinarily diverse composition. Glycan based probes have proved insightful to monitor polysaccharide bioassembly. Because sugar composition differs greatly, and there is a lack of commercially available glycans, acquiring a comprehensive library of bacteria specific glycans is lacking. The research presented here addressed the need for ubiquitous tools that could be applied broadly throughout various bacterial glycan assembly systems. To do this, we: (1) identified optimal conditions for introducing a new fluorophore and a "click-able" azido- tag to the polyisoprenoid toolbox; (2) demonstrate general utilization of polyisoprenoid probes with several initiating phosphoglycosyltransferases as well as the a heptasaccharide important for protein glycosylation in *C. jejuni*; and (3) recapitulate colanic acid biosynthesis in live cells and employ methods to detect it.

Scaling Chemoenzymatic Synthesis of Polyisoprenoid Probes

The combined chemo- and enzymatic preparation of polyisoprenoid tagged materials has several advantages over traditional synthetic approaches. For example, enzymes are known to catalyze in a regio- and stereospecific manor. Relaxed substrate specificity can also be advantageous to build glycans on non-native substrates that do not participate in catalysis, such as ω-tagged polyisoprenoids. The main limitation of this

approach lies in the scalability of biocatalytic reactions. Some considerations to address this included: methods to increase yield of recombinant UppS; volume/concentration scalability of substrates; reproducible phosphatase activity; and semi-preparatory method development to purify mixed polyisoprenoid monophosphates. Altogether, optimizing these steps led us to develop a more robust procedure to multi-milligram quantities of BP.

Two critical areas of success were essential for scaling the chemoenzymatic synthesis of bactoprenyl tags. The first was identifying a UppS enzyme that had broad specificity for tagged polyisoprenoids. Prior efforts used exclusively UppS from *B. fragilis*, which had markedly lower turnover with both the NBD fluorophore and azido-tag (data not shown). The fact that this was remedied by suppling a different species UppS, from *S. aureus*, suggests that there are structural differences between these enzymes that allows one to better tolerate nonnative tags. This is corroborated by the literature report in which a tri-floromethyl coumarin analogue could not be polymerized past the first isoprenoid addition.[56] Our empirical approach, however, was sufficient to produce the desired bactoprenyl diphosphate probes at ten-fold higher concentrations and volumes than previously reported. To what extent the size or shape of tagged geranyl diphosphates are suitable substrate replacements for UppS is not fully understood and could reveal exciting directions for chemoenzymatic synthesis of labeled polyisoprenoids.

In addition to UppS catalysis, optimizing for robust and reproducible mono dephosphorylation was also needed. Commercial sources of alkaline phosphatase had unpredictable activity from batch-to-batch. We found that potato acid phosphatase was more reliable, but was not amenable to basic buffering conditions required for UppS

activity. Therefore, we implemented a strategy to extract tagged polyisoprenoid diphosphates for subsequent dephosphorylation. This two-step procedure was critical for omitting additional purification in between di- and monophosphate formation which would result in significant losses of material. Currently, a purification bottleneck exists where tagged isoprenoids can be produced far more robustly than can be HPLC purified. Better methodologies for isolating large batches of mixed polyisoprenoids would greatly improve this process.

An alternative approach altogether was undertaken with azido- tagged neryl monophosphate. Purification of mixed polyisoprenoids could be avoided since direct synthesis of this probe was possible, unlike tagged bactoprenyl monophosphates. Additionally, monitoring enzymatic polymerization of labeled polyisoprenoids has thus far been reported with HPLC/MS. Removing the enzymatic step eliminates a barrier for labs without these instruments, making them broadly accessible to a wide audience. Analogues of neryl monophosphate are an exciting new addition to the tagged isoprenoid toolbox, particularly for downstream applications of glycoconjugates. Further investigation of glycosyltransferases activity is needed to evaluate if these probes are generally utilized substrates.

Isoprenoid Scaffold Replacements *in vitro* Glycan Assembly

Variation in polyisoprenoid substrate recognition has been well documented in the literature for glycosyltransferases.[41, 45, 46, 50, 71, 76, 110-112] Therefore, one of the research goals herein was to assess a broad array of polyisoprenoid utilizing enzymes. To date, two oligosaccharides have been built on fluorescently labeled bactoprenyl phosphate. This includes colanic acid and a capsular polysaccharide A from *E. coli* and *B. fragilis*

respectively.[26, 27] We selected glycosyltransferases with known functions to screen our tagged isoprenoids with, including several initiating glycosyltransferases important for building the cell envelope. In addition, we assembled a heptasaccharide important for pathogenicity from *C. jejuni* with azido-modified lipid scaffolds. These successes substantiate the general utilization of tagged polyisoprenoids throughout a variety of glycosyltransferase enzymes. Several important considerations arose during this investigation that could lead to better enzyme performance with these non-native substrates, such as co-solvent additives or hydrophobicity of the isoprenoid probe.

In vitro activity of glycosyltransferases are known to exhibit a wide degree of tolerance to various solvent additives like methanol, DMSO, or surfactants. These are largely believed to be enzyme specific, yet we also identified conditions where certain environments influenced enzyme activity with certain modified lipid scaffolds. For example the NBD fluorophore was used by the initiating glycosyltransferase WbaP only in the presence of *n*-propanol. The same was not true of the 2CN fluorophore, in which WbaP utilized this substrate. Additionally, CPS2E failed to catalyze the transfer of phospho-glucose to native BP in the presence of either DMSO or *n*-propanol. Yet, both of these conditions afforded the product with either the 2CN or NBD fluorophore. Methods to better predict activity based on the lipid scaffold could reduce iterative screening for each new conditions. Such analysis could reveal the behavior of these lipid scaffolds in aqueous environments, and whether or not this influences enzyme activity.

Various reports in the literature have limited success with short isoprenoids, such as nerol, for glycosyltransferase reactions.[41, 46, 50, 71, 76] To our surprise, ω-tagged neryl monophosphate was a suitable substrate for each step in the protein glycosylation

pathway in *C. jejuni*. This hydrophilic scaffold was soluble in complimentary enzyme conditions and did not require the addition of a co-solvent or added surfactant. In contrast, we found that one key benefit of elongated isoprenoids, while much lower in yield, was the ability to extract these hydrophobic glycoconjugates. This enabled us to rapidly perform sugar specificity analysis which would have taken considerably more time with the neryl probe. Both scaffolds ultimately have distinct advantages for reproducing bacterial surface oligosaccharides. Together these probe choices aid in expanding the variety of applications that could be exploited for downstream use.

Detection of Oligosaccharide Intermediates from Cell Extracts

The vast majority of rare bacterial glycans are not commercially available. Research efforts described above circumvented the need to synthesize rare glycans by focusing on pathways which do not use them, or utilizing pathways for which there were known biosynthetic routes. Methods to explore unknown pathways by detecting isoprenoid intermediates could rapidly enhance our understanding of the roles bacterial cell surfaces play in our health. To do this, we sought to recapitulate early stages of glycan assembly in their native environment, a bacterial cell. Importantly, this also avoids having to purchase or prepare sugar donors since the cell acts as a glycan factory to produce them for us.

The quantity of BP in *E. coli* has been theoretically estimated at around tens of thousands of molecules per cell.[133] This naturally low abundance has made it difficult to investigate how non-essential surface glycans are assembled in their native environment. Analytical methodologies in mass spectroscopy have played an essential role in detecting colanic acid intermediates, as well as genetic manipulation to increase transcriptional

regulation of the operon. Insight gained by using colanic acid as a model may provide a necessary foundation for investigating the dynamic assembly of surface glycans or even the sequestration of BP among different pathways. This could also be applied with complimentary characterization methods, such as NMR, for *in vivo* synthesized lipid-linked glycan materials with unknown chemical composition.

Around one third of recombinant therapeutics, such as insulin, originate from *E. coli*.[158] Complex biological materials such as these cannot be reasonably recreated synthetically and cellular machinery is instead engineered to optimize therapeutic formation. In the future, it may be possible to use this for obtaining complex glycoconjugates for therapeutic or detection technologies. This is distinctly advantageous to mitigate the scarcity of rare bacterial glycans, or significantly reduce the time burden to reproduce them chemoenzymatically. Perhaps it might be feasible to incorporate tagged isoprenoid probes in live cells to acquire naturally derived glycoconjugates. The use of tags presented here, such as a azido- handles, could further provide straightforward methods for facile recovery or purification of glycan intermediates for such advances.

This work presents three different strategies for investigating isoprenoid scaffolds to interrogate bacterial glycan bioassembly. The polyisoprenoid scaffold is a central lipid carrier throughout the assembly of many cell surface glycans. The composition of the bacterial cell surface is highly differentiated among bacteria and they take advantage of various different glycans. These surface saccharides can contribute to pathogenicity or bacterial survival.

REFERENCES

1. Sender, R.; Fuchs, S.; Milo, R., Revised Estimates for the Number of Human and Bacteria Cells in the Body. *PLoS Biol* **2016,** *14* (8), e1002533.
2. Rowland, I.; Gibson, G.; Heinken, A.; Scott, K.; Swann, J.; Thiele, I.; Tuohy, K., Gut microbiota functions: metabolism of nutrients and other food components. *Eur J Nutr* **2018,** *57* (1), 1-24.
3. Guinane, C. M.; Cotter, P. D., Role of the gut microbiota in health and chronic gastrointestinal disease: understanding a hidden metabolic organ. *Therap Adv Gastroenterol* **2013,** *6* (4), 295-308.
4. Maynard, C. L.; Elson, C. O.; Hatton, R. D.; Weaver, C. T., Reciprocal interactions of the intestinal microbiota and immune system. *Nature* **2012,** *489* (7415), 231-41.
5. Surana, N. K.; Kasper, D. L., The yin yang of bacterial polysaccharides: lessons learned from B. fragilis PSA. *Immunol Rev* **2012,** *245* (1), 13-26.
6. Kirk, J. A.; Banerji, O.; Fagan, R. P., Characteristics of the Clostridium difficile cell envelope and its importance in therapeutics. *Microbial Biotechnology* **2017,** *10* (1), 76-90.
7. Sambol, S. P.; Merrigan, M. M.; Tang, J. K.; Johnson, S.; Gerding, D. N., Colonization for the prevention of Clostridium difficile disease in hamsters. *Journal of Infectious Diseases* **2002,** *186* (12), 1781-1789.
8. Calabi, E.; Calabi, F.; Phillips, A. D.; Fairweather, N. F., Binding of Clostridium difficile surface layer proteins to gastrointestinal tissues. *Infection and Immunity* **2002,** *70* (10), 5770-5778.
9. Tra, V. N.; Dube, D. H., Glycans in pathogenic bacteria - potential for targeted covalent therapeutics and imaging agents. *Chem Commun* **2014,** *50* (36), 4659-4673.
10. Kumar, A.; Schweizer, H. P., Bacterial resistance to antibiotics: active efflux and reduced uptake. *Adv Drug Deliv Rev* **2005,** *57* (10), 1486-513.
11. Braun, V.; Bos, C.; Braun, M.; Killmann, H., Outer membrane channels and active transporters for the uptake of antibiotics. *J Infect Dis* **2001,** *183 Suppl 1*, S12-6.
12. Ghai, I.; Ghai, S., Understanding antibiotic resistance via outer membrane permeability. *Infect Drug Resist* **2018,** *11*, 523-530.
13. Vaara, M., Agents That Increase the Permeability of the Outer-Membrane. *Microbiol Rev* **1992,** *56* (3), 395-411.
14. Raetz, C. R.; Whitfield, C., Lipopolysaccharide endotoxins. *Annu Rev Biochem* **2002,** *71*, 635-700.
15. Frirdich, E.; Whitfield, C., Lipopolysaccharide inner core oligosaccharide structure and outer membrane stability in human pathogens belonging to the Enterobacteriaceae. *J Endotoxin Res* **2005,** *11* (3), 133-44.
16. Harris, S.; Piotrowska, M. J.; Goldstone, R. J.; Qi, R.; Foster, G.; Dobrindt, U.; Madec, J. Y.; Valat, C.; Rao, F. V.; Smith, D. G. E., Variant O89 O-Antigen of E-coli Is Associated With Group 1 Capsule Loci and Multidrug Resistance. *Frontiers in Microbiology* **2018,** *9*.

17. Lerouge, I.; Vanderleyden, J., O-antigen structural variation: mechanisms and possible roles in animal/plant-microbe interactions. *FEMS Microbiol Rev* **2002,** *26* (1), 17-47.
18. Do, T.; Page, J. E.; Walker, S., Uncovering the activities, biological roles, and regulation of bacterial cell wall hydrolases and tailoring enzymes. *J Biol Chem* **2020,** *295* (10), 3347-3361.
19. Pushkaran, A. C.; Nataraj, N.; Nair, N.; Gotz, F.; Biswas, R.; Mohan, C. G., Understanding the Structure-Function Relationship of Lysozyme Resistance in Staphylococcus aureus by Peptidoglycan O-Acetylation Using Molecular Docking, Dynamics, and Lysis Assay. *J Chem Inf Model* **2015,** *55* (4), 760-770.
20. O'Callaghan, R. J., The Pathogenesis of Staphylococcus aureus Eye Infections. *Pathogens* **2018,** *7* (1).
21. Baranwal, G.; Mohammad, M.; Jarneborn, A.; Reddy, B. R.; Golla, A.; Chakravarty, S.; Biswas, L.; Gotz, F.; Shankarappa, S.; Jin, T.; Biswas, R., Impact of cell wall peptidoglycan O-acetylation on the pathogenesis of Staphylococcus aureus in septic arthritis. *Int J Med Microbiol* **2017,** *307* (7), 388-397.
22. Danese, P. N.; Pratt, L. A.; Kolter, R., Exopolysaccharide production is required for development of Escherichia coli K-12 biofilm architecture. *J Bacteriol* **2000,** *182* (12), 3593-6.
23. Chen, L.; Wen, Y. M., The role of bacterial biofilm in persistent infections and control strategies. *Int J Oral Sci* **2011,** *3* (2), 66-73.
24. Kelly, J.; Jarrell, H.; Millar, L.; Tessier, L.; Fiori, L. M.; Lau, P. C.; Allan, B.; Szymanski, C. M., Biosynthesis of the N-linked glycan in Campylobacter jejuni and addition onto protein through Block transfer. *Journal of Bacteriology* **2006,** *188* (7), 2427-2434.
25. Herget, S.; Toukach, P. V.; Ranzinger, R.; Hull, W. E.; Knirel, Y. A.; von der Lieth, C. W., Statistical analysis of the Bacterial Carbohydrate Structure Data Base (BCSDB): characteristics and diversity of bacterial carbohydrates in comparison with mammalian glycans. *BMC Struct Biol* **2008,** *8*, 35.
26. Scott, P. M.; Erickson, K. M.; Troutman, J. M., Identification of the Functional Roles of Six Key Proteins in the Biosynthesis of Enterobacteriaceae Colanic Acid. *Biochemistry-Us* **2019,** *58* (13), 1818-1830.
27. Sharma, S.; Erickson, K. M.; Troutman, J. M., Complete Tetrasaccharide Repeat Unit Biosynthesis of the Immunomodulatory Bacteroides fragilis Capsular Polysaccharide A. *ACS Chem Biol* **2017,** *12* (1), 92-101.
28. Johnson, J. G.; Wilson, D. B., Role of a sugar-lipid intermediate in colanic acid synthesis by Escherichia coli. *J Bacteriol* **1977,** *129* (1), 225-36.
29. Patel, K. B.; Toh, E.; Fernandez, X. B.; Hanuszkiewicz, A.; Hardy, G. G.; Brun, Y. V.; Bernards, M. A.; Valvano, M. A., Functional characterization of UDP-glucose:undecaprenyl-phosphate glucose-1-phosphate transferases of Escherichia coli and Caulobacter crescentus. *J Bacteriol* **2012,** *194* (10), 2646-57.
30. Rihn, B.; Coulais, C.; Bottin, M. C.; Martinet, N., Evaluation of non-radioactive labelling and detection of deoxyribonucleic acids. Part One: Chemiluminescent methods. *J Biochem Biophys Methods* **1995,** *30* (2-3), 91-102.

31. Baskin, J. M.; Prescher, J. A.; Laughlin, S. T.; Agard, N. J.; Chang, P. V.; Miller, I. A.; Lo, A.; Codelli, J. A.; Bertozzi, C. R., Copper-free click chemistry for dynamic in vivo imaging. *P Natl Acad Sci USA* **2007,** *104* (43), 16793-16797.
32. Siegrist, M. S.; Whiteside, S.; Jewett, J. C.; Aditham, A.; Cava, F.; Bertozzi, C. R., (D)-Amino acid chemical reporters reveal peptidoglycan dynamics of an intracellular pathogen. *ACS Chem Biol* **2013,** *8* (3), 500-5.
33. Clark, E. L.; Emmadi, M.; Krupp, K. L.; Podilapu, A. R.; Helble, J. D.; Kulkarni, S. S.; Dube, D. H., Development of Rare Bacterial Monosaccharide Analogs for Metabolic Glycan Labeling in Pathogenic Bacteria. *ACS Chem Biol* **2016,** *11* (12), 3365-3373.
34. Dube, D., Glycans in pathogenic bacteria - potential for selective targeting. *Abstr Pap Am Chem S* **2016,** *251*.
35. DeMeester, K. E.; Liang, H.; Jensen, M. R.; Jones, Z. S.; D'Ambrosio, E. A.; Scinto, S. L.; Zhou, J.; Grimes, C. L., Synthesis of Functionalized N-Acetyl Muramic Acids To Probe Bacterial Cell Wall Recycling and Biosynthesis. *J Am Chem Soc* **2018,** *140* (30), 9458-9465.
36. Wu, B. L.; Woodward, R.; Wen, L. Q.; Wang, X.; Zhao, G. H.; Wang, P. G., Synthesis of a Comprehensive Polyprenol Library for the Evaluation of Bacterial Enzyme Lipid Substrate Specificity. *Eur J Org Chem* **2013,** *2013* (36), 8162-8173.
37. Saldias, M. S.; Patel, K.; Marolda, C. L.; Bittner, M.; Contreras, I.; Valvano, M. A., Distinct functional domains of the Salmonella enterica WbaP transferase that is involved in the initiation reaction for synthesis of the O antigen subunit. *Microbiol-Sgm* **2008,** *154*, 440-453.
38. Patel, K. B.; Furlong, S. E.; Valvano, M. A., Functional analysis of the C-terminal domain of the WbaP protein that mediates initiation of O antigen synthesis in Salmonella enterica. *Glycobiology* **2010,** *20* (11), 1389-1401.
39. Lehrer, J.; Vigeant, K. A.; Tatar, L. D.; Valvano, M. A., Functional characterization and membrane topology of Escherichia coli WecA, a sugar-phosphate transferase initiating the biosynthesis of enterobacterial common antigen and O-antigen lipopolysaccharide. *J Bacteriol* **2007,** *189* (7), 2618-28.
40. Cochrane, R. V. K.; Alexander, F. M.; Boland, C.; Fetics, S. K.; Caffrey, M.; Cochrane, S. A., From plant to probe: semi-synthesis of labelled undecaprenol analogues allows rapid access to probes for antibiotic targets. *Chem Commun (Camb)* **2020,** *56* (61), 8603-8606.
41. Liu, F.; Vijayakrishnan, B.; Faridmoayer, A.; Taylor, T. A.; Parsons, T. B.; Bernardes, G. J. L.; Kowarik, M.; Davis, B. G., Rationally Designed Short Polyisoprenol-Linked PglB Substrates for Engineered Polypeptide and Protein N-Glycosylation. *Journal of the American Chemical Society* **2014,** *136* (2), 566-569.
42. Ye, X. Y.; Lo, M. C.; Brunner, L.; Walker, D.; Kahne, D.; Walker, S., Better substrates for bacterial transglycosylases. *J Am Chem Soc* **2001,** *123* (13), 3155-6.
43. Musumeci, M. A.; Hug, I.; Scott, N. E.; Ielmini, M. V.; Foster, L. J.; Wang, P. G.; Feldman, M. F., In vitro activity of Neisseria meningitidis PglL O-oligosaccharyltransferase with diverse synthetic lipid donors and a UDP-activated sugar. *J Biol Chem* **2013,** *288* (15), 10578-87.

44. Al-Dabbagh, B.; Mengin-Lecreulx, D.; Bouhss, A., Purification and characterization of the bacterial UDP-GlcNAc:undecaprenyl-phosphate GlcNAc-1-phosphate transferase WecA. *J Bacteriol* **2008,** *190* (21), 7141-6.
45. Auger, G.; van Heijenoort, J.; Mengin-Lecreulx, D.; Blanot, D., A MurG assay which utilises a synthetic analogue of lipid I. *Fems Microbiology Letters* **2003,** *219* (1), 115-119.
46. Woodward, R.; Yi, W.; Li, L.; Zhao, G.; Eguchi, H.; Sridhar, P. R.; Guo, H.; Song, J. K.; Motari, E.; Cai, L.; Kelleher, P.; Liu, X.; Han, W.; Zhang, W.; Ding, Y.; Li, M.; Wang, P. G., In vitro bacterial polysaccharide biosynthesis: defining the functions of Wzy and Wzz. *Nat Chem Biol* **2010,** *6* (6), 418-23.
47. Zhang, Y.; Fechter, E. J.; Wang, T. S.; Barrett, D.; Walker, S.; Kahne, D. E., Synthesis of heptaprenyl-lipid IV to analyze peptidoglycan glycosyltransferases. *J Am Chem Soc* **2007,** *129* (11), 3080-1.
48. Al-Dabbagh, B.; Olatunji, S.; Crouvoisier, M.; El Ghachi, M.; Blanot, D.; Mengin-Lecreulx, D.; Bouhss, A., Catalytic mechanism of MraY and WecA, two paralogues of the polyprenyl-phosphate N-acetylhexosamine 1-phosphate transferase superfamily. *Biochimie* **2016,** *127*, 249-57.
49. Patel, K. B.; Ciepichal, E.; Swiezewska, E.; Valvano, M. A., The C-terminal domain of the Salmonella enterica WbaP (UDP-galactose:Und-P galactose-1-phosphate transferase) is sufficient for catalytic activity and specificity for undecaprenyl monophosphate. *Glycobiology* **2012,** *22* (1), 116-122.
50. Chen, M. M.; Weerapana, E.; Ciepichal, E.; Stupak, J.; Reid, C. W.; Swiezewska, E.; Imperiali, B., Polyisoprenol specificity in the Campylobacter jejuni N-linked glycosylation pathway. *Biochemistry-Us* **2007,** *46* (50), 14342-8.
51. Breukink, E.; van Heusden, H. E.; Vollmerhaus, P. J.; Swiezewska, E.; Brunner, L.; Walker, S.; Heck, A. J. R.; de Kruijff, B., Lipid II is an intrinsic component of the pore induced by nisin in bacterial membranes. *Journal of Biological Chemistry* **2003,** *278* (22), 19898-19903.
52. Han, W. Q.; Wu, B. L.; Li, L.; Zhao, G. H.; Woodward, R.; Pettit, N.; Cai, L.; Thon, V.; Wang, P. G., Defining Function of Lipopolysaccharide O-antigen Ligase WaaL Using Chemoenzymatically Synthesized Substrates. *Journal of Biological Chemistry* **2012,** *287* (8), 5357-5365.
53. Mostafavi, A. Z.; Lujan, D. K.; Erickson, K. M.; Martinez, C. D.; Troutman, J. M., Fluorescent probes for investigation of isoprenoid configuration and size discrimination by bactoprenol-utilizing enzymes. *Bioorg Med Chem* **2013,** *21* (17), 5428-35.
54. Dodbele, S.; Martinez, C. D.; Troutman, J. M., Species differences in alternative substrate utilization by the antibacterial target undecaprenyl pyrophosphate synthase. *Biochemistry-Us* **2014,** *53* (30), 5042-50.
55. Troutman, J. M.; Erickson, K. M.; Scott, P. M.; Hazel, J. M.; Martinez, C. D.; Dodbele, S., Tuning the production of variable length, fluorescent polyisoprenoids using surfactant-controlled enzymatic synthesis. *Biochemistry-Us* **2015,** *54* (18), 2817-27.
56. Chen, A. P.; Chen, Y. H.; Liu, H. P.; Li, Y. C.; Chen, C. T.; Liang, P. H., Synthesis and application of a fluorescent substrate analogue to study ligand interactions for undecaprenyl pyrophosphate synthase. *J Am Chem Soc* **2002,** *124* (51), 15217-24.

57. Teng, K. H.; Chen, A. P.; Kuo, C. J.; Li, Y. C.; Liu, H. G.; Chen, C. T.; Liang, P. H., Fluorescent substrate analog for monitoring chain elongation by undecaprenyl pyrophosphate synthase in real time. *Anal Biochem* **2011,** *417* (1), 136-41.
58. Whitfield, C., Biosynthesis and assembly of capsular polysaccharides in Escherichia coli. *Annual Review of Biochemistry* **2006,** *75*, 39-68.
59. Ranjit, D. K.; Young, K. D., Colanic Acid Intermediates Prevent De Novo Shape Recovery of Escherichia coli Spheroplasts, Calling into Question Biological Roles Previously Attributed to Colanic Acid. *Journal of Bacteriology* **2016,** *198* (8), 1230-1240.
60. Cain, B. D.; Norton, P. J.; Eubanks, W.; Nick, H. S.; Allen, C. M., Amplification of the Baca Gene Confers Bacitracin Resistance to Escherichia-Coli. *Journal of Bacteriology* **1993,** *175* (12), 3784-3789.
61. Jorgenson, M. A.; Young, K. D., Interrupting Biosynthesis of O Antigen or the Lipopolysaccharide Core Produces Morphological Defects in Escherichia coli by Sequestering Undecaprenyl Phosphate. *Journal of Bacteriology* **2016,** *198* (22), 3070-3079.
62. Bertozzi, C. R.; Kiessling, L. L., Chemical glycobiology. *Science* **2001,** *291* (5512), 2357-2364.
63. Cartee, R. T.; Forsee, W. T.; Bender, M. H.; Ambrose, K. D.; Yother, J., CpsE from type 2 Streptococcus pneumoniae catalyzes the reversible addition of glucose-1-phosphate to a polyprenyl phosphate acceptor, initiating type 2 capsule repeat unit formation. *Journal of Bacteriology* **2005,** *187* (21), 7425-7433.
64. Merino, S.; Jimenez, N.; Molero, R.; Bouamama, L.; Regue, M.; Tomas, J. M., A UDP-HexNAc:Polyprenol-P GalNAc-1-P Transferase (WecP) Representing a New Subgroup of the Enzyme Family. *Journal of Bacteriology* **2011,** *193* (8), 1943-1952.
65. Wu, Y. W.; Alexandrov, K.; Brunsveld, L., Synthesis of a fluorescent analogue of geranylgeranyl pyrophosphate and its use in a high-throughput fluorometric assay for Rab geranylgeranyltransferase. *Nat Protoc* **2007,** *2* (11), 2704-2711.
66. Kiessling, L. L.; Splain, R. A., Chemical approaches to glycobiology. *Annu Rev Biochem* **2010,** *79*, 619-53.
67. Ko, T. P.; Chen, Y. K.; Robinson, H.; Tsai, P. C.; Gao, Y. G.; Chen, A. P.; Wang, A. H.; Liang, P. H., Mechanism of product chain length determination and the role of a flexible loop in Escherichia coli undecaprenyl-pyrophosphate synthase catalysis. *J Biol Chem* **2001,** *276* (50), 47474-82.
68. Fujii, H.; Koyama, T.; Ogura, K., Efficient enzymatic hydrolysis of polyprenyl pyrophosphates. *Biochim Biophys Acta* **1982,** *712* (3), 716-8.
69. Lehrer, J.; Vigeant, K. A.; Tatar, L. D.; Valvano, M. A., Functional characterization and membrane topology of Escherichia coli WecA, a sugar-phosphate transferase initiating the biosynthesis of enterobacterial common antigen and O-antigen lipopolysaccharide. *J Bacteriol* **2007,** *189* (7), 2618-2628.
70. Al-Dabbagh, B.; Mengin-Lecreulx, D.; Bouhss, A., Purification and Characterization of the Bacterial UDP-GlcNAc: Undecaprenyl-Phosphate GlcNAc-1-Phosphate Transferase WecA. *J Bacteriol* **2008,** *190* (21), 7141-7146.
71. Chen, L.; Men, H.; Ha, S.; Ye, X. Y.; Brunner, L.; Hu, Y.; Walker, S., Intrinsic lipid preferences and kinetic mechanism of Escherichia coli MurG. *Biochemistry-Us* **2002,** *41* (21), 6824-33.

72. Entova, S.; Guan, Z.; Imperiali, B., Investigation of the conserved reentrant membrane helix in the monotopic phosphoglycosyl transferase superfamily supports key molecular interactions with polyprenol phosphate substrates. *Arch Biochem Biophys* **2019**, 108111.
73. Chattopadhyay, A.; London, E., Parallax Method for Direct Measurement of Membrane Penetration Depth Utilizing Fluorescence Quenching by Spin-Labeled Phospholipids. *Biochemistry-Us* **1987,** *26* (1), 39-45.
74. Huster, D.; Muller, P.; Arnold, K.; Herrmann, A., Dynamics of membrane penetration of the fluorescent 7-nitrobenz-2-oxa-1,3-diazol-4-yl (NBD) group attached to an acyl chain of phosphatidylcholine. *Biophys J* **2001,** *80* (2), 822-831.
75. Furlong, S. E.; Ford, A.; Albarnez-Rodriguez, L.; Valvano, M. A., Topological analysis of the Escherichia coli WcaJ protein reveals a new conserved configuration for the polyisoprenyl-phosphate hexose-1-phosphate transferase family. *Sci Rep* **2015,** *5*, 9178.
76. Ye, X. Y.; Lo, M. C.; Brunner, L.; Walker, D.; Kahne, D.; Walker, S., Better substrates for bacterial transglycosylases. *J Am Chem Soc* **2001,** *123* (13), 3155-3156.
77. Li, L.; Woodward, R. L.; Han, W. Q.; Qu, J. Y.; Song, J.; Ma, C.; Wang, P. G., Chemoenzymatic synthesis of the bacterial polysaccharide repeating unit undecaprenyl pyrophosphate and its analogs. *Nat Protoc* **2016,** *11* (7), 1280-1298.
78. Turek, T. C.; Gaon, I.; Gamache, D.; Distefano, M. D., Synthesis and evaluation of benzophenone-based photoaffinity labeling analogs of prenyl pyrophosphates containing stable amide linkages. *Bioorg Med Chem Lett* **1997,** *7* (16), 2125-2130.
79. Das, D.; Tnimov, Z.; Nguyen, U. T. T.; Thimmaiah, G.; Lo, H.; Abankwa, D.; Wu, Y. W.; Goody, R. S.; Waldmann, H.; Alexandrov, K., Flexible and General Synthesis of Functionalized Phosphoisoprenoids for the Study of Prenylation in vivo and in vitro. *Chembiochem* **2012,** *13* (5), 674-683.
80. Davisson, V. J.; Woodside, A. B.; Neal, T. R.; Stremler, K. E.; Muehlbacher, M.; Poulter, C. D., Phosphorylation of Isoprenoid Alcohols. *J Org Chem* **1986,** *51* (25), 4768-4779.
81. Luchansky, S. J.; Hang, H. C.; Saxon, E.; Grunwell, J. R.; Yu, C.; Dube, D. H.; Bertozzi, C. R., Constructing azide-labeled cell surfaces using polysaccharide biosynthetic pathways. *Methods Enzymol* **2003,** *362*, 249-72.
82. Shieh, P.; Siegrist, M. S.; Cullen, A. J.; Bertozzi, C. R., Imaging bacterial peptidoglycan with near-infrared fluorogenic azide probes. *Proc Natl Acad Sci U S A* **2014,** *111* (15), 5456-61.
83. Bertozzi, C. R., Chemical approaches to glycobiology. *Faseb J* **2000,** *14* (8), A1410-A1410.
84. Young, N. M.; Brisson, J. R.; Kelly, J.; Watson, D. C.; Tessier, L.; Lanthier, P. H.; Jarrell, H. C.; Cadotte, N.; St Michael, F.; Aberg, E.; Szymanski, C. M., Structure of the N-linked glycan present on multiple glycoproteins in the Gram-negative bacterium, Campylobacter jejuni. *J Biol Chem* **2002,** *277* (45), 42530-9.
85. Karlyshev, A. V.; Everest, P.; Linton, D.; Cawthraw, S.; Newell, D. G.; Wren, B. W., The Campylobacter jejuni general glycosylation system is important for attachment to human epithelial cells and in the colonization of chicks. *Microbiology (Reading)* **2004,** *150* (Pt 6), 1957-1964.

86. Kelly, J.; Jarrell, H.; Millar, L.; Tessier, L.; Fiori, L. M.; Lau, P. C.; Allan, B.; Szymanski, C. M., Biosynthesis of the N-linked glycan in Campylobacter jejuni and addition onto protein through block transfer. *J Bacteriol* **2006,** *188* (7), 2427-34.
87. Nothaft, H.; Davis, B.; Lock, Y. Y.; Perez-Munoz, M. E.; Vinogradov, E.; Walter, J.; Coros, C.; Szymanski, C. M., Engineering the Campylobacter jejuni N-glycan to create an effective chicken vaccine. *Sci Rep* **2016,** *6*, 26511.
88. O'Neil, C. L.; Stine, K. J.; Demchenko, A. V., Immobilization of glycans on solid surfaces for application in glycomics. *J Carbohydr Chem* **2018,** *37* (4), 225-249.
89. Monzo, A.; Guttman, A., Immobilization techniques for mono- and oligosaccharide microarrays. *Qsar Comb Sci* **2006,** *25* (11), 1033-1038.
90. Tommasone, S.; Allabush, F.; Tagger, Y. K.; Norman, J.; Kopf, M.; Tucker, J. H. R.; Mendes, P. M., The challenges of glycan recognition with natural and artificial receptors. *Chem Soc Rev* **2019,** *48* (22), 5488-5505.
91. Troutman, J. M.; Imperiali, B., Campylobacter jejuni PglH is a single active site processive polymerase that utilizes product inhibition to limit sequential glycosyl transfer reactions. *Biochemistry-Us* **2009,** *48* (12), 2807-16.
92. Morrison, J. P.; Troutman, J. M.; Imperiali, B., Development of a multicomponent kinetic assay of the early enzymes in the Campylobacter jejuni N-linked glycosylation pathway. *Bioorg Med Chem* **2010,** *18* (23), 8167-71.
93. Glover, K. J.; Weerapana, E.; Chen, M. M.; Imperiali, B., Direct biochemical evidence for the utilization of UDP-bacillosamine by PglC, an essential glycosyl-1-phosphate transferase in the Campylobacter jejuni N-linked glycosylation pathway. *Biochemistry-Us* **2006,** *45* (16), 5343-50.
94. Olivier, N. B.; Chen, M. M.; Behr, J. R.; Imperiali, B., In vitro biosynthesis of UDP-N,N'-diacetylbacillosamine by enzymes of the Campylobacter jejuni general protein glycosylation system. *Biochemistry-Us* **2006,** *45* (45), 13659-69.
95. Teng, K. H.; Liang, P. H., Undecaprenyl diphosphate synthase, a cis-prenyltransferase synthesizing lipid carrier for bacterial cell wall biosynthesis. *Mol Membr Biol* **2012,** *29* (7), 267-73.
96. Coker, O. O.; Palittapongarnpim, P., Current understanding of de novo synthesis of bacterial lipid carrier (undecaprenyl phosphate): More enzymes to be discovered. *Afr J Microbiol Res* **2011,** *5* (18), 2555-2565.
97. Glover, K. J.; Weerapana, E.; Imperiali, B., In vitro assembly of the undecaprenylpyrophosphate-linked heptasaccharide for prokaryotic N-linked glycosylation. *Proc Natl Acad Sci U S A* **2005,** *102* (40), 14255-9.
98. Das, D.; Kuzmic, P.; Imperiali, B., Analysis of a dual domain phosphoglycosyl transferase reveals a ping-pong mechanism with a covalent enzyme intermediate. *Proc Natl Acad Sci U S A* **2017,** *114* (27), 7019-7024.
99. Schoenhofen, I. C.; McNally, D. J.; Vinogradov, E.; Whitfield, D.; Young, N. M.; Dick, S.; Wakarchuk, W. W.; Brisson, J. R.; Logan, S. M., Functional characterization of dehydratase/aminotransferase pairs from Helicobacter and Campylobacter: enzymes distinguishing the pseudaminic acid and bacillosamine biosynthetic pathways. *J Biol Chem* **2006,** *281* (2), 723-32.
100. Nothaft, H.; Liu, X.; Li, J.; Szymanski, C. M., Campylobacter jejuni free oligosaccharides: function and fate. *Virulence* **2010,** *1* (6), 546-50.

101. Nothaft, H.; Liu, X.; McNally, D. J.; Li, J.; Szymanski, C. M., Study of free oligosaccharides derived from the bacterial N-glycosylation pathway. *Proc Natl Acad Sci U S A* **2009,** *106* (35), 15019-24.
102. Reid, A. J.; Scarbrough, B. A.; Williams, T. C.; Gates, C. E.; Eade, C. R.; Troutman, J. M., General Utilization of Fluorescent Polyisoprenoids with Sugar Selective Phosphoglycosyltransferases. *Biochemistry-Us* **2020,** *59* (4), 615-626.
103. Park, S.; Gildersleeve, J. C.; Blixt, O.; Shin, I., Carbohydrate microarrays. *Chem Soc Rev* **2013,** *42* (10), 4310-26.
104. Vijayakumar, S.; Merkx-Jacques, A.; Ratnayake, D. B.; Gryski, I.; Obhi, R. K.; Houle, S.; Dozois, C. M.; Creuzenet, C., Cj1121c, a novel UDP-4-keto-6-deoxy-GlcNAc C-4 aminotransferase essential for protein glycosylation and virulence in Campylobacter jejuni. *J Biol Chem* **2006,** *281* (38), 27733-43.
105. Mostafavi, A. Z.; Troutman, J. M., Biosynthetic Assembly of the Bacteroides fragilis Capsular Polysaccharide A Precursor Bactoprenyl Diphosphate-Linked Acetamido-4-amino-6-deoxygalactopyranose. *Biochemistry-Us* **2013,** *52* (11), 1939-1949.
106. Labadie, G. R.; Viswanathan, R.; Poulter, C. D., Farnesyl diphosphate analogues with omega-bioorthogonal azide and alkyne functional groups for protein farnesyl transferase-catalyzed ligation reactions. *J Org Chem* **2007,** *72* (24), 9291-7.
107. De Schutter, J. W.; Morrison, J. P.; Morrison, M. J.; Ciulli, A.; Imperiali, B., Targeting Bacillosamine Biosynthesis in Bacterial Pathogens: Development of Inhibitors to a Bacterial Amino-Sugar Acetyltransferase from Campylobacter jejuni. *J Med Chem* **2017,** *60* (5), 2099-2118.
108. Olivier, N. B.; Chen, M. M.; Behr, J. R.; Imperiali, B., In vitro biosynthesis of UDP-N,N '-diacetylbacillosamine by enzymes of the Campylobacter jejuni general protein glycosylation system. *Biochemistry-Us* **2006,** *45* (45), 13659-13669.
109. Rick, P. D.; Barr, K.; Sankaran, K.; Kajimura, J.; Rush, J. S.; Waechter, C. J., Evidence that the wzxE gene of Escherichia coli K-12 encodes a protein involved in the transbilayer movement of a trisaccharide-lipid intermediate in the assembly of enterobacterial common antigen. *Journal of Biological Chemistry* **2003,** *278* (19), 16534-16542.
110. Perlstein, D. L.; Wang, T. S.; Doud, E. H.; Kahne, D.; Walker, S., The role of the substrate lipid in processive glycan polymerization by the peptidoglycan glycosyltransferases. *J Am Chem Soc* **2010,** *132* (1), 48-9.
111. Men, H. B.; Park, P.; Ge, M.; Walker, S., Substrate synthesis and activity assay for MurG. *Journal of the American Chemical Society* **1998,** *120* (10), 2484-2485.
112. Ramirez, A. S.; Boilevin, J.; Mehdipour, A. R.; Hummer, G.; Darbre, T.; Reymond, J. L.; Locher, K. P., Structural basis of the molecular ruler mechanism of a bacterial glycosyltransferase. *Nat Commun* **2018,** *9* (1), 445.
113. Miller, W. L.; Matewish, M. J.; McNally, D. J.; Ishiyama, N.; Anderson, E. M.; Brewer, D.; Brisson, J. R.; Berghuis, A. M.; Lam, J. S., Flagellin glycosylation in Pseudomonas aeruginosa PAK requires the O-antigen biosynthesis enzyme WbpO. *J Biol Chem* **2008,** *283* (6), 3507-18.
114. Pan, L.; Farouk, M. H.; Qin, G.; Zhao, Y.; Bao, N., The Influences of Soybean Agglutinin and Functional Oligosaccharides on the Intestinal Tract of Monogastric Animals. *Int J Mol Sci* **2018,** *19* (2).

115. Wacker, M.; Linton, D.; Hitchen, P. G.; Nita-Lazar, M.; Haslam, S. M.; North, S. J.; Panico, M.; Morris, H. R.; Dell, A.; Wren, B. W.; Aebi, M., N-linked glycosylation in Campylobacter jejuni and its functional transfer into E-coli. *Science* **2002,** *298* (5599), 1790-1793.
116. Studier, F. W., Protein production by auto-induction in high density shaking cultures. *Protein Expr Purif* **2005,** *41* (1), 207-34.
117. Chhetri, G.; Kalita, P.; Tripathi, T., An efficient protocol to enhance recombinant protein expression using ethanol in Escherichia coli. *Methodsx* **2015,** *2*, 385-391.
118. Rath, A.; Glibowicka, M.; Nadeau, V. G.; Chen, G.; Deber, C. M., Detergent binding explains anomalous SDS-PAGE migration of membrane proteins. *Proc Natl Acad Sci U S A* **2009,** *106* (6), 1760-5.
119. Chehade, K. A. H.; Andres, D. A.; Morimoto, H.; Spielmann, H. P., Design and synthesis of a transferable farnesyl pyrophosphate analogue to Ras by protein farnesyltransferase. *J Org Chem* **2000,** *65* (10), 3027-3033.
120. Labadie, G. R.; Viswanathan, R.; Poulter, C. D., Farnesyl diphosphate analogues with omega-bioorthogonal azide and alkyne functional groups for protein farnesyl transferase-catalyzed Ligation reactions. *J Org Chem* **2007,** *72* (24), 9291-9297.
121. Xu, H. J.; Zhao, Y. Q.; Zhou, X. F., Palladium-catalyzed Heck reaction of aryl chlorides under mild conditions promoted by organic ionic bases. *J Org Chem* **2011,** *76* (19), 8036-41.
122. Whitfield, C.; Paiment, A., Biosynthesis and assembly of Group 1 capsular polysaccharides in Escherichia coli and related extracellular polysaccharides in other bacteria. *Carbohyd Res* **2003,** *338* (23), 2491-2502.
123. Chen, J.; Lee, S. M.; Mao, Y., Protective effect of exopolysaccharide colanic acid of Escherichia coli O157:H7 to osmotic and oxidative stress. *Int J Food Microbiol* **2004,** *93* (3), 281-6.
124. Mao, Y.; Doyle, M. P.; Chen, J., Insertion mutagenesis of wca reduces acid and heat tolerance of enterohemorrhagic Escherichia coli O157:H7. *J Bacteriol* **2001,** *183* (12), 3811-5.
125. Ophir, T.; Gutnick, D. L., A role for exopolysaccharides in the protection of microorganisms from desiccation. *Appl Environ Microbiol* **1994,** *60* (2), 740-5.
126. Prigent-Combaret, C.; Prensier, G.; Le Thi, T. T.; Vidal, O.; Lejeune, P.; Dorel, C., Developmental pathway for biofilm formation in curli-producing Escherichia coli strains: role of flagella, curli and colanic acid. *Environ Microbiol* **2000,** *2* (4), 450-64.
127. Goebel, W. F., Colanic acid. *Proc Natl Acad Sci U S A* **1963,** *49*, 464-71.
128. Stevenson, G.; Andrianopoulos, K.; Hobbs, M.; Reeves, P. R., Organization of the Escherichia coli K-12 gene cluster responsible for production of the extracellular polysaccharide colanic acid. *J Bacteriol* **1996,** *178* (16), 4885-93.
129. Harding, C. M.; Haurat, M. F.; Vinogradov, E.; Feldman, M. F., Distinct amino acid residues confer one of three UDP-sugar substrate specificities in Acinetobacter baumannii PglC phosphoglycosyltransferases. *Glycobiology* **2018,** *28* (7), 522-533.
130. Rosano, G. L.; Ceccarelli, E. A., Recombinant protein expression in Escherichia coli: advances and challenges. *Front Microbiol* **2014,** *5*, 172.
131. Schaffer, C.; Wugeditsch, T.; Messner, P.; Whitfield, C., Functional expression of enterobacterial O-polysaccharide biosynthesis enzymes in Bacillus subtilis. *Appl Environ Microbiol* **2002,** *68* (10), 4722-30.

132. van Heijenoort, J., Lipid intermediates in the biosynthesis of bacterial peptidoglycan. *Microbiol Mol Biol Rev* **2007,** *71* (4), 620-35.
133. Piepenbreier, H.; Diehl, A.; Fritz, G., Minimal exposure of lipid II cycle intermediates triggers cell wall antibiotic resistance. *Nat Commun* **2019,** *10* (1), 2733.
134. Luo, S.; McNeill, M.; Myers, T. G.; Hohman, R. J.; Levine, R. L., Lon protease promotes survival of Escherichia coli during anaerobic glucose starvation. *Arch Microbiol* **2008,** *189* (2), 181-185.
135. Van Melderen, L.; Aertsen, A., Regulation and quality control by Lon-dependent proteolysis. *Res Microbiol* **2009,** *160* (9), 645-51.
136. Gottesman, S.; Trisler, P.; Torres-Cabassa, A., Regulation of capsular polysaccharide synthesis in Escherichia coli K-12: characterization of three regulatory genes. *J Bacteriol* **1985,** *162* (3), 1111-9.
137. Jorgenson, M. A.; Kannan, S.; Laubacher, M. E.; Young, K. D., Dead-end intermediates in the enterobacterial common antigen pathway induce morphological defects in Escherichia coli by competing for undecaprenyl phosphate. *Mol Microbiol* **2016,** *100* (1), 1-14.
138. Eade, C. R.; Wallen, T. W.; Gates, C. E.; Oliverio, C. L.; Scarbrough, B. A.; Reid, A. J.; Jorgenson, M. A.; Young, K. D.; Troutman, J. M., Making the Enterobacterial Common Antigen Glycan and Measuring Its Substrate Sequestration. *ACS Chem Biol* **2021**.
139. Whitfield, C.; Roberts, I. S., Structure, assembly and regulation of expression of capsules in Escherichia coli. *Mol Microbiol* **1999,** *31* (5), 1307-19.
140. Henderson, J. C.; O'Brien, J. P.; Brodbelt, J. S.; Trent, M. S., Isolation and chemical characterization of lipid A from gram-negative bacteria. *J Vis Exp* **2013,** (79), e50623.
141. Stout, V., Identification of the promoter region for the colanic acid polysaccharide biosynthetic genes in Escherichia coli K-12. *J Bacteriol* **1996,** *178* (14), 4273-80.
142. Wall, E.; Majdalani, N.; Gottesman, S., The Complex Rcs Regulatory Cascade. *Annu Rev Microbiol* **2018,** *72*, 111-139.
143. Castanie-Cornet, M. P.; Cam, K.; Jacq, A., RcsF is an outer membrane lipoprotein involved in the RcsCDB phosphorelay signaling pathway in Escherichia coli. *Journal of Bacteriology* **2006,** *188* (12), 4264-4270.
144. Ebel, W.; Trempy, J. E., Escherichia coli RcsA, a positive activator of colanic acid capsular polysaccharide synthesis, functions To activate its own expression. *J Bacteriol* **1999,** *181* (2), 577-84.
145. Adcox, H. E.; Vasicek, E. M.; Dwivedi, V.; Hoang, K. V.; Turner, J.; Gunn, J. S., Salmonella Extracellular Matrix Components Influence Biofilm Formation and Gallbladder Colonization. *Infect Immun* **2016,** *84* (11), 3243-3251.
146. Amer, A. O.; Valvano, M. A., Conserved aspartic acids are essential for the enzymic activity of the WecA protein initiating the biosynthesis of O-specific lipopolysaccharide and enterobacterial common antigen in Escherichia coli. *Microbiology (Reading)* **2002,** *148* (Pt 2), 571-582.
147. Charette, M. F.; Henderson, G. W.; Markovitz, A., ATP hydrolysis-dependent protease activity of the lon (capR) protein of Escherichia coli K-12. *Proc Natl Acad Sci U S A* **1981,** *78* (8), 4728-32.

148. Navasa, N.; Rodriguez-Aparicio, L.; Martinez-Blanco, H.; Arcos, M.; Ferrero, M. A., Temperature has reciprocal effects on colanic acid and polysialic acid biosynthesis in E-coli K92. *Appl Microbiol Biot* **2009,** *82* (4), 721-729.
149. Clarke, D. J., The Rcs phosphorelay: more than just a two-component pathway. *Future Microbiol* **2010,** *5* (8), 1173-84.
150. Meredith, T. C.; Mamat, U.; Kaczynski, Z.; Lindner, B.; Holst, O.; Woodard, R. W., Modification of lipopolysaccharide with colanic acid (M-antigen) repeats in Escherichia coli. *J Biol Chem* **2007,** *282* (11), 7790-8.
151. Hong, Y. Q.; Liu, M. A.; Reeves, P. R., Progress in Our Understanding of Wzx Flippase for Translocation of Bacterial Membrane Lipid-Linked Oligosaccharide. *Journal of Bacteriology* **2018,** *200* (1).
152. Kramer, N. E.; Smid, E. J.; Kok, J.; de Kruijff, B.; Kuipers, O. P.; Breukink, E., Resistance of Gram-positive bacteria to nisin is not determined by lipid II levels. *FEMS Microbiol Lett* **2004,** *239* (1), 157-61.
153. Dietrich, C. P.; Colucci, A. V.; Strominger, J. L., Biosynthesis of the peptidoglycan of bacterial cell walls. V. Separation of protein and lipid components of the particulate enzyme from Micrococcus lysodeikticus and purification of the endogenous lipid acceptors. *J Biol Chem* **1967,** *242* (13), 3218-25.
154. Grant, W. D.; Sutherland, I. W.; Wilkinson, J. F., Exopolysaccharide colanic acid and its occurrence in the Enterobacteriaceae. *J Bacteriol* **1969,** *100* (3), 1187-93.
155. Sutherland, I. W., Enzymic hydrolysis of colanic acid. *Eur J Biochem* **1971,** *23* (3), 582-7.
156. Huang, Y. H.; Ferrieres, L.; Clarke, D. J., The role of the Rcs phosphorelay in Enterobacteriaceae. *Res Microbiol* **2006,** *157* (3), 206-12.
157. Datsenko, K. A.; Wanner, B. L., One-step inactivation of chromosomal genes in Escherichia coli K-12 using PCR products. *Proc Natl Acad Sci U S A* **2000,** *97* (12), 6640-5.
158. Huang, C. J.; Lin, H.; Yang, X., Industrial production of recombinant therapeutics in Escherichia coli and its recent advancements. *J Ind Microbiol Biotechnol* **2012,** *39* (3), 383-99.